TRANSIENT VOLTAGE-GATED POTASSIUM CHANNELS IN CULTURED HIPPOCAMPAL ASTROCYTES

A Thesis

Submitted to

The College of Graduate Studies and Research

In Partial Fulfillment of the Requirements

For the Degree of Doctor of Philosophy

In the Department of Physiology

University of Saskatchewan

Saskatoon

By

Lane K. Bekar

PERMISSION OF USE STATEMENT

In presenting this thesis in partial fulfillment of the requirements for a Postgraduate Degree from the University of Saskatchewan, I agree that the Libraries of this University may make it freely available for inspection. I further agree that permission for copying of this thesis in any manner, in whole or in part, for scholarly purposes may be granted by the professor or professors who supervised my thesis work or, in their absence, by the Head of the Department or the Dean of the College in which my thesis was done. It is understood that any copy or publication or use of this thesis or parts thereof for financial gain shall not be allowed without my written permission. It is also understood that due recognition shall be given to me and to the University of Saskatchewan in any scholarly use which may be made of any material in my thesis.

Requests for permission to copy or to make other use of material in this thesis in whole or part should be addressed to:

Head of the Department of Physiology,
University of Saskatchewan,
107 Wiggins Road,
Saskatoon, Saskatchewan,
Canada S7N 5E5

ABSTRACT

In the nervous system, the roles of Kv channels are well established as being critical for regulating action potential frequency, membrane potential, and neurotransmitter release. However, their role in glial cells, a non-excitable cell type, is yet to be fully understood. Whole-cell current kinetics, pharmacology, immunocytochemistry and RT-PCR were used to characterize A-type current in hippocampal astrocyte cultures to better understand its function. Pharmacological analysis suggests that ~70%, 10% and less than 5% of total A-current is associated with Kv4, Kv3 and Kv1 channels, respectively. In addition, pharmacology and kinetics provide novel evidence for a significant contribution of KChIP accessory proteins to astrocytic A-channel composition. Localization of the *Shaw* Kv3.4 channel to astrocytic processes and the *Shal* Kv4.3 channel to soma suggest that these channels serve a specific function. Since astrocytes are known to be subjected to neuronal firing frequencies of up to 200 Hz in the hippocampus, the role of A-currents in membrane voltage oscillations was assessed. Although TEA-sensitive delayed-rectifying currents are involved in the extent of repolarization, 4-AP-sensitive A-currents serve to increase the rate.

Astrocytes and HEK293 cells were used to investigate the mechanism of the previously found $GABA_A$ induced anion-mediated reduction of Kv channels in more detail. Astrocytes demonstrate an anion concentration specific depolarizing effect on inactivating A-type (also termed transient voltage-gated) K^+ channel activation kinetics whereas a hyperpolarizing effect was seen upon expression of Kv4.2 or Kv1.4 in HEK293 cells, but only after disruption of the cytoskeleton using cytochalasin D. It is hypothesized that cytoskeletal interactions and Cl^--mediated effects are mediated through N-terminal conformational stabilities.

In summary, the results indicate that hippocampal astrocytes *in vitro* express multiple A-type Kv channel α-subunits with accessory, Ca^{2+}-sensitive cytoplasmic subunits that appear to be specifically localized to subcellular membrane compartments. Functions of these channels remain to be determined in a physiological setting, but suggest that A-type Kv channels enable astrocytes to respond rapidly with membrane voltage oscillations to high frequency incoming signals, possibly synchronizing astrocyte function to neuronal activity. Furthermore, studies of anion and cytoskeletal effects on Kv channels demonstrate channel function to be highly localized/targeted and susceptible to changes in ionic environment.

ACKNOWLEDGEMENTS

I would like to thank Dr. W. Walz, my supervisor, for the opportunity to pursue my interests in neurophysiology and for having enough confidence in me to allow me to follow my own interests, even when that meant it was outside the research field of his expertise. I would also like to thank him and all the members of my advisory committee for their guidance, patience and support throughout the course of my Ph.D program.

I would like to extend special thanks to Dr. Thomas Fisher, Dr. Michel Desautels, Dr. Prakash Sulakhe and Dr. Nigel West for their help and discussions on manuscripts and writing of this thesis.

During my Ph.D program I was supported by a scholarship from the College of Graduate Studies and Research of the University of Saskatchewan. The work in this thesis was supported by grants from the Canadian Institutes of Health Research and the Heart and Stroke Foundation of Saskatchewan.

DEDICATION

I dedicate this thesis to:

My fiancée, Kai Wang, for loving me and providing that spark in my life that lets me know I can accomplish anything I set my mind to.

TABLE OF CONTENTS

LIST OF TABLES

LIST OF FIGURES

LIST OF ABBREVIATIONS

4-AP – 4-aminopyridine

A1 – type 1 adenosine receptor

AA – arachidonic acid

AHP – afterhyperpolarization

AMPA – α-amino-3-hydroxy-5-methylisoxazole-4-propionic acid

AQP-4 – aquaporin-4

A-type/A-current – inactivating outward potassium channel/current

BBB – blood brain barrier

CFTR – cystic fibrosis transmembrane regulator

Chl-T/chloramines-T – N-Chloro-p-toluene-sulfonamide

CHO – Chinese hamster ovary

Cxn43 – connexin-43

DAG- diacylglycerol

DMEM – Dulbecco's modified eagle's medium

DMSO - dimethylsulfoxide

DPPX – dipeptidyl aminopeptidase-like protein

EETs – epoxyeicosatrienoic acids

eGFP – enhanced green fluorescent protein

EGTA – ethylene glycol bis-(β-aminoethyl ether) N,N,N',N'-tetraacetic acid

ETYA – eicosatetraynoic acid

FBS – fetal bovine serum

FCS – fetal calf serum

FITC – fluorescein isothiocyanate

GABA – γ-amino butyric acid

GAPDH – glyceraldehyde phosphate dehydrogenase

GDNF – glial derived neurotrophic factor

GFAP – glial fibrillary acidic protein

GFP – green fluorescent protein

HEK293 – human embryonic kidney cell line

HEPES – Hydroxyethylpeperazine ethanesulfonic acid

HS – horse serum

IP3 – inositol 3-phosphate

KChAP – potassium channel associated protein

KChIP – potassium channel interacting protein

KIS – potassium channel inactivation suppressor

MiRPs – minK related peptides

mRNA – messenger RNA

NADP+ - nicotinamide adenine dinucleotide phosphate oxidized

NADPH – nicotinamide adenine dinucleotide phosphate reduced

NCS-1 – neuronal calcium sensor-1

NMDA – N-methyl-D-aspartate

NO – nitric oxide

NT - neurotransmitter

$P2X_7$ – purinergic type 2X splice variant 7 receptor

PGs - prostaglandins

PSD-95 – post synaptic density protein

Redox – reduction/oxidation

REM – rapid eye movement

RT-PCR – reverse transcriptase polymerase chain reaction

S1-6 – transmembrane segments 1-6

SH – sulfhydryl

T1 – tetramerization domain

tBHP – tert-butyl hydrogen peroxide

TEA - tetraethylammonium

TGFα – transforming growth factor-α

TRITC – tetramethylrhodamine isothiocyanate

V½ - voltage of 50% activation or inactivation

1.0 - GENERAL INTRODUCTION

This thesis investigates voltage-gated potassium channel expression and function in astrocytes and explores the previously found anion-mediated effects (Bekar and Walz 1999) on these channels in astrocytes and on isolated Kv channels expressed in HEK293 cells. As a result, the introduction will begin with a short structural and functional background of voltage-gated potassium channels with emphasis on structures that become pertinent to work performed herein. Following this, basic astrocytic function in the complex CNS is briefly covered with emphasis on the astrocyte-neuronal interactions illustrating the importance for astrocytes being synchronized with their environment. The complex neuronal-astrocytic interactions will provide a backdrop for postulating a reason for the complex voltage-gated channel repertoire in this so-called non-excitable cell type.

1.1 Voltage-gated Potassium Channels

Due to large intracellular stores of negatively charged particles and solutes in the nucleus and cytoplasm, cells have had to develop means for preventing osmotic gradients leading to cell swelling and eventual lysis. Plant cells accomplish this by forming a second thick cell wall to withstand large hydrostatic forces. Animal cells, on the other hand, took a different approach by allowing establishment and maintenance of electrochemical gradients across a selectively permeable single bilayer lipid membrane. In this way the cell can avoid influx of neutralizing charged particles with their concurrent osmotic effects. With the establishment of large Na^+, K^+, and Ca^{2+} gradients, fast electrical signaling was made possible.

> Electricity plays an unavoidable role in biology. Whenever solutes like phosphate compounds, amino acids, or inorganic ions are transported across membranes, the movement of their charge constitutes an electrical current that produces a voltage difference across the membrane. Beyond managing to keep this accumulation of charge from getting too far out of balance, all living cells have developed the ability to exploit a transmembrane electrical potential as an intermediate in the storage of energy and the synthesis of ATP (Yellen, 2002).

Voltage-gated potassium channels are found in many cell types, both excitable and non-excitable. Their presence is especially noted in tissues comprising nervous, cardiovascular and endocrine systems. Mutations in these important channels may lead to altered electrical activity of the heart and neurological dysfunction. In many cases, the functional role of these channels is unknown, likely due to the overwhelming diversity of the channels in addition to the variable distribution throughout tissues and across species. In the nervous system, potassium channels contribute to regulation of the cells membrane potential which, in neurons, influences the frequency of action potential firing and thereby flow of information. Movement and concentration of extracellular potassium in the central nervous system is also regulated through potassium channel expression in glial cells, a non-excitable cell type. By means of their

extensive gap junctional coupling and potassium homeostatic capabilities, the astrocytic syncytium plays a large role in regulating neuronal excitability. Taken together, glial and neuronal potassium channels are instrumental in information processing and maintaining proper nervous system function.

In the cardiovascular system, potassium channels are responsible for repolarization and hyperpolarization of cardiac and smooth muscle tissue, respectively. In smooth muscle tissue, hyperpolarization plays a crucial role in determining vascular tone. Changes in tone regulate the diameter of small resistance arteries thereby controlling blood pressure and flow. In cardiac tissue, the rate of repolarization regulates rhythmicity of contractions. As one can see, potassium channels play significant roles in both nervous and cardiovascular tissue. However, their importance reaches beyond these tissues. Potassium channels are found in nearly all cells and are functionally very diverse; an evident prerequisite to being able to fulfill their diverse functions in many different specialized tissues.

1.1.1 Kv channel α-subunits

Voltage-gated potassium α-subunits have six transmembrane domains, with both amino and carboxy termini residing on the cytosolic side of the membrane (Fig. 1.1A). Channels are formed when four identical (homomeric) or four unique (heteromeric) alpha subunits assemble to form a pore in a membrane (Fig. 1.1B). The voltage sensitivity required for activation of the channel is imparted by the positively charged S4 segment, while the 'pore loop' linker between S5 and S6 (called H5) as well as S6 and the S4-S5 loop grants K^+ selectivity to the channel (Fig. 1.1A; Slesinger et al. 1993; Aiyar et al. 1994; for review see Jan and Jan, 1997, Coetzee et al. 1999 and Yellen 2002).

The number of Kv channel α-subunits discovered seems to be continually growing allowing for a huge diversity in channel properties (Fig. 1.1C). There are four major pore forming α-subunit families (Kv1-4) that yield functional channels upon expression in different expression systems. Additional membrane α-subunits (Kv5, 6, 8 and 9), and cytoplasmic Kvβ- or potassium channel interacting protein (KChIPs) subunits appear to function in a modulatory role creating still greater potential for functional Kv channel diversity.

Tetramerization of the Kv channel subunits is highly dependent on an ~120 amino acid N-terminal domain termed the tetramerization domain (T1). Formation of a functional channel occurs, as mentioned above, in a homogeneous or heterogeneous fashion but is limited to channels within the same subfamily (Jan and Jan 1992; Kreusch et al. 1998; Bixby et al. 1999; Strang et al. 2001) due to small T1 sequence differences (Xu et al. 1995; Bixby et al. 1999). The T1 N-terminal domain is situated hanging like a gondola directly below the channel (Fig. 1.2 right; Fig. 1.3) and is highly conserved among the Kv1.x – Kv4.x α-subunits. What is interesting about this functional protein interaction domain is that, in contrast to most assembly domain interfaces (Jones and Thornton 1997), this subunit interface is highly polar in nature making the interaction much less stable (Fig. 1.2 inset). It is proposed that this instability, in such an important interaction site, serves a functional role (Minor et al. 2000). Replacement of the T1 domain with a structurally unrelated four-stranded coiled-coil tetramerization domain (Harbury et al. 1993), in addition to scanning mutagenesis of the individual polar residues, demonstrated the T1 domain to be highly important in determining gating kinetics of the channel (Minor et al. 2000; Cushman et al. 2000; see Discussion 6.2.2).

In addition to containing the tetramerization domain, the amino (N) terminus is involved in N-type rapid inactivation ('ball and chain') in the *Shaker* Kv1.4 and *Shaw* Kv3.3-4 α-subunits.

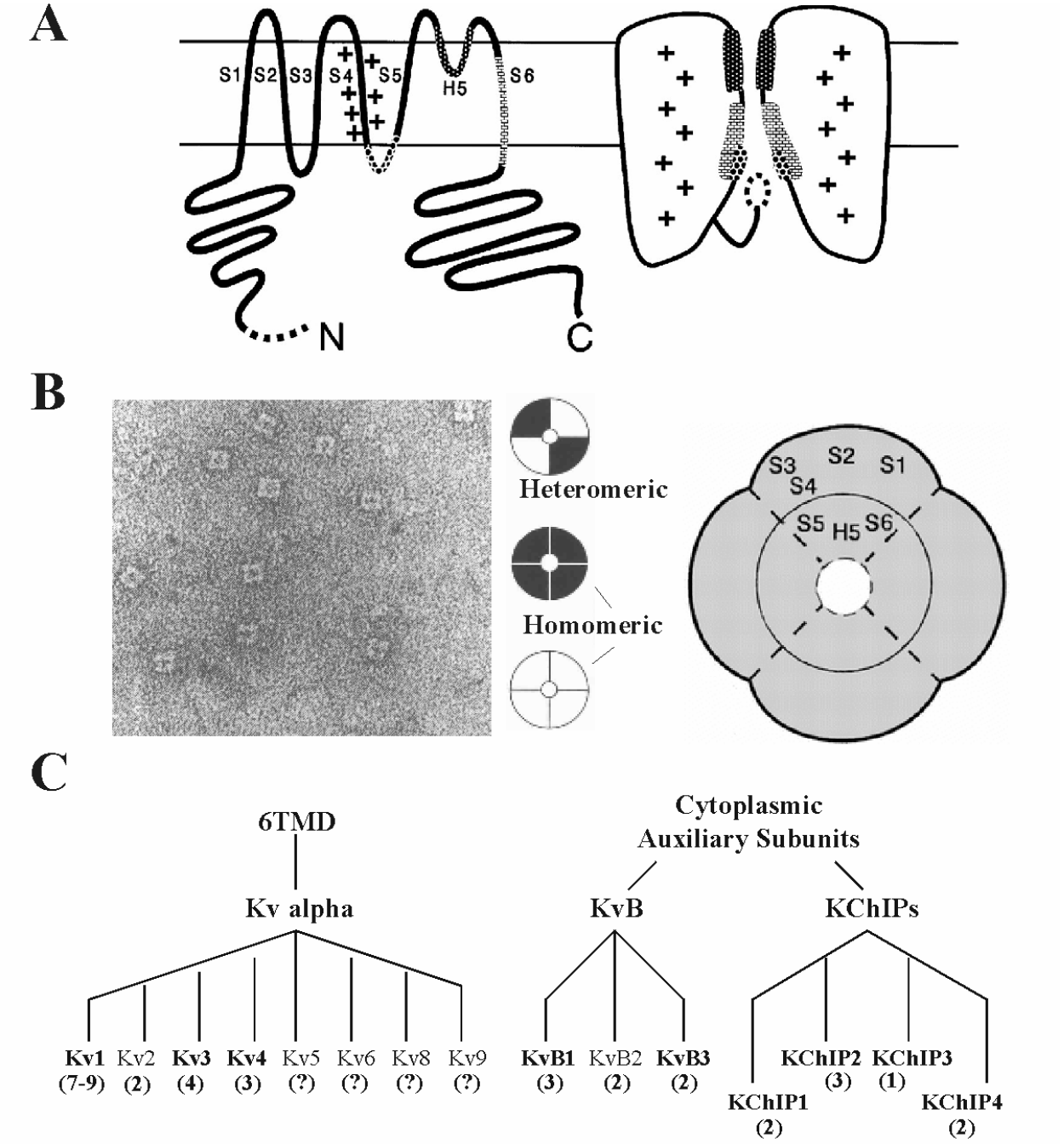

Figure 1.1. Kv channel alpha subunit structure and multimerization. A) Structural elements of the voltage-gated potassium channel for demonstration of site specific functions. The N-terminal inactivation particle, the S4 voltage sensor, the S4-S5 loop that interacts with the inactivation particle, and the H5 and S6 segments responsible for the permeation pathway are illustrated with respect to orientation in the 3-dimensional structure (compare left to right; from Jan and Jan 1997). B) Kv channels are made up of 4 alpha-subunits (right). Homomeric channels are formed from identical subunits and heteromeric channels from different subunits (center; Ashcroft 2000). Note the fourfold symmetry of the purified *Shaker* channels in the picture taken on an electron microscope (left; from Li et al. 1994). C) Schematic representation of the 6 transmembrane voltage-gated potassium channel subfamily (left; from Coetzee et al. 1999) and accessory beta- and KChIP subunits (right; from Pongs et al. 1999). The number of known splice variants for each is displayed in parentheses.

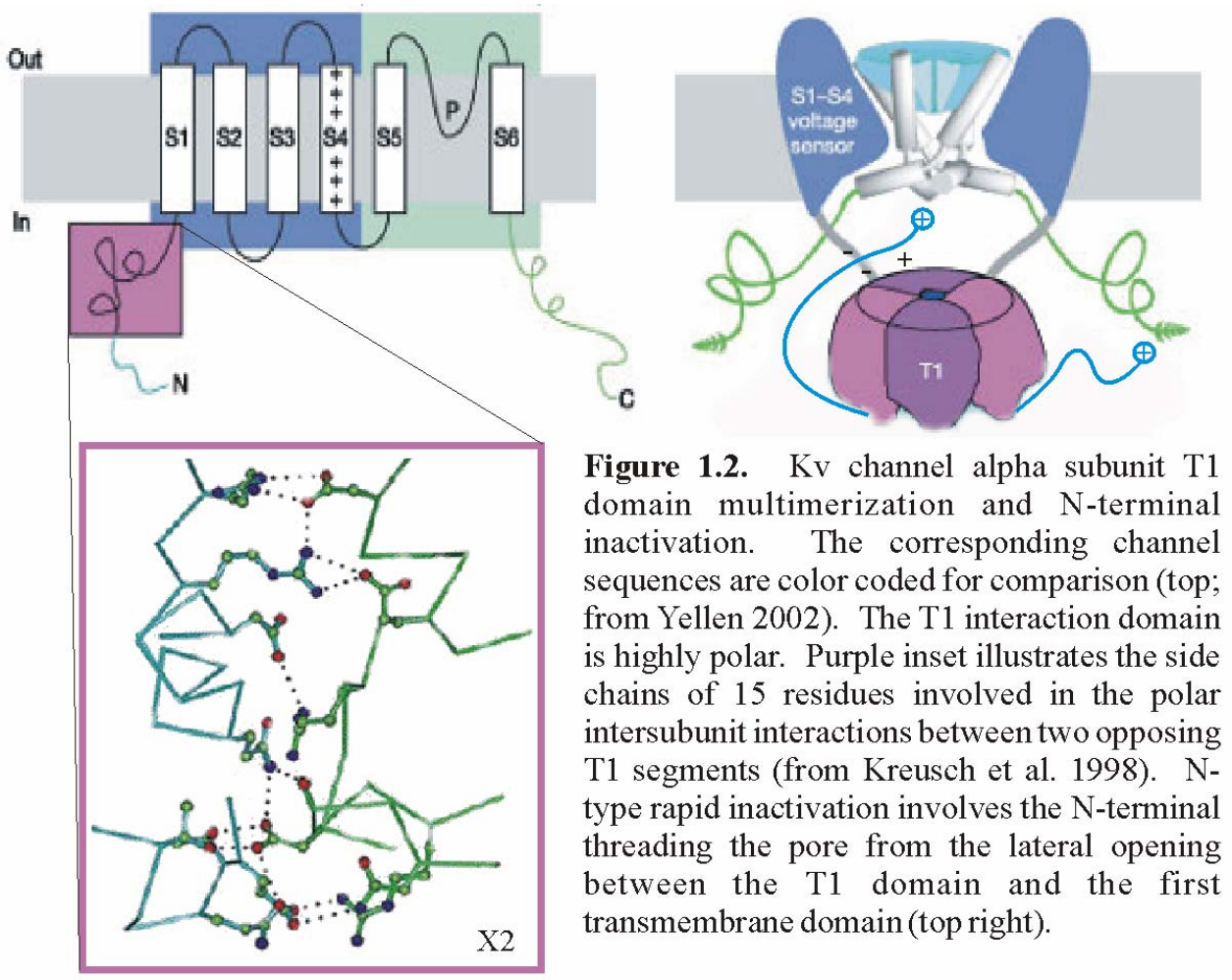

Figure 1.2. Kv channel alpha subunit T1 domain multimerization and N-terminal inactivation. The corresponding channel sequences are color coded for comparison (top; from Yellen 2002). The T1 interaction domain is highly polar. Purple inset illustrates the side chains of 15 residues involved in the polar intersubunit interactions between two opposing T1 segments (from Kreusch et al. 1998). N-type rapid inactivation involves the N-terminal threading the pore from the lateral opening between the T1 domain and the first transmembrane domain (top right).

The inactivation 'ball and chain' was shown to enter the lateral opening between the T1 domain and the channel, as mutations in the T1-S1 linker influence the inactivation process (Fig. 1.2 right; Gulbis et al. 2000). The 'ball' binds to the intracellular loop between transmembrane segments S4 and S5 resulting in the obstruction of the intracellular mouth of the pore. Although the *Shal* Kv4 α-subunit family also demonstrates rapid inactivation kinetics, the mechanism for inactivation block is less clear. It was shown that N- and C-terminal domains of the Kv4.1 channels interact with each other and together determine the fast phase of the complex multiphase inactivation kinetics (Jerng and Covarrubias 1997). Residues residing on the channels S4-S5 loop (note the consistency with 'ball and chain' inactivation) and the C-terminal end of S6 adjacent to the inner pore are thought to be responsible for both channel closing and the slower phases of inactivation kinetics (Jerng et al. 1999). Interestingly however, a recent study (Gebauer et al. 2004) demonstrated that, although inactivation energetics and structural determinants associated with *Shal* Kv4 channels differs from *Shaker* Kv1, many aspects of the rapid inactivation are the same with the first 40 N-terminal residues acting like the inactivation ball.

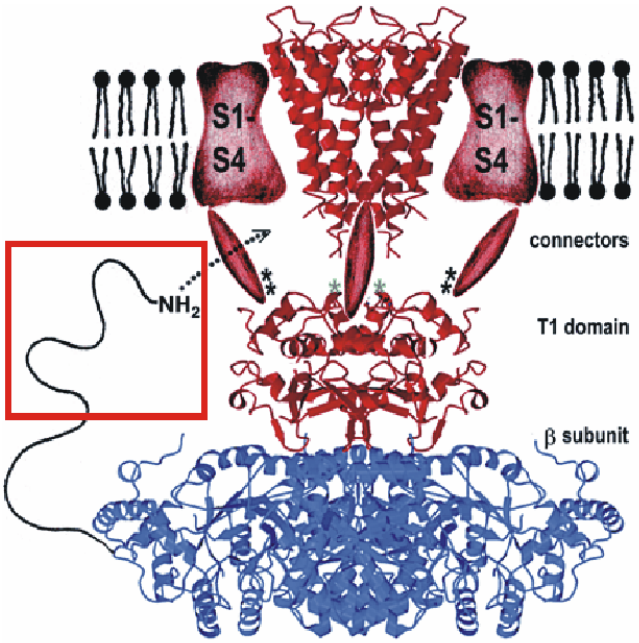

Figure 1.3. Composite model of a voltage-dependent potassium channel (from Gulbis et al. 2000). The alpha-subunit is in red and the beta-subunit in blue. Note that beta-subunit N-terminal inactivation is identical to alpha-subunit inactivation (Fig. 1.2). The red box represents the fact that not all beta-subunits contain an inactivation domain.

1.1.2 Kv channel accessory subunits

Although only a limited number of Kvα-subunit channels demonstrate N-type inactivation on their own, auxiliary cytoplasmic β-subunits with a similar N-terminal 'ball' domain may also interact with *Shaker* Kv1 family *α*-subunit N-terminals to create an N-type inactivating channel (Fig. 1.3; Rettig et al. 1994; Heinemann et al. 1996; Pongs et al. 1999; Gulbis et al. 2000). However, not every β-subunit is capable of this N-type inactivation. The Kvβ2 family does not contain the N-terminal 'ball' domain and thus does not create a rapidly inactivating channel. N-type inactivation, therefore, must not be its only function. Indeed, additional studies have demonstrated that Kvβ subunits also affect *Shaker* Kv1 family gating kinetics (England et al. 1995; Uebele et al. 1996, 1998; Accili et al. 1997) distinct from N-terminal-mediated inactivation. Furthermore, it has been demonstrated that Kvβ-subunits increase amplitude and confer O_2-sensitivity to Kv channels (Wang et al. 1996; Perez-Garcia et al. 1999; Peri et al. 2001; Bahring et al. 2001; Tipparaju et al. 2005) via an internal oxido-reductase binding site (Peri et al. 2001). The oxido-reductase catalytic site may be important in Kv1.4 channel targeting to the membrane as mutations in the site reduced Kvβ2-mediated effects on amplitude (at plasma membrane) but not total internal membrane associated Kv1.4-Kvβ2 complexes (Peri et al. 2001). This implies that Kvβ subunits are also involved in channel targeting. Consistent with this functional role, it is very interesting to note that Kvβ-subunits also bind to the C-termini of *Shal* Kv4 channels (Nakahira et al. 1996; Yang et al. 2001) that are known to be involved in channel targeting (Rivera et al. 2003) leading to an increase in channel surface expression (Yang et al. 2001). Therefore, although Kvβ subunits most notably affect gating of *Shaker* family Kv1 channels, evidence is now accumulating for them as chaperones in targeting of both *Shaker* and *Shal* subfamilies as well as sensors of the redox state of the cell linking O_2 levels with Kv channel function.

Additional cytoplasmic *Shal* Kv4 channel accessory subunits have been uncovered within the last five years. These subunits have been named potassium channel interacting proteins (KChIPs) and are members of the larger neuronal calcium sensor recoverin gene subfamily (An

et al. 2000). To date, there are four known KChIP genes with multiple splice variants (Fig. 1.1C). KChIPs bind to Kv4 channel N-terminal T1 domains and modulate expression density, inactivation kinetics and recovery from inactivation (An et al. 2000; Nakamura et al. 2001; Beck et al. 2002; Holmqvist et al. 2002; Morohashi et al. 2002; Patel et al. 2002, 2004; Wang et al. 2002; Boland et al. 2003; Shibata et al. 2003; Van Hoorick et al. 2003). Gating kinetics are also often affected by the different KChIP binding to the highly electrostatic T1 N-terminal domain (discussed in section 1.1.4). KChIPs contain four EF-hand-like Ca^{2+}-binding motifs linking KChIP modulation of Kv4 channel members to intracellular Ca^{2+} levels (An et al. 2000). Ca^{2+} binding to KChIPs is thought to remove the KChIP-mediated slowing of inactivation kinetics without altering the KChIP-mediated increase in recovery from inactivation (Patel et al. 2002, 2004). Therefore, similar to β-subunit effects on Kv1 family members with a link to cellular redox state, KChIPs modulate functions of Kv4 family members with a link to intracellular Ca^{2+}. However, it is important to note that Kv4 family channels, in contrast to Kv1, appear to bind both Kvβ-subunits as well as KChIPs, potentially rendering them sensitive to both redox state and intracellular Ca^{2+}.

Additional factors have been found to interact and modulate *Shal* Kv4 family channels. These include neuronal calcium sensor-1 (NCS-1; also known as frequenin; Nakamura et al. 2001), K^+ channel accessory protein (KChAP; Kuryshev et al. 2000, 2001), CD26-related dipeptidyl aminopeptidase-like protein (DPPX; Nadal et al. 2001, 2003; Strop et al. 2004), the scaffolding protein PSD-95 (Wong et al. 2002) and minK-related peptides (MiRPs; Abbott et al. 2001; Zhang et al. 2001). These proteins have all been shown to modulate Kv4 channel kinetics or amplitude in some fashion through binding. They do not play a role in the context of this investigation and are therefore not discussed here. They have been mentioned in order to help illustrate some of the difficulties involved when interpreting results obtained in different expression systems (Uebele et al. 1996; Petersen and Nerbonne 1999) as well as the complexity of functional channels *in vivo*.

1.1.3 Cytoskeletal interactions with Kv channels

Recently discovered interactions of Kv channels with cytoskeletal elements provide insight into channel targeting and localization mechanisms. Disruption of the actin cytoskeleton appears to disrupt many different ion channels (Cantiello et al. 1991; Maguire et al. 1998; Wang et al. 2004). More specific studies now demonstrate that Kv channels interact with the cytoskeleton in synaptic terminals through post synaptic density protein, 95 kDa (PSD-95) (Laube et al. 1996; Burke et al. 1999; Jugloff et al. 2000; Wong et al. 2002) or even the exocytotic apparatus protein syntaxin 1A (Fili et al. 2001). This PSD-95 binding is thought to occur through a PDZ binding domain on the C-terminal (Kim et al. 1995) and/or the N-terminal (Jugloff et al. 2000; Eldstrom et al. 2002) of Kvα-subunits. Still other cytoskeletal elements such as filamin (Petrecca et al. 2000) and α-actinin-2 (Maruoka et al. 2000; Cukovic et al. 2001) may also play a role in these complex interactions. Many of these interactions alter channel density and targeting of the respective channels. However, it is not widely known if these interactions can modify channel kinetics. Lotan's group (Levin et al. 1996; Jing et al. 1997, 1999; Singer-Lahat et al. 1999) have clearly demonstrated that a cytoskeletal interaction with the Kv1.1β1.1 complex regulates the degree of rapid inactivation that can be controlled through phosphorylation of a serine residue on the C-terminal of the α-subunit. Fedida's group, on the other hand, did not show any effect of cytoskeletal disruption on Kv1.5 (Maruoka et al. 2000) or Kv4.2 (Wang et al. 2004) channel gating kinetics. Therefore, the functional impact cytoskeletal interactions have on

channel localization, targeting and behavior remains to be determined on a channel-to-channel basis.

1.1.4 Potassium channels as effector systems

Potassium channel opening is dependent upon the concerted action of multiple intracellular and extracellular factors that must culminate in the conformational changes necessary for opening of the ion selective path. Recent studies by Minor et al. (2000) and Cushman et al. (2000) demonstrated that mutations in polar residues lining the T1 tetramerization interface stabilize or destabilize the gondola-like T1 tetramer conformation. Furthermore, as these mutations also result in significant changes in gating kinetics, it is proposed that channel gating is accompanied by conformational changes in cytoplasmic T1 tetramers (Minor et al. 2000; Yi et al. 2001). Because conformational changes involved in channel opening are linked to accompanying conformational changes in the cytoplasmic T1 tetramer, Kv channels are amenable to cytoplasmic factor-mediated modulation of T1 conformation stability (Yi et al. 2001). This implies that anything that stabilizes or alters the conformation of the cytoplasmic T1 domain, such as accessory subunit binding, phosphorylation or modification by other regulatory molecules, can have an impact on channel kinetics and therefore function. As the T1 tetramer is known to interact with the C-terminal (Schulteis et al. 1996; Hatano et al. 2004) it is also conceivable that both N-terminal and C-terminal modifications affect channel function in a manner consistent with alterations in channel conformational stabilities. Thus, binding of cytoskeletal elements, Kvβ-subunits, KChIPs, calcium, NADP+ or arachidonic acid directly or indirectly to Kvα-subunit domains may all result in changes of channel function through a common mechanism relating to the energetics associated with channel conformational changes. A good example of this conformation hypothesis is provided by the Ca^{2+}-dependent and independent KChIP2 modifications of Kv4.3 (Patel et al. 2004). It is proposed that the KChIP-mediated effect on recovery from inactivation is a result of direct binding of the KChIP to the N-terminal of the Kv4.3 channel (affect gating – conformational change?) whereas the slowing of inactivation is dependent on KChIP Ca^{2+} binding (Fig. 1.4; Patel et al. 2002, 2004). As Ca^{2+}-binding to EF-hand structures results in conformational sequestration of polar residues with concomitant exposure of hydrophobic amino acids (Ikura 1996; Lewit-Bentley and Rety 2000), alterations in KChIP interactions with other parts of the channel may be exposed leading to the Ca^{2+}-dependent effect (Fig. 1.4; Patel et al. 2004).

1.1.5 Electrostatic interactions and charge screening impact channel gating behavior

The conformational hypothesis mentioned in the previous section does not apply only to binding and modulation by peptides and kinases. Inorganic salts are bountiful and under continual flux in biological systems. Since Franz Hofmeister (1888) first described anions ability to precipitate proteins from whole egg white, solutes have been known to affect surface charges at water-air and water-protein interfaces (Collins and Washabaugh 1985) that can ultimately affect protein conformational stability (Washabaugh and Collins 1986; Curtis et al. 1998; Jelesarov et al. 1998; Collins 2004). Studies on the BK Ca^{2+}-activated K^+ channel (MacKinnon et al. 1989; Park et al. 2003) or the *Shaker* K^+ channel (Elinder et al. 1998; Elinder and Arhem 1999; Islas and Sigworth 2001) demonstrate that channel behavior can be modified by charge screening with different salt solution concentrations. In addition, detailed anion replacement studies of L-type Ca^{2+} currents in rod photoreceptors (Thoreson and Stella 2000) also

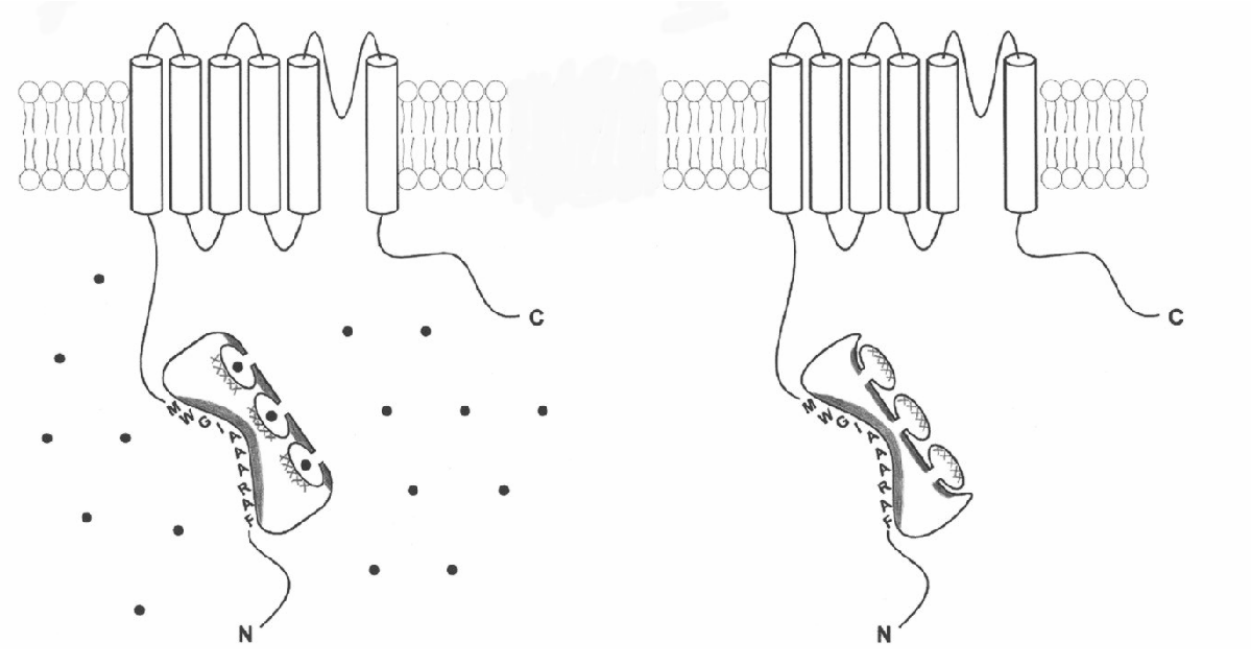

Figure 1.4. Proposed model for KChIP2-Kv4.3 interactions (from Patel et al. 2004). Hydrophobic surfaces of the KChIP molecules are shaded, hydrophilic surfaces are crosshatched. Ca^{2+} ions are indicated as black dots. KChIPs bind to the N-termini of Kv4.3 channels via a hydrophobic crevice. The steric effects of KChIP binding to the Kv4.3 N-terminus leads to slower closed-state inactivation kinetics and faster recovery kinetics independent of Ca^{2+}. Only 3 of the 4 EF-hands in KChIPs bind Ca^{2+} with the EF-hand domains facing opposite the hydrophobic crevice. When Ca^{2+} bound, the EF-hands expose a hydrophobic surface on the KChIP molecule (left) whereas when unbound, a hydrophilic surface is exposed (right). These conformational changes govern Ca^{2+}-dependent processes, namely open-state macroscopic inactivation. Therefore, binding alone alters conformational stability, with additional binding of Ca^{2+} altering that stability further.

demonstrated a functional hyperpolarizing shift in channel activation due to electrostatic interactions of Cl^- concentration changes. Therefore, it should be emphasized that changes in ion concentrations can have profound impact on ion channel gating kinetics (changes in electrostatic field potentials).

1.2 Astrocytes

Astrocytes or astroglial (glia – glue) were once thought to be "stuffing" for maintaining the structural integrity of the neuronal architecture. The past century has seen major advancements in understanding the role of astrocytes in the complex central nervous system. It is now known that astrocytes play a crucial role in maintaining a proper environment for neuronal activity. This includes establishment and maintenance of the blood brain barrier (BBB) and glial limitans (surface of brain), removal and metabolism of neurotransmitters, maintenance of extracellular K^+ and H^+ levels, ensheathment and isolation of synaptic complexes, as well as providing energy substrates for their demanding neighbours, the neuron. Additionally, it is only within the last 5-

10 years that astrocytes are being recognized as being key players in synaptic function and as playing a direct role in information processing through their ability to regulate and modulate synapse strength by means of syncytial calcium waves and transmitter release (Araque et al. 1999, 2001; Newman 2003; Ransom et al. 2003).

1.2.1 Astrocyte homeostatic functions

1.2.1.1 Regulation of $[K^+]_o$

Glial cells are well known for their role in regulating extracellular K^+ ion concentrations. Potassium spatial buffering is the capacity of astrocytes to redistribute locally elevated extracellular K^+ following neuronal activity to sites of low $[K^+]_o$ in order to prevent subsequent changes in membrane excitability (Kreisman and Smith 1993; D'Ambrosio et al. 1999). Due to the tortuosity and lack of extracellular space (ECS) in the complex mammalian CNS (Chen and Nicholson 2000), the bulk of this redistribution is achieved through the high selective potassium conductance of astrocytes associated with significant astrocytic gap junctional coupling (Konietzko and Muller 1994). As $[K^+]_o$ builds up, it results in a depolarization of the astrocytic membrane at the site of the K^+ elevation. This depolarization creates a potential difference across the astrocytic syncytium that results in a current, carried mostly by the K^+ ion, away from the site of depolarization. The complete current loop created consists of exclusive K^+ entry at the site of depolarization and exclusive K^+ exit at sites farther away with the extracellular currents carried by the bulk ions in the extracellular space (Na^+, Cl^-, Reichenbach 1991; Newman 1996). Astrocytes possess both active and passive transport systems for taking up extracellular K^+ (for review see Walz 2004). Passive K^+ uptake involves the $Na^+/K^+/2Cl^-$ cotransporter (Newman 1996) as well as inwardly rectifying potassium channels (Kir, Newman 1993; Ransom and Sontheimer 1995) coupled with Cl^- ion channels. Active transport involves the Na^+/K^+ ATPase. The glial Na^+/K^+ ATPase differs from its neuronal counterpart in that it has a different sensitivity to external K^+ ions. It was shown that the neuronal pump saturates as $[K^+]_o$ reaches 3 to 5 mM, whereas activity of the glial pump continues to rise until $[K^+]_o$ reaches 18 to 20 mM (Newman 1996; D'Ambrosio et al. 2002). On this basis, it is easy to see that the glial Na^+/K^+ pump is well suited for the uptake of K^+ in the physiological range of 3 to 20 mM $[K^+]_o$. Interestingly, it is not surprising to learn that both the passive and active systems work in concert. The passive cotransport mechanism is postulated to be linked to active transport (Na^+/K^+ ATPase) by creating a transmembrane Na^+ cycle (Walz and Hinks 1986). The Na^+ that enters the cell via the cotransport system provides the Na^+ to allow the Na^+/K^+ pump to remain active without dramatically altering intracellular Na^+ levels.

1.2.1.2 Regulation of pH

It is becoming evident that H^+ directly functions in modulating, gating and/or altering conductance of neurotransmitter and voltage-gated neuronal and glial channels (Moody 1984; Walz and Hinks 1987; Deitmer 1996). Furthermore, pH transients may be involved in the link between metabolism and activity as many of the glycolytic enzymes have been shown to be activated by intracellular alkalinization and suppressed by acidification near physiological pH (Deitmer and Rose 1996). Given that pH has the potential to modulate many cellular processes, the importance of regulation of both extracellular and intracellular pH becomes evident.

Regulation of pH in glial cells is accomplished by Cl^-/HCO_3^- exchange, Na^+/H^+ antiport and Na^+/HCO_3^- cotransport systems (Deitmer 1996; Deitmer and Rose 1996; Walz 1996; Bevensee et al. 1997). They may also have H^+ pumps (Deitmer and Rose 1996). Together, these transport mechanisms provide the astrocyte with several means to adjust, absorb and propagate pH transients. The most dominant mechanism under physiological conditions in glial cells appears to be the Na^+/HCO_3^- cotransporter. The stoichiometry of the cotransporter ($1Na^+:3HCO_3^-$, Bevensee et al. 1997) suggests that it operates near its equilibrium, close to the resting potential of the cell (Deitmer 1996). This means that with membrane depolarization there is an accompanying intracellular alkalinization (Grichtchenko and Chesler 1994), or, likewise, acidification upon membrane hyperpolarization. Therefore, modulation of both intra and extracellular pH is linked to cell membrane potential. With pH transients so intimately tied to activity and function, it isn't difficult to realize possible implications for pH in modulation of most cell-cell interactions.

Mild extracellular acidosis, which occurs concurrently with an intracellular alkalinization upon depolarization of astrocytic membranes (Ransom 1992), may be protective to neurons in times of extreme activity or pathology. A drop in extracellular pH helps limit excitotoxic damage to neurons during oxygen and glucose deprivation (Tombaugh and Sapolsky 1990) by inhibiting NMDA channel activation (glutamate channels are highly suspect in excitotoxic damage, Ransom 1992). The intracellular alkalinization of astrocytes upon increased $[K^+]_o$/depolarization serves also to increase gap junctional coupling (Spray and Bennett 1985; Enkvist and McCarthy 1994), thereby improving glial syncytial characteristics for K^+ spatial buffering and siphoning. Extracellular pH changes are also known to affect voltage-gated channels (Chesler 1990) and different membrane carriers (Walz and Hinks 1987), demonstrating significant secondary actions of H^+ in functioning of neurons and glia.

1.2.1.3 Neurotransmitter uptake

As glial cell processes envelop and encase the synaptic cleft, they are in an ideal position to intercept neurotransmitters that overflow the synapse. Astrocytes are equipped with the necessary transport systems and enzymes for removal of a large number of neurotransmitters/neuromodulators in the CNS (Martin 1996). These cells possess uptake and degradation systems for several transmitters including adenosine, aspartate, dopamine, GABA, glutamate, glycine, histamine, norepinephrine and serotonin (Martin 1996). Most of the known transport systems for uptake of transmitters derive energy from the driving forces of Na^+, K^+ or Cl^- gradients, thereby making these uptake systems electrogenic and thus most efficient under resting physiological conditions. However, because these uptake systems use ion gradients, under pathological conditions of high $[K^+]_o$ (spreading depression/injury) or even perhaps high neuronal activity, reversal of these cotransport uptake mechanisms may occur, resulting in release of additional neurotransmitter into the synaptic cleft (Martin 1996; Fellin and Carmignoto 2004). Astrocytes can avoid this situation by quickly degrading neurotransmitters, preventing buildup of internal transmitter concentrations (GABA and monoamines, Martin 1996). However, it is interesting to note that astrocytes maintain appreciable concentrations of glutamate and aspartate (Martin 1996); possibly meaning reversal of uptake for these transmitters has a functional role in synapse modulation (Araque et al. 1999, 2001; Newman 2003; Ransom et al. 2003). Although this may be the case, under pathological conditions reversal of the glutamate or aspartate uptake mechanisms could exacerbate excitotoxic conditions (Longuemare et al. 1999; Anderson and Swanson 2000; Fellin and Carmignoto 2004).

1.2.1.4 The blood-brain barrier, metabolic compartmentalization, and regulation of local blood flow

The role of astrocytes in blood-brain barrier (BBB) formation (and/or maintenance), the concept of metabolic compartmentalization and regulation of local blood flow are discussed together in this section due to anatomical convenience. Astrocytes are anatomically interposed between the brain microvasculature and neurons. Nearly all the surface area of brain microvasculature is covered by astrocytic endfeet terminals (Fig. 1.5; Harder et al. 1998; Nedergaard et al. 2003; Simard et al. 2003) forming a highly connected syncytium through connexin43 gap junctional coupling (Fig. 1.5D; Simard et al. 2003). In addition, recent demonstration of limited neighbouring astrocytic process interdigitation using enhanced green-fluorescent protein (eGFP)-expressing astrocytes in a cortical slice suggests that astrocytes may occupy their own non-overlapping microdomains (Fig. 1.6; Nedergaard et al. 2003), making each astrocyte responsible for energy demands of axons and neurons within its domain.

It is not yet known if glial cells or neurons initiate the formation of the BBB (Bauer and Bauer 2000). However, it is known that direct contact between astrocytes and endothelial cells is necessary for at least a fraction of the development (Tontsch and Bauer 1991). It is also thought that a substance secreted by astrocytes induces the junctional development, as astrocyte conditioned media appears to induce tight junctions *in vitro* (Rubin et al. 1991). Indeed, transforming growth factor α (TGFα) and glial-derived neurotrophic factor (GDNF) were subsequently found to be involved in BBB tight junction formation (Abbott 2002). Nevertheless, astrocyte conditioned media or contact with astrocytes alone does not appear to increase the electrical resistance of the BBB to that which is found in the adult CNS, strongly suggesting that additional CNS specific environmental factors are required (Rubin and Staddon 1999).

Considering the specialized arrangement with astrocytic endfeet covering all blood vessels, it appears that all energy substrates must pass through astrocytes on the way to neurons. Compartmentalization of energy metabolism in this situation seems to be the most efficient. Astrocytes are highly glycolytic and are the sole source of glycogen in the CNS (Brown et al. 2004, 2005). In contrast, neurons are primarily oxidative, using lactate provided by glycolysis and glycogenolysis in astrocytes (Brown et al. 2004). This compartmental separation (astrocyte/glycolysis vs neuron/oxidative phosphorylation) of metabolic processes provides the framework for the astrocyte-neuron lactate shuttle hypothesis (Magistretti et al. 1999; Kasischke et al. 2004; Pellerin and Magistretti 2004a, b) in which astrocytes provide neurons with lactate for oxidative phosphorylation and thereby supply a major portion of their energy requirements. This process is intimately linked with activity dependent energy expenditure (Fig. 1.7; Kasischke et al. 2004; Pellerin and Magistretti 2004a, b). Glutamate release at an excitatory synapse depolarizes the postsynaptic neuron with resultant action potentials stimulating Na^+/K^+ ATPase activity and increasing neuronal demand for energy substrates. Concurrently to this postsynaptic neuronal response, glutamate uptake (using the Na^+ gradient) into astrocytes from the synaptic cleft leads to Na^+-mediated activation of the astrocyte Na^+/K^+ ATPase which stimulates glycolysis (glucose utilization and lactate production). Lactate is then made available for the increased energy demands of the neurons. In this way, synaptic activity is directly coupled to energy substrate availability (Fig. 1.7).

In addition to glutamate uptake and metabolism by astrocytes, the glutamate released at the synapse activates metabotropic glutamate receptors on the astrocytes resulting in liberation of both IP_3 and DAG, which can both lead to production of arachidonic acid (AA). Breakdown of

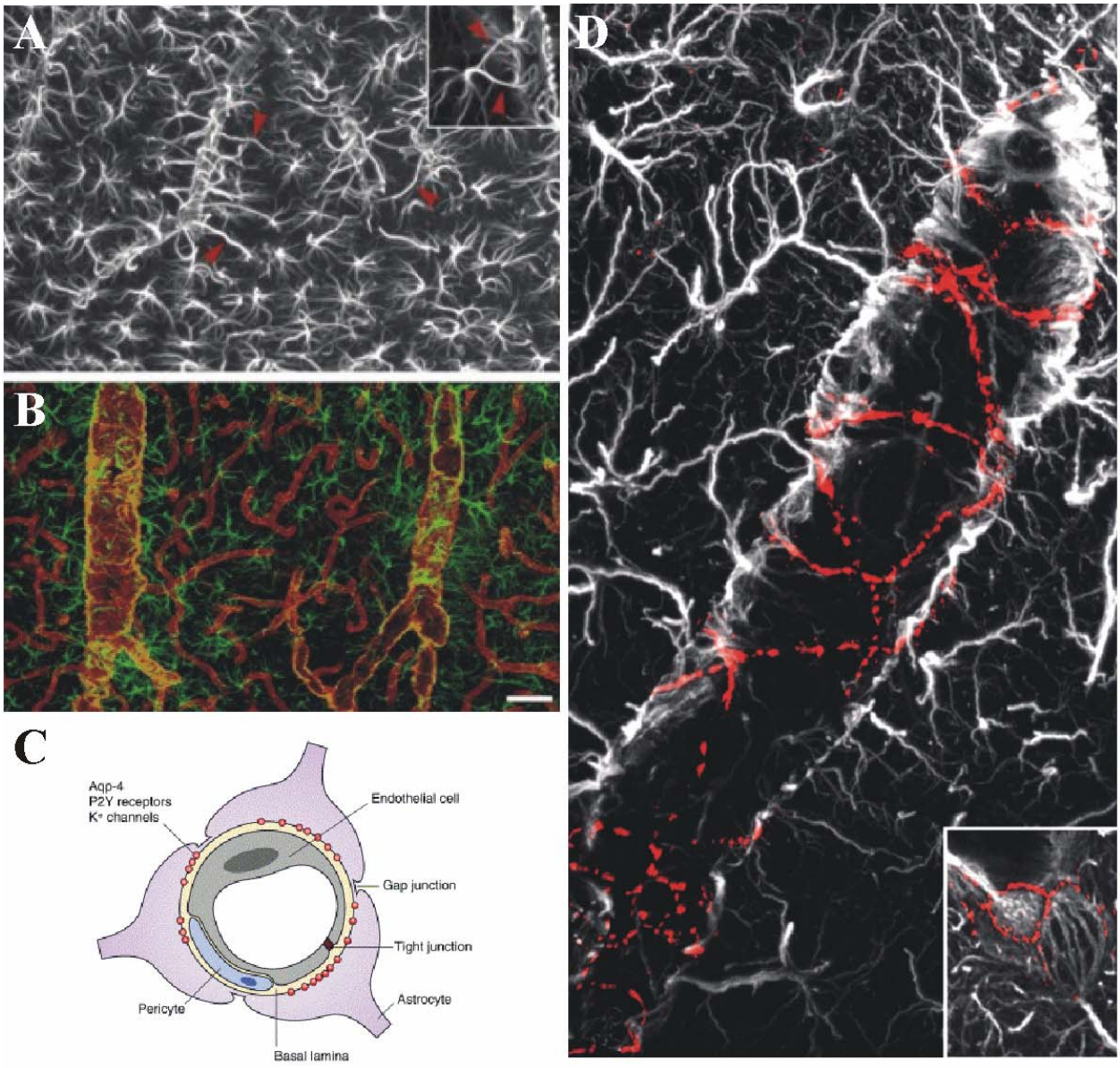

Figure 1.5. Highly coupled astrocytic endfeet completely cover CNS blood vessels. A) GFAP immunolabeled astrocytes in the cortex showing starlike shape and association of large branches with blood vessels (red arrowheads). B) Double immunolabeling for GFAP (green) and aquaporin-4 (red), a water channel specifically located in astrocytic endfeet. Note the endfeet labeling of all microvessels and the lack of GFAP in these fine processes. C) Schematic cross-section of the BBB demonstrating complete encasement of vessels by astrocytic endfeet tightly coupled by gap junctions. D) Double labeling for GFAP (white) and connexin-43 (red) demonstrating close knit layer of coupled astrocytic foot processes. A, B and D images taken from Simard and Nedergaard (2004); C is taken from Nedergaard et al. (2003).

AA by cytochrome P450 or COX enzymes leads to release of epoxyeicosatrienoic acids (EETs) and prostaglandins, respectively, which are known to be potent dilators of cerebral vessels (Fig. 1.8; Alkayed et al. 1996; Harder et al. 1998; Zonta et al. 2003b). This means that glutamate released in the synapse leads to an increase in blood flow as well as supply of energy substrates from astrocytes. Recent studies have shown that astrocytic calcium waves along connected astrocytic endfeet couple regional blood-flow to neuronal activity (Zonta et al. 2003a, b; Simard

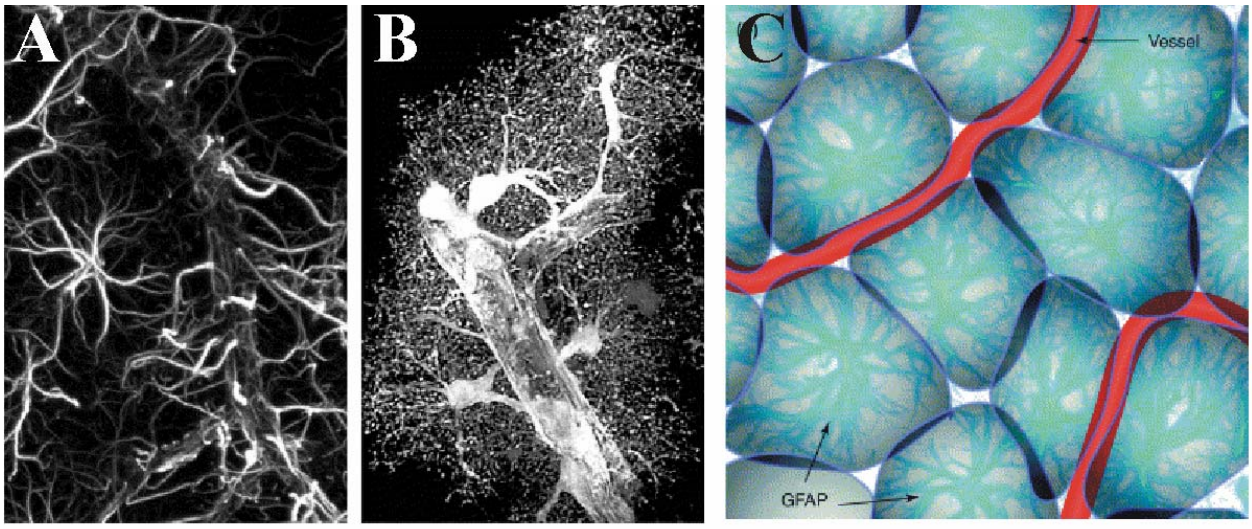

Figure 1.6. Morphological comparison of astrocytes using GFAP and eGFP. A) GFAP immunolabeling demonstrating star-like shape of astrocytes. GFAP labels the most prominant processes. B) Astrocytes visualized by overexpression of enhanced green fluorescence protein (eGFP). EGFP is cytosolic and reveals detailed astrocytic process morphology. Note the tremendous arborization of processes forming a 3D polyhedral shape with processes defining their individual territorial domain like that illustrated schematically in C. Images A and B are taken from Simard and Nedergaard (2004) and image C is from Nedergaard et al. (2003).

et al. 2003; Filosa et al. 2004; Mulligan and MacVicar 2004). It is thought that glutamate-mediated calcium transients and release of vasodilator substances on the brain microvessels links activity to blood flow and thus explains the very specific functional hyperemia seen in different brain regions (Lou et al. 1987). It is not clear what the dilator substance is, or whether there are multiple substances, but the prostaglandins and EETs are strong candidates (Alkayed et al. 1996; Harder et al. 1998; Zonta et al. 2003b).

1.2.2 Astrocytic signaling

1.2.2.1 Neurotransmitter receptors

As mentioned above, astrocytes ensheath synapses and cell bodies with their many cell processes, making them ideally situated for neurotransmitter and neuromodulator exposure. It is becoming increasingly clear that astrocytes have receptors for many of these substances (Verkhratsky and Kettenmann 1996; Porter and McCarthy 1997; Verkhratsky et al. 1998) including glutamate, GABA, purines and pyrimidines, monoamines (norepinephrine, dopamine, serotonin), acetylcholine, histamine, substance P, bradykinin, endothelins (Verkhratsky et al. 1998; Kettenmann and Steinhauser 2005) as well as prostaglandins, several hormones and cytokines/chemokines (Wesemann and Benveniste 2005). The ability of individual astrocytes to respond to these substances must clearly be a result of the environment and substances used by surrounding neurons. As astrocytes express both metabotropic (which represent the majority) and ionotropic receptors for many of the above mentioned ligands, there appear to be many different ways in which environmental factors can influence astrocyte function. However, the majority of ligands lead to changes in astrocyte intracellular Ca^{2+} concentrations (Verkhratsky et

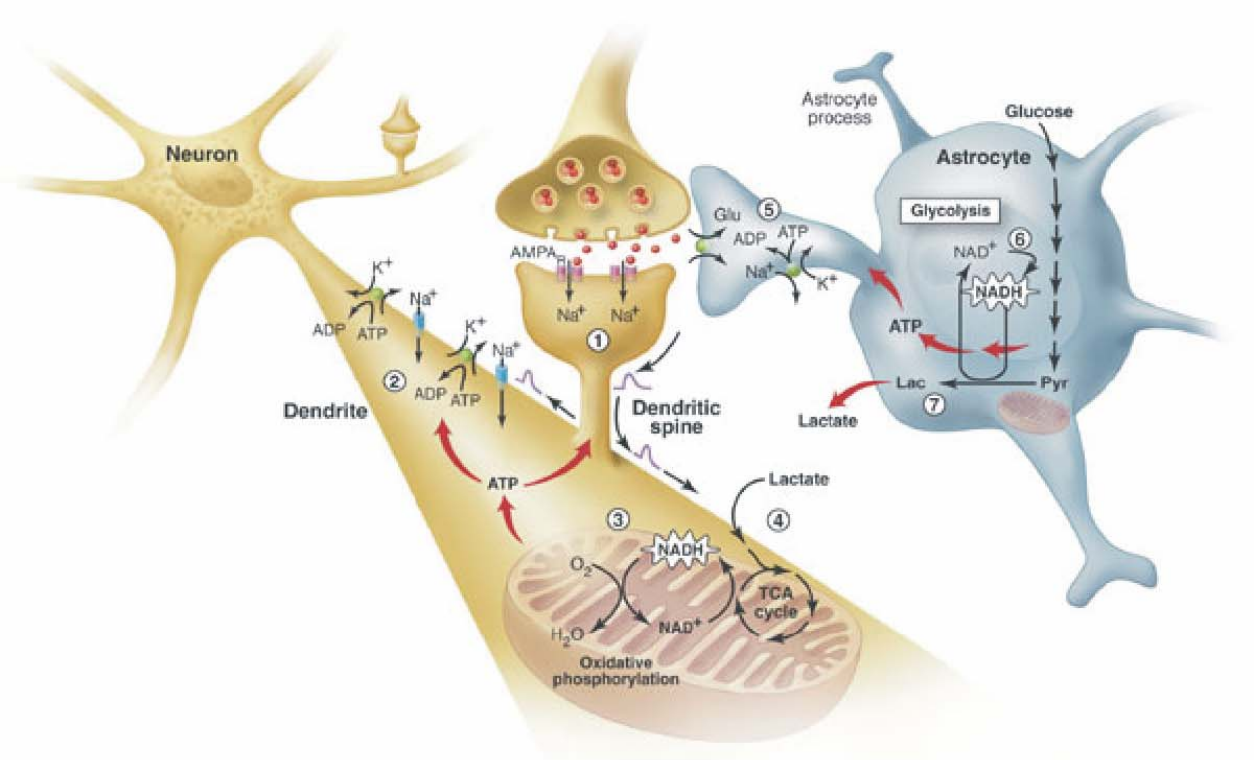

Figure 1.7. Compartmentalized activation of oxidative phosphorylation (respiration) in neurons (brown) and glycolysis in astrocytes (blue). **(1)** Stimulation of excitatory (glutamatergic) neurons activates postsynaptic AMPA receptors and induces an excitatory postsynaptic potential in the dendritic spine of the neuron. **(2)** The depolarization propagates from the dendritic spine to the dendrite, where it may cause further opening of voltage-gated sodium channels and activation of the Na^+/K^+ ATPase, leading to an increased demand for energy (ATP). **(3)** In response, oxidative phosphorylation is rapidly activated, causing a decrease in mitochondrial NADH content. **(4)** Recovery of mitochondrial NADH in dendrites is accomplished by stimulation of the TCA cycle, fueled largely by lactate from the extracellular pool. **(5)** In parallel, but delayed in time, glutamate reuptake in astrocytes (blue) activates the glial Na^+/K^+ ATPase. **(6)** The increased energy demand leads to a strong enhancement of glycolysis in the cytoplasm of astrocytes, as indicated by the large increase in cytosolic NADH. **(7)** To maintain the high glycolytic flux, NAD^+ must be regenerated via the conversion of pyruvate to lactate through the activity of the enzyme lactate dehydrogenase. Release of lactate into the extracellular space not only replenishes the extracellular pool, but also may sustain the late phase of neuronal activation. Figure and legend from Pellerin and Magistretti (2004a). This figure is a description of experimental work described in Kasischke et al. (2004).

al. 1998). This is not to say that down-stream events are all the same. Astrocytic $[Ca^{2+}]_i$ responses are very complex, encompassing different microdomains and/or the whole cell (Pasti et al. 1997; Grosche et al. 1999). Furthermore, calcium responses can be in the form of long-lasting elevations or oscillations with frequency dependent effects (Cornell-Bell et al. 1990; Pasti et al. 1997; Verkhratsky et al. 1998; Araque et al. 2001; Zonta and Carmignoto 2002; Cotrina and Nedergaard 2005). Therefore, accumulating evidence suggests that astrocytes play a role in signal processing through integration of intracellular calcium responses (Araque et al. 2001).

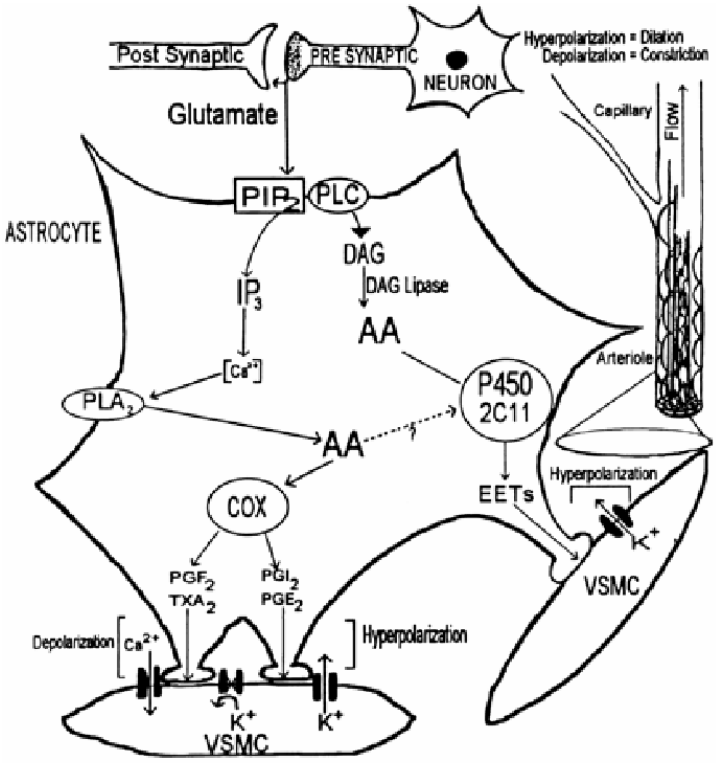

Figure 1.8. Astrocytic involvement in CNS functional hyperemia. Glutamate from active synapses can bind glutamate receptors on astrocytes, thus increasing intracellular calcium and AA release from astrocytic membranes by activation of phospholipase C, phospholipase A2, and DAG lipases. The free AA thus released can be metabolized by COX to prostaglandins and by P450 epoxygenases to EETs. Diffusion of these eicosanoids from astrocytic foot processes onto cerebral arterioles leads to modulation of cerebral vascular smooth muscle cell membrane potential and thus contractile tone. Figure and legend from Harder et al. (1998).

1.2.2.2 Neurotransmitter release

In addition to responding to what seems like every known signaling substance in the CNS, recent evidence supports the notion that astrocytes release neurotransmitter in response to elevations in intracellular Ca^{2+}, much like that in neuronal synaptic release (Araque et al. 1998b, 2001; Parpura and Haydon 2000; Pasti et al. 2001; Newman 2003; Kreft et al. 2004; Zhang et al. 2004a, b; Evanko et al. 2004; Fellin and Carmignoto 2004). In addition to Ca^{2+}-mediated vesicular release, astrocytes can also release substances through volume-sensitive anion channels, connexin hemichannels, $P2X_7$ receptors, reversal of glutamate transporters and diffusion release of lipid soluble messengers (Fig. 1.9; Ye et al. 2003; Fellin and Carmignoto 2004). Release of the different transmitter substances by astrocytes in response to different stimuli provides a

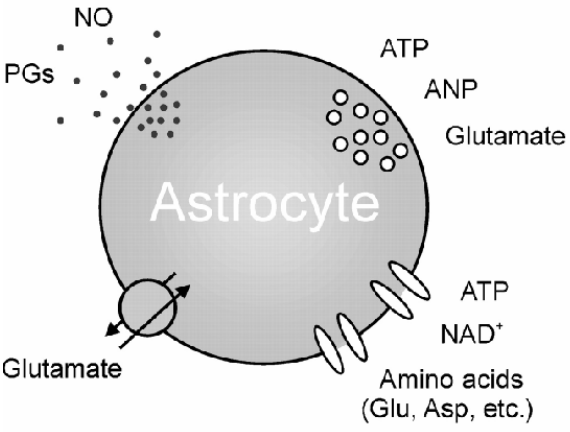

Figure 1.9. Multiple mechanisms of release of signaling molecules from astrocytes. The classical neurotransmitters glutamate and ATP can be released from astrocytes through a Ca^{2+}-dependent, most likely vesicular-mediated, mechanism. ATP, NAD^+, glutamate and other amino acids can also be released through the opening of large conductance channels, such as volume-sensitive anion channels, connexin hemichannels and $P2X_7$ receptors. Reverse operation of glutamate transporters represents an additional mechanism that can lead to a slow increase in extracellular glutamate concentration. Signaling molecules, such as PGs and NO, may diffuse freely across the membrane. Figure and legend from Fellin and Carmignoto (2004).

means of feedback, and possibly feedforward (Fellin and Carmignoto 2004), regulation that may be involved in learning and memory.

1.2.2.3 Regulation of synapse function

With astrocytes expressing functional receptors for the bulk of known neurotransmitters and modulators, and the fact that they can respond to these ligands with increases in intracellular Ca^{2+} with subsequent transmitter release, it is not difficult to envision how astrocytes play a role in modification of synapse activity and strength. It would take an entire review to describe the potential mechanisms behind glial synapse modification (see Araque et al. 1999/2001, Newman 2003 and Fellin and Carmignoto 2004 for reviews), therefore only the anatomical and physiological framework will be illustrated in this section.

As mentioned above, astrocytes are anatomically positioned between neuronal synapses and blood vessels, coordinating blood flow and metabolism with synaptic activity. In addition, they may integrate environmental signals leading to calcium waves and oscillations throughout the

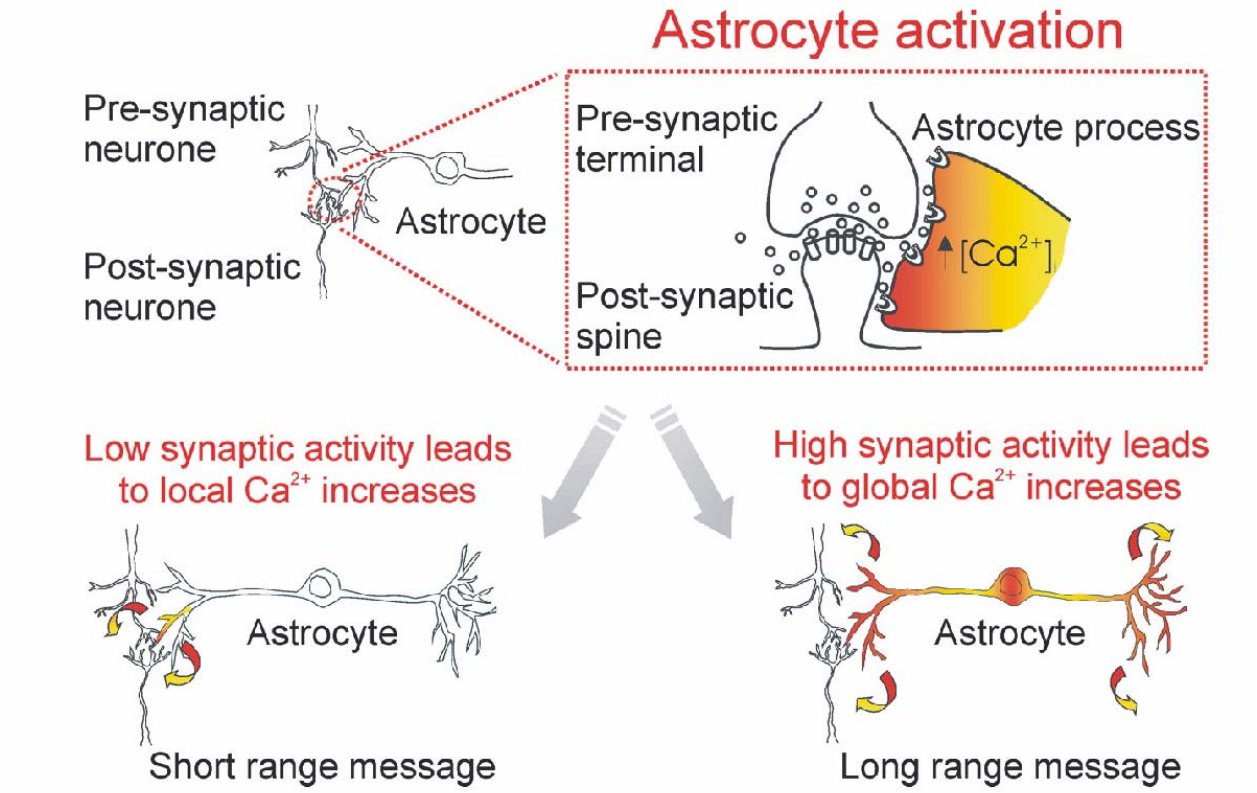

Figure 1.10. Schematic illustrating feedback and feedforward astrocyte signaling. Low synaptic activity triggers $[Ca^{2+}]_i$ elevations which remain restricted to activated astrocyte processes. This short-distance message evokes in astrocytes a Ca^{2+}-dependent release of neuroactive agents that may work as a feedback mechanism to locally affect neuronal transmission. High neuronal activity triggers a Ca^{2+} signal which propagates to other processes, and possibly other astrocytes, and is oscillatory in nature. This long-distance message works as a feedforward mechanism to transfer information on neuronal activity to other cells remote from the initial site of activation at the astrocyte process. Figure and legend from Fellin and Carmignoto (2004).

astrocytic syncytium capable of stimulating neurons and synapses at a distance. Due to long astrocytic processes, Ca^{2+} signaling may occur locally in the process ensheathing the synapse or, if the stimulus is strong enough, may propagate to the soma and distant processes (Fig. 1.10). In this way, the astrocyte encodes the strength of synaptic activity, relaying that information to adjacent synapses and, potentially, distant neurons and synapses (Pasti et al. 1997; Fellin and Carmignoto 2004). This signaling arrangement correlates well with the fact that the high frequency burst firing in the hippocampus necessary for memory consolidation (Buzsaki et al. 1987; Staba et al. 2002), would result in the feedforward long-distance calcium oscillations and waves in astrocytes (Latour et al. 2001; Hirase et al. 2004) that are thought to play a role in long-term potentiation and modification of synaptic connections (Dani et al. 1992; Kang et al. 1998; Liu et al. 2004). Figure 1.11 illustrates some of the mechanisms involved in the feedback and feedforward responses in astrocytes during synaptic activity.

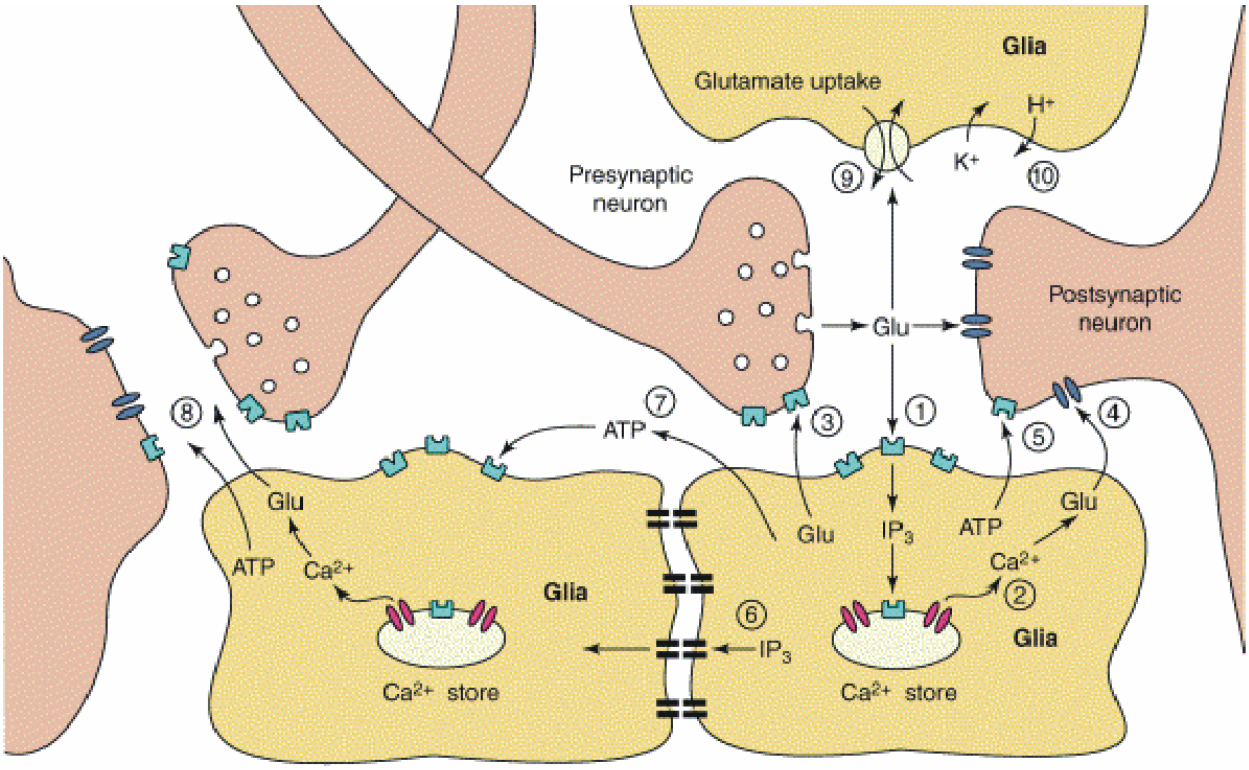

Figure 1.11. Summary of proposed mechanisms of glial regulation of synaptic transmission. Release of glutamate (Glu) from the presynaptic terminal activates glial receptors (1), evoking an increase in Ca2+ levels (2) and the release of glutamate from glia. Glutamate activation of presynaptic receptors (3) regulates transmitter release, while activation of postsynaptic receptors (4) directly depolarizes neurons. Stimulation of glia also elicits the release of ATP, which inhibits postsynaptic neurons by activating A1 receptors (5). Activation of glia might also evoke an intercellular Ca2+ wave, which propagates between glia by diffusion of IP_3 through gap junctions (6) and by release of ATP (7), and results in the modulation of distant synapses (8). Glia also modulate synaptic transmission by uptake of glutamate (9) and by regulating extracellular K+ and H+ levels (10). Figure and legend from Newman (2003).

1.3 Objectives for the Present Investigations

Specific objectives of this thesis were to:

> **Specific Objective 1)** Characterize functional transient (A-type) channel expression in cultured astrocytes in order to aid in understanding the significance of channel expression in this non-excitable cell type.

Rationale: Voltage-gated potassium channels are found in both excitable and non-excitable cell types. They are involved in neuronal and muscular electrical excitability, rhythmicity of heart rate, as well as modulation of secretion from certain endocrine cells. In the nervous system, the roles of Kv channels are well established as being critical for regulating action potential frequency, membrane potential, and neurotransmitter release (Pongs 1999). However, their role in glial cells, a non-excitable cell type, is yet to be fully understood. Voltage-gated potassium channels in astrocytes can be sub-classified as delayed rectifiers, transient A-type and inwardly rectifying channels (Barres et al. 1990; Sontheimer and Waxman 1993; Sontheimer 1994). Surprisingly, although many studies have looked at the pharmacological profile of voltage-gated potassium channels in astrocytes (Bordey and Sontheimer 1999), little is known regarding functional channel subunit expression, of inactivating A-type (also termed transient voltage-gated) channels in particular.

> **Specific Objective 2)** Assess whether A-type inactivating channels in astrocytes affect the rate of membrane repolarization and provide a link for A-current function in GABA and glutamate receptor-mediated responses.

Rationale: Although astrocytes have been demonstrated to express many different voltage-gated channels (Lascola et al. 1998; Ullrich et al. 1998; Latour et al. 2003; Bordey and Sontheimer 2000), it is still not clear what role these channels play in normal physiological function. Much has been learned regarding function of inactivating potassium channels in neurons (Hoffman et al. 1997; Hoffman and Johnston 1998; Watanabe et al. 2002; Christie and Westbrook 2003) and cardiomyocytes (Nerbonne 2000; Oudit et al. 2001; Caballero et al. 2004; Tamargo et al. 2004). In these preparations, inactivating Kv channels have been shown to affect the rate of repolarization and thereby be important in frequency modulation of action potential firing. Although much is known regarding Kv channel involvement in glial cell cycle progression (Gallo et al. 1996; Knutson et al. 1997; Ghiani et al. 1999; MacFarlane and Sontheimer 2000), a physiological function for A-type inactivating channels in this nonexcitable cell have yet to be demonstrated. Interestingly however, two recent studies (Lew et al. 2004; Vautier et al. 2004) have demonstrated that inactivating A-type channels may be able to regulate cell cycle as well, but may be related to pathological scenarios only. Since glial cells are known to express these channels under normal physiological conditions and that astrocytes are known to be subjected to neuronal firing frequencies of up to 200 Hz in the hippocampus (Staba et al. 2002; Klausberger et al. 2003, 2004; Kunec and Bose 2003; Ponomarenko et al. 2003), inactivating potassium channels may serve a similar function in astrocytes as they do in neurons.

Specific Objective 3) Investigate the mechanism of anion-mediated effects on Kv channels in both astrocytes and HEK293 cells in isolation.

Rationale: Although chloride is implicated in many cellular processes (Higashijima et al. 1987; Perutz et al. 1994; Lenz et al. 1997; Thoreson et al. 1997; Thoreson and Stella 2000), a physiologically significant role of this ion as an intracellular modulator of channel function has not been convincingly demonstrated. It has previously been shown that $GABA_A$ receptor activation in astrocytes results in a receptor-mediated chloride current with a concurrent block of outward potassium currents (Bekar et al. 1999; Bekar and Walz 1999). Although the block appears directly dependent on chloride flux through the receptor channel (Bekar and Walz 1999), the mechanism of this blockade and its link to the $GABA_A$ receptor is unknown. However, a similar situation exists with the astrocytic ionotropic glutamate receptor, where cation currents are followed by potassium channel blockade. In this case it was found that net sodium influx through the receptor with an increase in internal sodium concentration is responsible for the secondary potassium channel blockade (Robert and Magistretti 1997). Sodium increases alone were able to reduce outward potassium currents by competitive block in the channel pore at highly depolarized potentials. Anions such as chloride must affect potassium channels in a different manner as the potassium selective filter would not allow the negatively charged chloride ions to enter.

2.0 - MATERIALS AND METHODS

2.1 Cell Culture

2.1.1 Hippocampal Astrocytes

Primary cultures of hippocampal astrocytes were prepared from 1-day-old Wistar rat pups. Animals were anesthetized with Methoxyflurane (Janssen Pharmaceutica, Canada) and decapitated. Hippocampi were removed aseptically and cells were mechanically dissociated using an 80 μM Nitex filter. The cells were seeded (10^5 cells/35 mm dish) in Dulbecco's modified Eagle's medium (DMEM, Gibco-BRL) containing 20% low endotoxin (≤ 10 EU/ml) defined donor horse sera (Hyclone) and incubated at 37ºC in humidified 5% CO_2/95% O_2. After 3 days, the culture medium was replaced with DMEM containing 10% low endotoxin horse sera. Medium replacement was then repeated twice a week for the continuation of the culture process. Cells were used for whole cell patch recordings when cells formed a confluent monolayer (~ 10-12 days).

2.1.2 HEK293 cells (ATCC)

Frozen HEK cells in 5% DMSO and 20% horse serum containing DMEM (cryovial containing ~3 x 10^6 cells in 1 ml) were rapidly thawed at 37ºC and added to 10 mls DMEM and spun at 1000 rpm for 5 minutes. The supernatant was removed and the cell pellet was resuspended in 10% horse serum DMEM for plating out in T75 (250 ml) culture flasks. Media was changed every 2 to 3 days. Cells were passaged and replated prior to reaching confluence.

2.2 HEK293 Cell Transfection

HEK cells were plated in 10% horse serum containing DMEM at $8x10^5$ cells/flask (50 ml) one day prior to transfection. On the day of transfection, the media was replaced with 5 mls of DMEM containing 10% horse serum without antibiotics. Plasmid DNA containing the cDNA of channel of interest and a GFP-containing plasmid (pIRES2-eGFP, Clontech) were diluted in a glass vial containing raw DMEM without antibiotics or serum (400 μl). In a separate glass vial, Lipofectamine 2000 (Invitrogen) was also diluted (400 μl) and subsequently added to the vial containing the diluted cDNA within 5 minutes. The mixture (800 μl) was then allowed to sit for ~30 minutes at room temperature for Lipofectamine-plasmid complexes to form before adding mixture dropwise to the 50 ml culture flask. Cultures were incubated for 4-24 hours in the culture incubator before removing the media and adding fresh 10% horse serum DMEM with antibiotics. Cells were allowed to grow for up to 48 hours after transfection at which time the cells were trypsinized (removed), counted and replated in 35 mm dishes at $3x10^5$ cells/dish for subsequent patch experiments following cell attachment.

2.3 Electrophysiology

For electrophysiological recordings, 35 mm culture dishes were placed on an inverted microscope (Zeiss Axiovert 10 – equipped with epifluorescence) and perfused by a gravity fed 16 gauge needle. Perfusate was removed using a vacuum pump attached to an aspirator (Harvard Apparatus) that reduced fluctuations in volume. Extracellular perfusate contained (in mM) NaCl 126, Na gluconate 24, KCl 3.5, $CaCl_2$ 2, $MgCl_2$ 2, glucose 10, HEPES 5, and pH adjusted to 7.3 with NaOH. Borosilicate capillaries containing a thin filament (Harvard Apparatus), with a 1.5 mm outer diameter and 0.33 mm wall thickness, were pulled to a tip diameter of less than 1 μm on a Flaming/Brown micropipette puller (Model P-97, Sutter Instruments) showing resistance of 2-4 MΩ when filled with (in mM) KCl 130, $CaCl_2$ 0.5, $MgCl_2$ 2, Na_2ATP 3, EGTA 5, HEPES 10, and pH adjusted to 7.3 with KOH. The drugs 4-aminopyridine (4-AP), N-chloro-p-toluene-sulfonamide (chloramine-T), tert-butyl hydrogen peroxide (tBHP), tetraethylammonium (TEA), and 5,8,11,14-eicosatetraynoic acid (ETYA) were applied through the gravity fed perfusion system. All chemicals were obtained from BDH (Toronto, Canada) or Sigma (St. Louis, MO) unless otherwise stated.

For different intracellular Cl^- concentrations, the corresponding gluconate salt was used to replace Cl^-. For the Cl^- replacement experiments in Chapter 5.0, Cl^- was completely replaced with I^- and gluconate salts in both intracellular and extracellular solutions. For perforated patch clamp experiments, gramicidin was dissolved in DMSO to create a 5 mg/ml stock solution (sonicated ~ 20 seconds), which was then diluted to a working concentration between 30 and 40 μg/ml in an intracellular solution containing (in mM) KCl 70, KF 70, HEPES 30, NaCl 10 and pH 7.2 immediately prior to experiments. Fluoride is added because of its known blocking effects on K^+ currents and thereby large effect on membrane potential, allowing rapid determination of patch viability. Pipettes were dipped in gramicidin-free intracellular solution for 15-30 s to fill by capillary action and then back-filled with gramicidin solution to prevent perforation of cells prior to seal formation. Gramicidin stock was prepared fresh daily.

Patch clamp recordings were obtained using an Axopatch-200B amplifier. Whole cell data were acquired with an acquisition frequency of 10 kHz, filtered at 2 kHz and stored using a PC computer equipped with the Digidata 1200 digital/analog converter and PClamp 8.2.0.231 software (Axon Instruments). For select current-clamp experiments, cells were recorded in voltage-clamp initially and then switched to current-clamp mode with zero current injection for monitoring resting membrane responses. Electrophysiological protocols are illustrated and explained in Box 1.

2.4 Immunocytochemistry

Double labeling immunocytochemistry was performed using antibodies specific for Kv1.4, Kv3.4 or Kv4.3 in conjunction with the specific astrocytic marker (in culture) glial fibrillary acidic protein (GFAP). Cultures were fixed in 4% paraformaldehyde in phosphate buffered saline for 30 minutes and blocked with antibody diluent at room temperature for 1 hour. Next, the primary polyclonal rabbit anti-GFAP antibody (1:500; DAKO Corporation, Carpinteria, CA) was applied in combination with the monoclonal anti-Kv1.4 antibody (1:100; Upstate Biotechnology, Lake Placid, NY) and incubated overnight at 4ºC. Alternately, the primary polyclonal rabbit anti-Kv3.4 or Kv4.3 antibodies (1:100; Alomone Labs, Jerusalem, Israel) were applied in combination with the polyclonal goat anti-GFAP (1:200; Santa Cruz Biotechnology Inc., Santa Cruz, CA) and incubated overnight at 4ºC. Goat anti-mouse TRITC (1:200 for Kv1.4)

Box 1. Voltage protocols used in inactivating K^+ channel analysis

Voltage subtraction protocol for isolation of inactivating current. Identical series of overlayed voltage jumps for 500 ms with corresponding current traces (top) ranging from -100 to +80 mV in 20 mV steps from a prior short 2 ms holding at -80 mV. The different whole-cell current components were separated using steady state inactivation behavior of underlying inactivating channels. Pre-hyperpolarizing (left, -120 mV) the cell for 300 ms enables 100% channel activation (all voltage-gated channels) whereas pre-depolarizing (middle, -40 mV) for 300 ms allows inactivation of A-type inactivating voltage-gated channels. If the non-inactivating current component (middle) is subtracted from the total current, the voltage-sensitive inactivating K^+ current can be isolated.

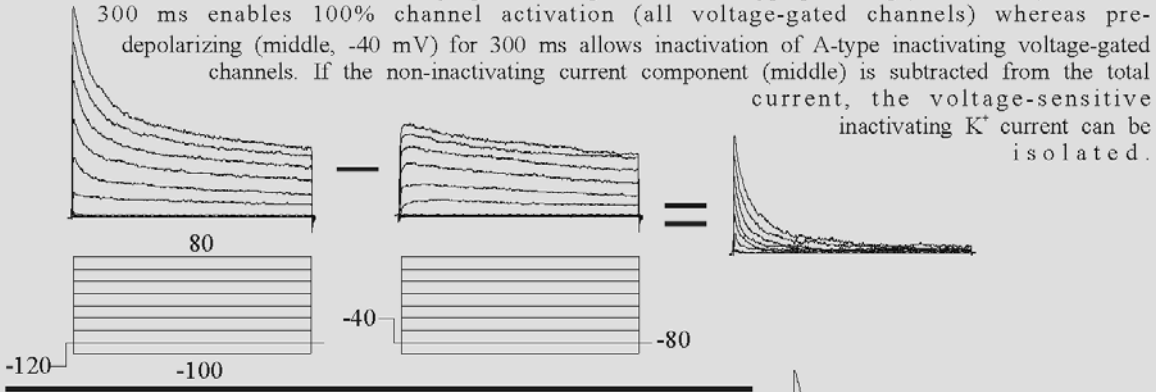

Simplified voltage protocol for isolating A-type current during pharmacological manipulation. Same theory as mentioned above for using steady-state channel kinetics. However, one protocol contains both prehyper- and predepolarizing pulses consecutively. This protocol is then applied every 3 seconds while administering drugs in the perfusate. Complete subtraction of the 100 ms voltage jumps to 80 mV renders isolated A-currents as shown above. The second jump is used alone for assessing non-inactivating currents for comparison.

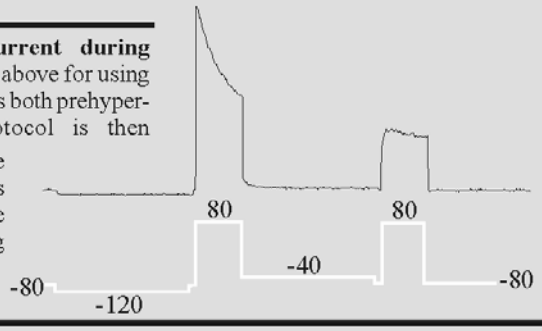

Voltage-protocol for steady-state activation and inactivation channel kinetics.

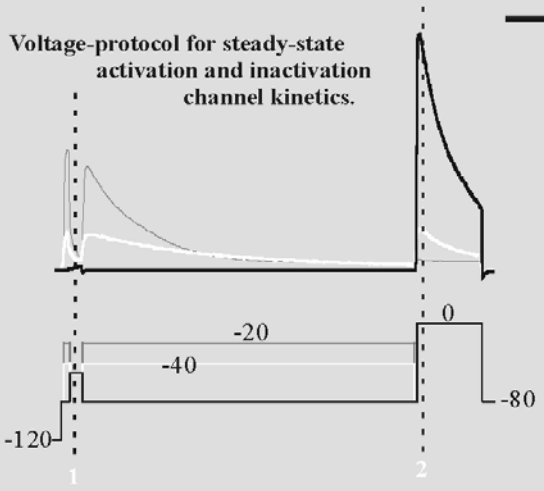

The voltage jump protocol and representative current recordings are color-coded for better understanding of what is happening. The black trace is -80 mV or common to all traces. The white represents jumps to -40 and the grey to -20 mV. Tail currents for activation are measured at 1, with steady-state inactivation measured at dashed line 2.

The black trace allows full inactivating current to the last jump to 0 mV (far right). The white trace demonstrates pre-activation of some of the channels (intermediate current at left and middle of tracing) allowing ~85% of the channels to move into the inactivated state (right jump to 0 mV again). The third grey trace activates 100% of inactivating channels (right) allowing inactivation (middle) with 0 current available for jump to 0 mV (right jump to 0 mV).

Current clamp protocols for assessing role of A-current in repolarization. Square (400 pA, 20 ms) and rapid (1 nA, 0.5 ms) current injection protocols were used to look at spiking behaviour always found in astrocyte cultures. Rapid injections allowed uninhibited repolarization for observation of A-current role using pharmacological methods.

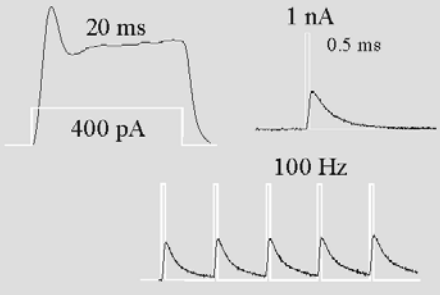

or donkey anti-rabbit FITC (1:200 for Kv3.4 and Kv4.3) were applied in conjunction with donkey anti-rabbit FITC (1:100) or donkey anti-goat TRITC (1:200) antibodies for 3 hours at room temperature in the dark. Cultures were washed and coverslips mounted with Citifluor (Marivac Laboratories) to minimize quenching. Digital images were taken with a Cool CCD Spot RT Color camera on an Olympus IX71 inverted fluorescence equipped microscope.

2.5 RNA isolation and RT-PCR analysis

Total RNA was isolated from confluent monolayer cultures of rat brain astrocytes by scraping cells in 1 ml of TRIZOL reagent (Invitrogen) containing guanidine thiocyanate and phenol. After addition of 0.2 ml of chloroform, tubes were centrifuged at 12,000 g for 15 min at 4°C. RNA in the supernatant solution was precipitated by adding an equal volume of ice-cold isopropanol and pelleted by centrifugation at 12,000 g for 10 min at 4°C and washed with 75% ethanol. RNA pellets were resuspended in RNase free water (Invitrogen). RT-PCR was performed using SuperScript One-Step RT-PCR with Platinum *Taq* from Invitrogen. Both reverse transcription and cDNA amplification were performed in a 50 µl reaction mixture containing 300 ηg of total RNA, 25 µl of the proprietary 2X reaction buffer containing 0.4 mM of each dNTP and 2.4 mM $MgSO_4$ and 1 µl RT/Platinum *Taq* mix containing SuperScript II Reverse Transcriptase and *Taq* DNA Polymerase. Sense and anti-sense primers (0.2 µM) were added and volume was brought to 50 µl with RNase free water. The annealing temperature for PCR reaction cycles was adjusted according to the optimal annealing temperatures for each specific primer set. PCR products in a 6 µl aliquot were subjected to electrophoresis in 2.0% agarose gel in 1x TEA buffer and visualized with ethidium bromide. All primers were designed based on the specific region for selected Kvα-, β-, and KChIP-subunits (Table 1).

2.6 Data Analysis

For analysis of receptor-mediated effects in chapters 4.0 and 5.0, all K^+ currents and receptor currents were normalized to cell capacitance to yield current densities (pA/pF). For analysis of the different K^+ currents during receptor activation, receptor current was subtracted from the total current at 80 mV. Because receptor currents display ohmic behavior, the receptor current at -80 mV (there is little-to-no voltage-gated channel activity at this voltage) was used to calculate the receptor current at 80 mV, given the driving forces for the different receptor-mediated ion currents (Cl^- for muscimol and Na^+/K^+ for kainate). Receptor current could not, however, be subtracted from perforated-patch experiments because the Cl^- equilibrium potential was not known. Therefore, only effects of muscimol on A-type currents could be evaluated (the protocol for A-current isolation allows complete subtraction of both receptor and delayed current). All values for concomitant inhibition of K^+ currents were normalized to receptor current density instead of cell capacitance alone. The rationale for normalizing in this manner is that K^+ current block is dependent on current flow through the receptor ionophore (Borges and Kettenmann, 1995; Robert and Magistretti, 1997; Bekar and Walz, 1999).

2.7 Statistics

Steady-state activation and inactivation data were normalized and fit with a Boltzmann function. All inactivation time constants were obtained by fitting a single exponential function to

Table 2.1. Oligonucleotide primers for Kvα and accessory β/KChIP subunits

Standard Name	Fragment Size, bp	Sense and Antisense	Location
Kv1.4	762	TCTCTTACAACTGGAAC	40-60
(M32867)		GGCCTCCTGACTGGTAA	782-801
Kvß1.1	431	GGGAAGCAATGCAAGTC	324-343
(X70662)		GCCTTTCTTCTTGATGAT	735-754
Kvß1.2	171	TGCTTGGGTCTTGGAAC	371-390
(AF131935)		GCCTTTCTTCTTGATGAT	522-541
Kvß1.3	285	GAAGTGGAGATGAACTG	217-236
(AF131936)		GCCTTTCTTCTTGATGAT	482-501
Kvß2	141	ATAGCCTGGTGCCTGAG	1514-1533
(X76724)		AATGCTGTCGATCTCGT	1635-1654
Kvß3	178	GAGTGATTGCACCCTTT	1631-1650
(X76723)		CACGGTGAAAGGATATG	1789-1808
Kv3.3	202	GGCGACAGCGGTAAGAT	481-501
(M84210)		GGTAGTAGTTGAGCACG	658-682
Kv3.4	202	AGACGATGAGCGGGAGT	936-955
(X62841)		CAGGCAGAAGGTGGTAA	1116-1137
Kv4.1	467	CGGACAAATGCTGTGCG	1386-1407
(M64226)		TAGGGGAGGAAGGTTGA	1829-1852
Kv4.2	522	ACCCCTGATCACTCTTGT	515-535
(S64320)		AGAGCACTCTCTCCTGT	1015-1036
Kv4.3	270	CTCCCTCAGCTTCCGCC	541-562
(U42975)		CTGCTGGGTGCCGCGAA	789-810
KChIP1a	206	ATGGGGGCCGTCATGGG	1-20
(AY082658)		ACCACACCACTGGGGCA	186-201
KChIP1b	239	ATGGGGGCCGTCATGGG	1-20
(AY142709)		ACCACACCACTGGGGCA	259-274
KChIP2a	324	GCTCCTATGACCAGCTT	53-73
(AAF81755)		CCTCGTTGACAATCCTA	367-387
KChIP2b	270	GCTCCTATGACCAGCTT	53-73
(AAF81756)		CCTCGTTGACAATCCTA	302-322
KChIP2c	174	GCTCCTATGACCAGCTT	53-73
(AAF81757)		CCTCGTTGACAATCCTA	206-226
KChIP3	299	GAGGACCAAGGAAGGA	6-25
(AB043892)		TCTTGAAGCCTCGGTAC	285-304
KChIP4a	197	GAATGTGAGGAGGGTGG	41-61
(AF302044)		CACTGGGGCATTCATTC	180-199
KChIP4b	299	GAATGTGAGGAGGGTGG	41-61
(AF305072)		CACTGGGGCATTCATTC	280-299

GenBank accession number is shown in parentheses.

the decaying phase of currents. All values obtained are expressed as mean ± standard error of the mean. Statistical comparisons were performed using SigmaStat (Jandel Scientific) and Excel (Microsoft) software. A two-way analysis of variance followed by a Bonferonni multiple comparison was performed on both the I-V data series and receptor-mediated responses in study III for demonstration of concentration- or anion-dependent effects. For comparisons of cell kinetics or pharmacological experiments, both paired and unpaired *t*-tests were used when appropriate to establish significance between groups. Results were deemed statistically significant at $p < 0.05$.

3.0 - COMPLEX EXPRESSION AND LOCALIZATION OF INACTIVATING KV CHANNELS IN CULTURED HIPPOCAMPAL ASTROCYTES

Astrocytes are the most numerous cells in the nervous system and appear to fulfill a wide range of neuronal support functions as outlined in the introduction. As essential to these homeostatic functions, astrocytes express many ligand (Whitaker-Azmitia et al. 1993; Matsutani and Yamamoto 1997; Porter and McCarthy 1997; Gebremedhin et al. 2003) and voltage-gated (Lascola et al. 1998; Ullrich et al. 1998; Latour et al. 2003; Bordey and Sontheimer 2000) channels. Astrocytic voltage-gated potassium channels can be sub-classified as delayed rectifiers, rapidly inactivating A-type and inwardly rectifying channels (Barres et al. 1990; Sontheimer and Waxman 1993; Sontheimer 1994). Although studies have addressed astrocytic sodium (Oh and Waxman 1994, 1995; Oh et al. 1994, 1997; Black et al. 1994, 1995; Reese and Caldwell 1999; Gautron et al. 2001; Aronica et al. 2003) and calcium channel (Latour et al. 2003) subunit expression, little is known regarding functional potassium channel subunit expression, of inactivating A-type channels in particular.

Of the Kv channel subunits thus far examined in glial cells, the *Shaker* family of voltage-gated potassium channels has received the most attention. The Kv1.1, 1.2, 1.3, 1.5, and 1.6 mRNA transcripts were found in mouse cortical astrocyte cultures using the RT-PCR approach (Smart et al. 1997). Confirmation of expression at the protein level for Kv1.5 using antisense technology (Roy et al. 1996) and Kv1.6 using immunocytochemistry (Smart et al. 1997) was also found in cultured astrocytes. Expression of Kv1.4 has only been demonstrated in Schwann cells (Sobko et al. 1998) and the oligodendrocyte cell lineage (Attali et al. 1997; Edwards et al. 2002), although it appears that astrocytes may upregulate Kv1.4 expression in a rat spinal cord injury model (Edwards et al. 2002). In addition to *Shaker* channels, only Kv2.1, 3.1 and 3.2 channel expression has been shown in Schwann cells (Sobko et al. 1998). Thus, knowledge of the Kv channel α-subunits involved in the makeup of astrocytic inactivating A-type currents is lacking. Also, the presence of accessory cytoplasmic β- (for *Shaker* α) and potassium channel interacting protein (KChIP; for *Shal* α) subunits, which have the capacity to create or modulate rapidly inactivating Kv currents (Pongs et al. 1999; Heinemann et al. 1996; Manganas and Trimmer 2000; An et al. 2000; Takimoto et al. 2002; Morohashi et al. 2002; Holmqvist et al. 2002), have not been evaluated in any glial cell type.

Considering the absence of information regarding the molecular identity of inactivating A-type channels, the objective of the following study was to better characterize A-type channel expression in cultured astrocytes in hopes of furthering our understanding of the function of these rapidly inactivating potassium currents.

3.1 Kv channel pharmacology reveals Shal subfamily dominance and presence of KChIPs

Pharmacological studies were conducted on isolated inactivating A-type currents in astrocytes using the voltage subtraction protocol described in Figure 3.1A. The isolated A-type current activated around -50 mV with peak currents averaging 1.96 ± 0.20 nA and showed nearly

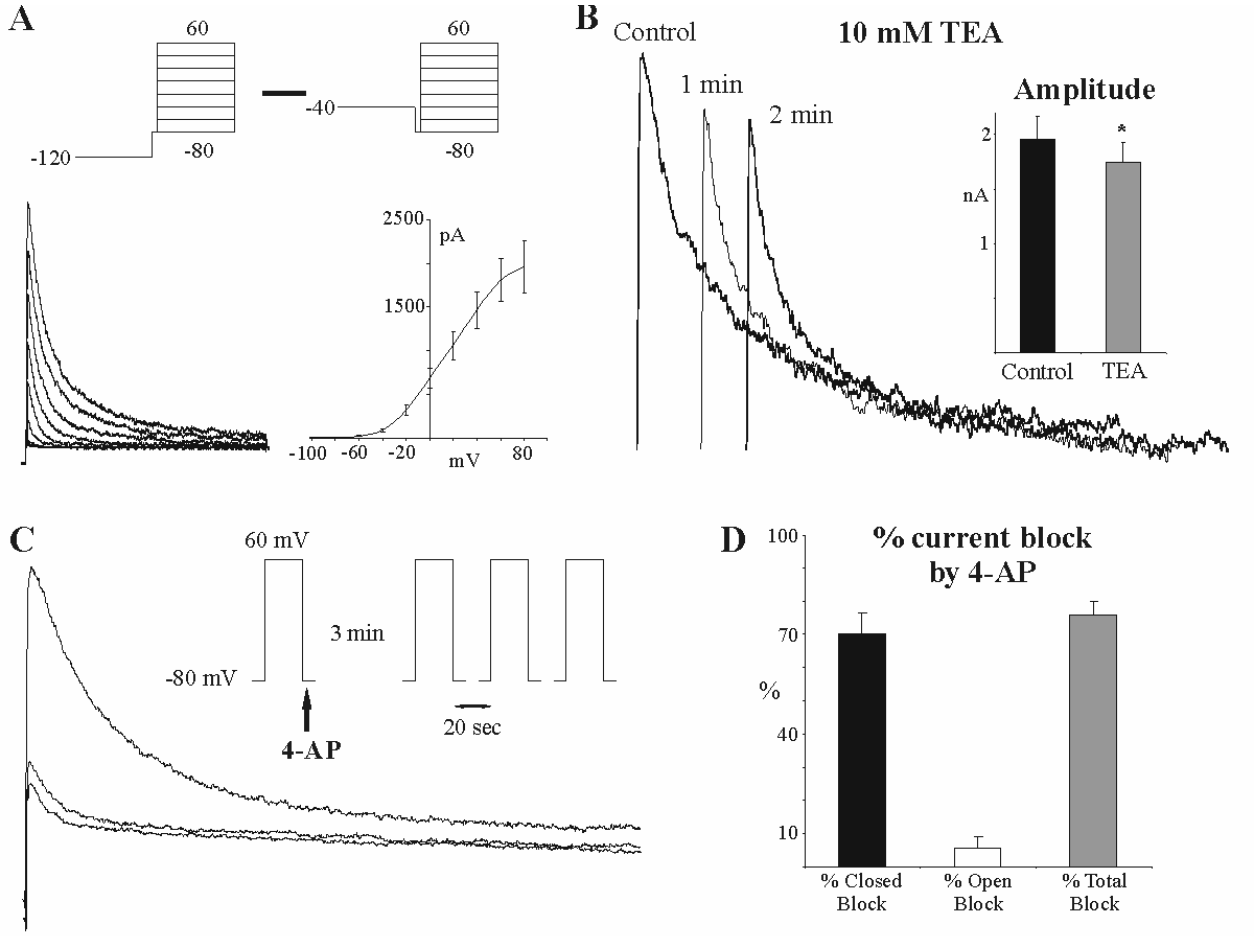

Figure 3.1. Pharmacological breakdown of inactivating A-type currents in cultured hippocampal astrocytes. A) Example of voltage isolated current pattern with average IV relationship using the subtraction protocol illustrated. B) Perfusion with 10 mM TEA resulted in an ~10% block of voltage isolated A-current at +60 mV. C) 4 mM 4-AP state-dependent block was subsequently determined in the presence of 10 mM TEA. An average of 3 traces for comparison were taken prior to 3 minutes of 4-AP perfusion with ensuing traces representing closed and open state block, respectively (see voltage protocol illustrated). D) Percentage of inactivating A-current blocked by 4-AP application as illustrated in C.

complete inactivation within the 500 ms voltage jumps (Fig. 3.1A). The impact of TEA on these isolated A-type currents was evaluated using the voltage subtraction protocol with a voltage jump from -80 to +60 mV repeated every 20 seconds. Perfusion with 10 mM TEA resulted in a 10 ± 2.5% steady-state block of A-current amplitude (Fig. 3.1B; n = 22). Although TEA is largely used as a blocker of delayed rectifying Kv channels, Kv3 (*Shaw*) family subunits display a high sensitivity to block by TEA, making it, under the voltage subtraction protocol used, a selective antagonist for Kv3.3 or Kv3.4 inactivating A-type channels (Riazanski et al. 2001; Fernandez et al. 2003). Subsequent pharmacological sensitivity to channel state-dependent 4-AP block was used to discriminate Kv4 family A-currents from those of Kv1, as 4-AP binds to Kv4 channels in the closed state and Kv1 in the open state (Tseng 1999). Voltage jumps from -80 to +60 mV were used as illustrated in Figure 3.1C. The A-current amplitude immediately following 3 minutes of 4-AP perfusion was determined as closed-state block with the subsequent maximum block upon additional voltage jumps representing open-state block. As this protocol was performed in the presence of 10 mM TEA, application of 4 mM 4-AP demonstrated an additional

70 ± 6.1% closed-state block and a 5.6 ± 3.6% open-state block, representing a total 4-AP block of 76 ± 4.3% (Fig. 3.1D; n = 9). These results are consistent with the majority of the TEA-insensitive A-current being made up of Kv4 family subunits. The small open state block observed may suggest a Kv1 family contribution consisting of Kv1.4 or other Kv1α subunits with Kvβ-subunits. Additionally, the small open-state block may be a result of insufficient perfusion with 4-AP in this particular experimental design; this possibility was not further explored.

Additional pharmacological studies using the nonhydrolyzable analog of arachidonic acid eicosotetraynoic acid (ETYA; 10 μM) confirm that Kv4 family channels are the dominant A-current. Furthermore, ETYA pharmacology demonstrates the functional presence of a calcium sensitive potassium channel interacting protein (KChIP; Fig. 3.2). Arachidonic acid (AA; as well as ETYA) has been shown to be a potent, selective inhibitor of Kv4 (*Shal*) family subunits (~50% in *Xenopus* oocytes and CHO cells; Villarroel and Schwarz 1996 and Holmqvist et al. 2001, respectively). In addition, KChIP modification of the rate of Kv4 channel inactivation is also disrupted by AA (Holmqvist et al. 2001). ETYA was used because AA metabolites are known to have many downstream effects in astrocytes (Harder et al. 1998; Gnatenco et al. 2002; Ferroni et al. 2003). To avoid dilution of ETYA-mediated Kv4 effects with contaminating ETYA insensitive Kv3.3/3.4 currents, these studies were conducted in the presence of 10 mM TEA and the voltage subtraction method was utilized as in Figure 3.1A. Application of 10 μM ETYA resulted in a 38 ± 3.9% block in amplitude from 1.32 ± 0.26 nA to 0.83 ± 0.20 nA (n = 7; Fig. 3.2), demonstrating again a Kv4 family specific effect in astrocytes. Interestingly, when normalized to control traces (Fig. 3.2A inset), ETYA also showed a significant 37 ± 7.0% decrease in the time constant (tau) of inactivation from 31 ± 4.5 to 18 ± 1.9 ms (Fig. 3.2B), consistent with effects on Kv4/KChIP complexes (Holmqvist et al. 2001).

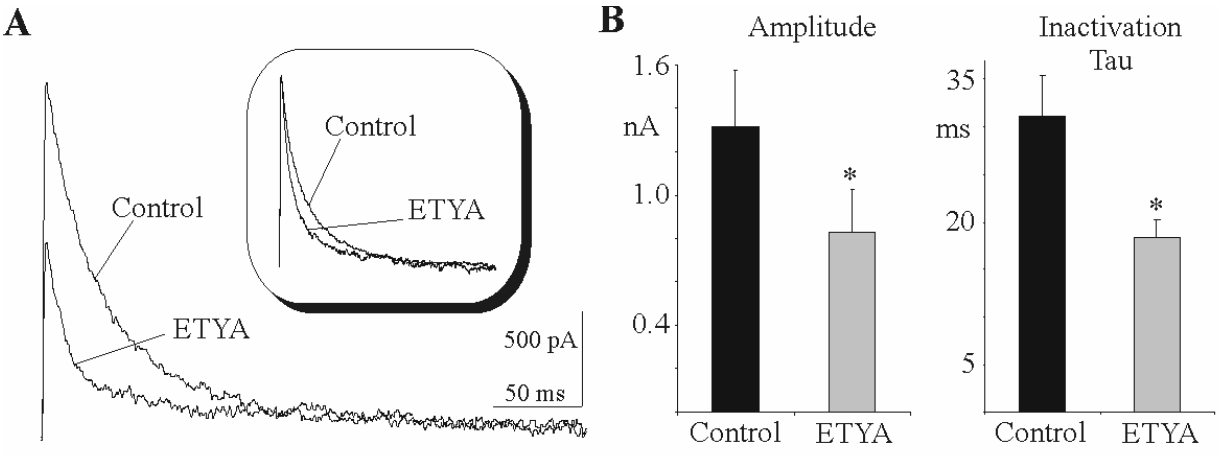

Figure 3.2. Effect of the arachidonic acid analog ETYA on astrocytic A-currents. A) Voltage jump protocols identical to that in Fig. 3.1B demonstrate a sizeable ETYA block of outward A-type currents in astrocytes. Averaging (n = 7) and normalization of current traces in the presence and absence of ETYA also demonstrates an additional affect on rate of inactivation (inset). B) Comparison of both amplitude and inactivation rates in presence and absence of ETYA. * indicates $P < 0.05$.

3.2 Complex astrocytic A-type kinetics are consistent with Shal (Kv4) subfamily expression

Astrocytic current patterns were compared to current patterns of Kv1.4 and Kv4.2 expressed in HEK293 cells in order to help clarify the Kvα subunits involved in the astrocytic A-type inactivating current pattern (Fig. 3.3). A-type inactivating outward K^+ currents make up 73

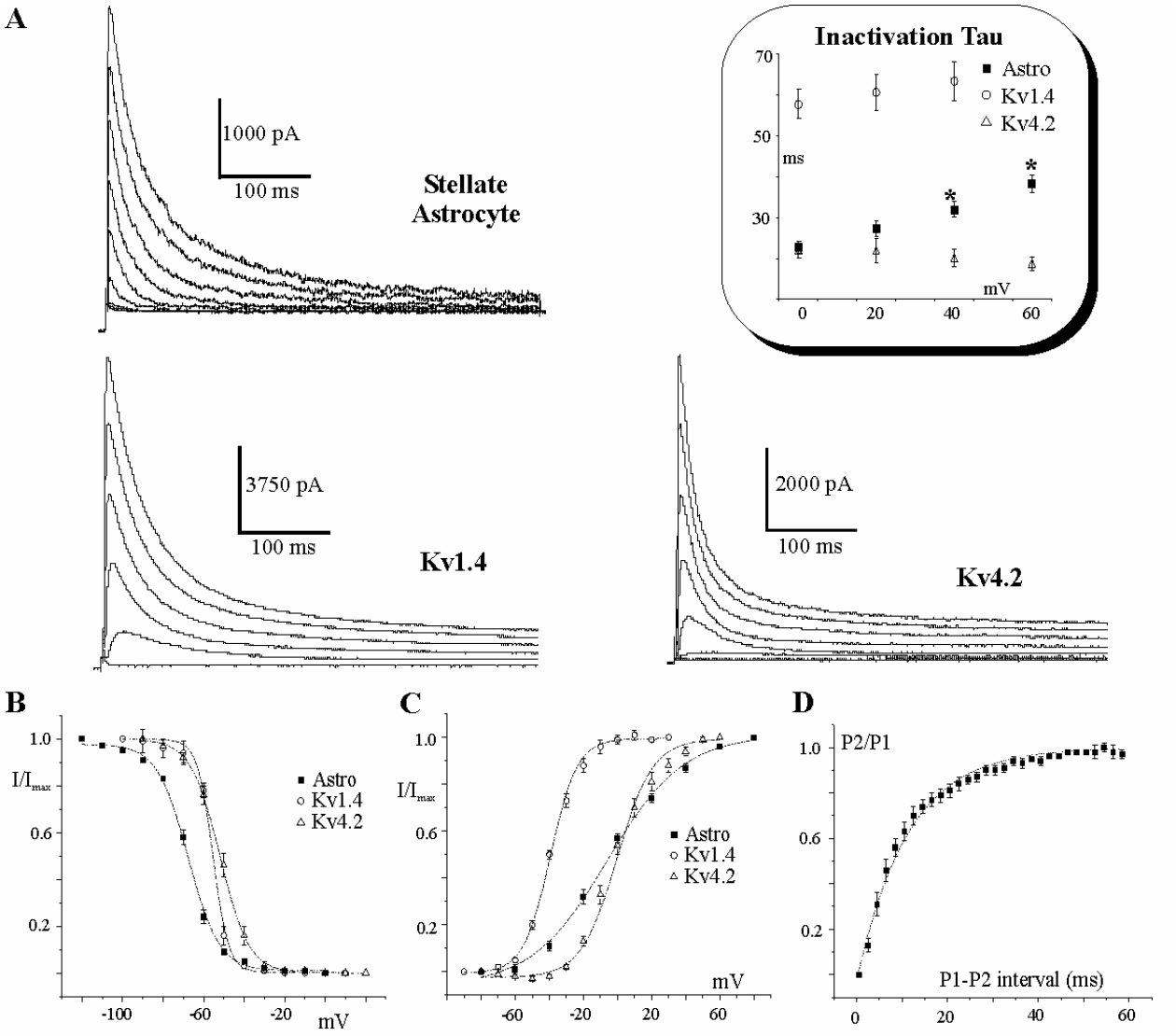

Figure 3.3. Comparison of astrocytic A-current kinetics with Kv1.4 and Kv4.2 currents expressed in HEK293 cells. A) Whole cell current patterns of inactivating A-type currents for comparison of rates of inactivation. Astrocyte currents were derived using the subtraction of voltage jump protocols illustrated in Fig. 3.1A. Inactivation tau is plotted versus voltage for comparison of the three different current patterns (inset). B) Steady-state inactivation kinetics. C) Steady-state activation kinetics and D) Reactivation kinetics. Note the rapid reactivation kinetics. Kv1.4 reactivation was greater than 2000X slower and so was not plotted on graph. * indicates $P < 0.05$.

± 0.9 % (n=19) of total outward current in astrocytes as determined using a subtraction protocol based on voltage inactivation properties of A-type inactivating currents. The isolated A-type current kinetics were then compared to inactivating currents expressed in HEK cells (Fig. 3.3). Astrocytes and HEK cells expressing either Kv1.4 or Kv4.2 demonstrated sizeable rapidly inactivating current patterns (Fig. 3.3A). The rate of current inactivation was fit to single exponential curves and inactivation rate constants (tau) were plotted at multiple voltages for comparison (Fig. 3.3A inset). Astrocytic inactivation rates most closely resemble that of the rate of Kv4.2 inactivation. Kv1.4 inactivation rates were almost twice that of astrocytes. Although inactivation rates resemble those of Kv4.2 in HEK cells, astrocytic inactivation demonstrates a decrease in rate at more depolarized potentials. This departure from Kv4.2 kinetics may be due to additional A-type channel involvement, but is also consistent with the possible involvement of

additional cytoplasmic accessory subunits (An et al. 2000; Holmqvist et al. 2002), such as that illustrated earlier in astrocytes by ETYA pharmacology.

Comparison of steady-state channel kinetics also provides support for astrocytic currents being comprised of Kv4 family inactivating α-subunits. Steady-state inactivation kinetics show astrocytes (n = 21) to have a more hyperpolarized half inactivation point than both Kv1.4 (n = 5) and Kv4.2 (n = 9) in HEK cells (-67.79 ± 0.97, -54.99 ± 0.88 and -51.25 ± 1.38, respectively; Fig. 3.3B). However, the Kv4.2 slope width is the same as that of astrocytes (6.90 ± 0.60 vs. 6.58 ± 0.27) while Kv1.4 shows a significantly steeper slope (3.84 ± 0.54; Fig. 3.3B). Considering KChIP subunits had a dramatic ~40 mV hyperpolarizing effect on Kv4.2 channel steady-state activation expressed in CHO cells (An et al. 2000) and an ~9 mV hyperpolarizing shift on steady-state inactivation but not activation in HEK cells (Van Hoorick et al. 2003), it is possible, once again, that the hyperpolarizing shift in astrocytic steady-state inactivation compared to Kv4.2 in HEK cells is a result of accessory subunit expression. Astrocytic activation kinetics demonstrate a slope width significantly longer than kinetics in HEK cells (20.17 ± 0.93, 9.67 ± 1.07 and 12.09 ± 0.66 for astrocytes, Kv1.4 and Kv4.2 respectively; Fig. 3.3C). However, astrocyte half activation (-1.83 ± 1.73; n = 37) shows a greater similarity to Kv4.2 (-1.27 ± 1.80; n = 10) than Kv1.4 (-38.85 ±0.69; n = 16) (Fig. 3.3C). Astrocytic reactivation demonstrates the greatest similarity to the Kv4 subfamily because of their rapid reactivation kinetics. Reactivation kinetics for cultured astrocytes shows a time constant of 10.15 ± 1.07 ms (n = 8; Fig. 3.3D) compared to a much longer 2650 ms (n = 2) for Kv1.4 in HEK cells (data not shown). These reactivation kinetics are more rapid than findings by Van Hoorick et al. (2003) in HEK cells where Kv4.2 demonstrated recovery time constants of 242 ms alone, or half that with KChIP1a or KChIP1b. Taken together, although there are definite differences with comparison to Kv4.2 alone, astrocytic kinetics appear consistent with the possibility that inactivating currents are comprised of a combination of the three Kv4 subfamily members with additional cytoplasmic accessory subunits.

3.3 Lack of effect with redox reagents suggests Shal subfamily as dominant A-type channel in astrocytes

It is now widely known that many Kv channels are sensitive to oxidation (Ruppersberg et al. 1991; Vega-Saenz de Miera and Rudy 1992; Rettig et al. 1994; Duprat et al. 1995; Stephens et al. 1996; Tanaka et al. 1998; Ciorba et al. 1999). This phenomenon is thought to be central to atherogenesis and development of hypertension as free radicals are heavily involved in the development of these pathologies. Many inactivating Kv channels possess cysteine residues on the cytoplasmic N-terminal (Fig. 3.4A). The sulfhydryl group of this cysteine has been shown to form a disulfide bridge with a sulfhydryl group located elsewhere on the protein under oxidizing conditions, effectively anchoring the N-terminal and altering N-type ('ball and chain') rapid inactivation kinetics (Ruppersberg et al. 1991; Rettig et al. 1994; Stephens et al. 1996; Fig. 3.4B). This phenomenon can be exploited to aid in determination of functional inactivating Kvα-subunits as, although the *Shaker* (Kv1) and *Shaw* (Kv3) subfamilies contain an oxidizable N-terminal cystine, the *Shal* (Kv4) subfamily does not (Fig. 3.4A). In fact, rapid inactivation of *Shal* subfamily members is a result of residues surrounding the pore region (Jerng and Covarrubias 1997; Jerng et al. 1999) rather than the N-terminal 'ball and chain' type. With the use of either chloramine-T or tBHP for oxidizing the sulfhydryl groups no significant effect on inactivation rate was found (Fig. 3.4C), however there was a small effect on amplitude. Interestingly, chloramine-T decreased the amplitude whereas tBHP increased it (Fig. 3.4C and D,

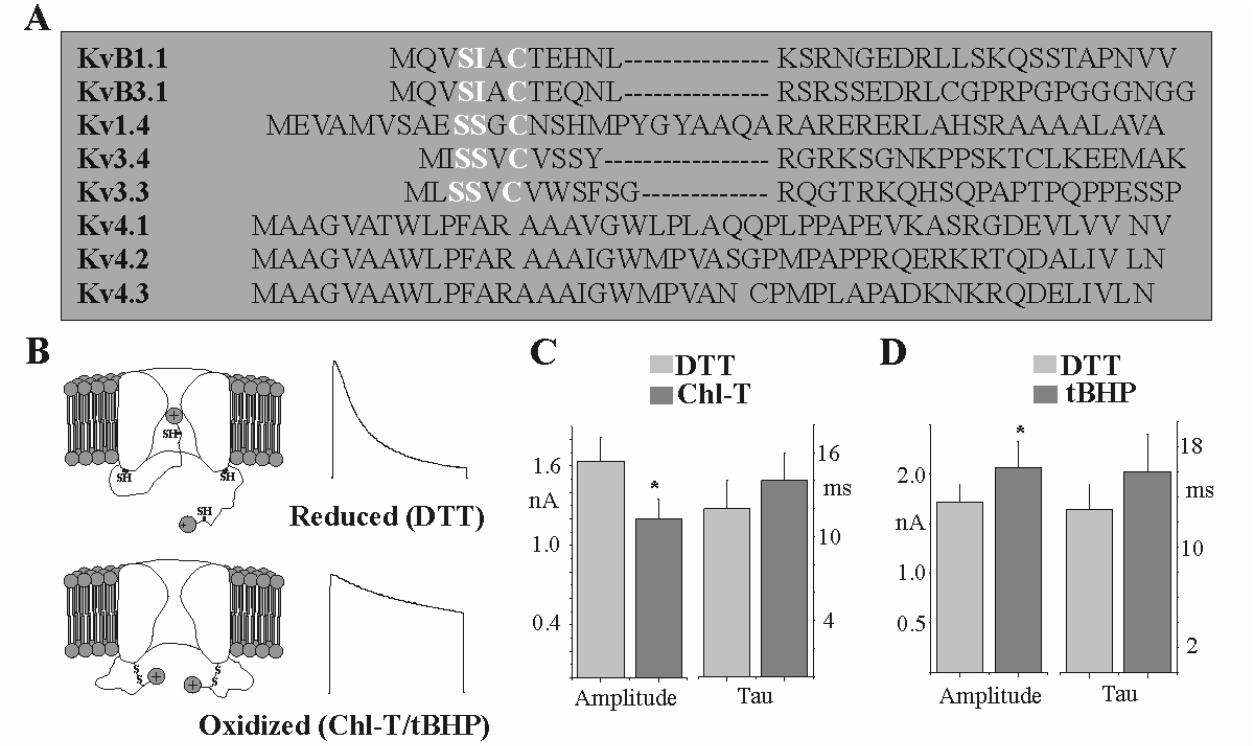

Figure 3.4. Oxidizing agents can be used to aid identification of gene families behind A-current expression in astrocytes. A) Protein sequence alignments of the N-terminal regions of the different alpha- and beta-subunits able to confer rapid 'ball and chain' N-type inactivation. B) Schematic correlating sulfhydryl (SH) redox state with Kv1.4 channel time-dependent inactivation in HEK293 cells. C) and D) Comparison of both amplitude and inactivation tau of astrocytic A-currents in the presence of the reducing agent dithiothreitol (DTT) with that in the presence of the oxidizing agent chloramine-T (Chl-T; C) or tert-butyl hydrogen peroxide (tBHP; D). * means $P < 0.05$

respectively). These effects on amplitude may be a result of oxidizable residues located near the pore region (Schlief et al. 1996). In contrast, the oxidizing agents had a dramatic effect on the rate of inactivation of Kv1.4 expressed in HEK cells (see current traces in Fig. 3.4B).

3.4 Immunocytochemistry and RT-PCR support astrocytic Kv channel pharmacology and kinetics

Due to pharmacological determination of expression for several A-type inactivating channel subunits and the interesting finding that A-current kinetics in astrocytes are more complicated then those of Kv4.2 expression alone in HEK cells, immunocytochemical and RT-PCR analysis was performed to provide additional insight into astrocytic A-current complexity. Glial fibrillary acidic protein positive, stellate astrocytes in culture were probed using specific antibodies for a single member from each of the three Kv channel subfamilies. Expression patterns demonstrate site-specific targeting with Kv3.4 localized primarily to cell processes and Kv4.3 channels showing intense staining throughout both cell soma and processes (Fig. 3.5A and B, respectively). The observation that Kv4.3 immunostaining is dominant in the cell soma is consistent with whole-cell patch-clamp kinetics and pharmacology in this study. Kv1.4 immunostaining could only be discriminated from background levels with extremely long exposures, suggesting minimal to no expression (Fig. 3.6A-C). As a positive control, however,

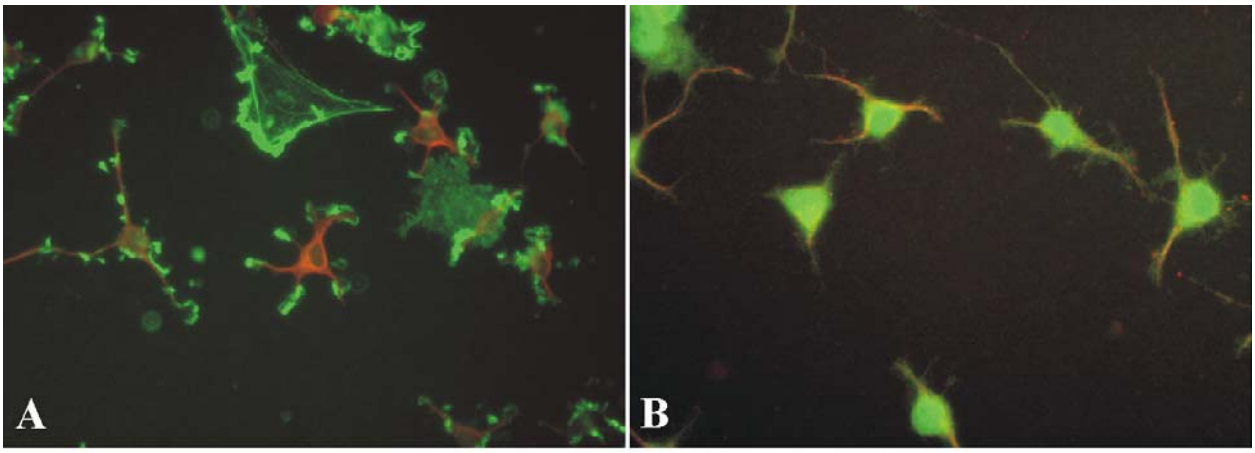

Figure 3.5. Immunocytochemical evaluation of *Shaw* and *Shal* Kv channels in stellate GFAP$^+$ cultured astrocytes. A) The *Shaw* Kv3.4 subunit (green) labels GFAP$^+$ (red) cell processes and demonstrates a punctuate staining pattern suggesting cytoskeletal localization. B) The *Shal* Kv4.3 subunit (green) labels GFAP$^+$ (red) cell bodies intensely with more diffuse staining in the processes.

prominent Kv1.4 staining could be obtained in transiently transfected HEK293 cells (Fig. 3.6D-F).

RT-PCR analysis was also used to examine expression of the Kv channel subunits from the three Kv channel subfamilies. As the *Shal* subfamily appears to dominate whole-cell A-type current patterns, Kv4.1-4.3 and the potassium channel interacting proteins (KChIPs) known to interact with *Shal* subfamily members were examined (Fig. 3.7A). Hippocampal astrocyte cultures (>95% GFAP-positive) demonstrated prominent mRNA for the three *Shal* family members as well as multiple splice variants of the different accessory KChIPs (Fig. 3.7A) known to affect Kv4 channel expression and kinetics (An et al. 2000; Takimoto et al. 2002; Morohashi et al. 2002; Holmqvist et al. 2002). Screening for the two members Kv3.3 and Kv3.4 from the

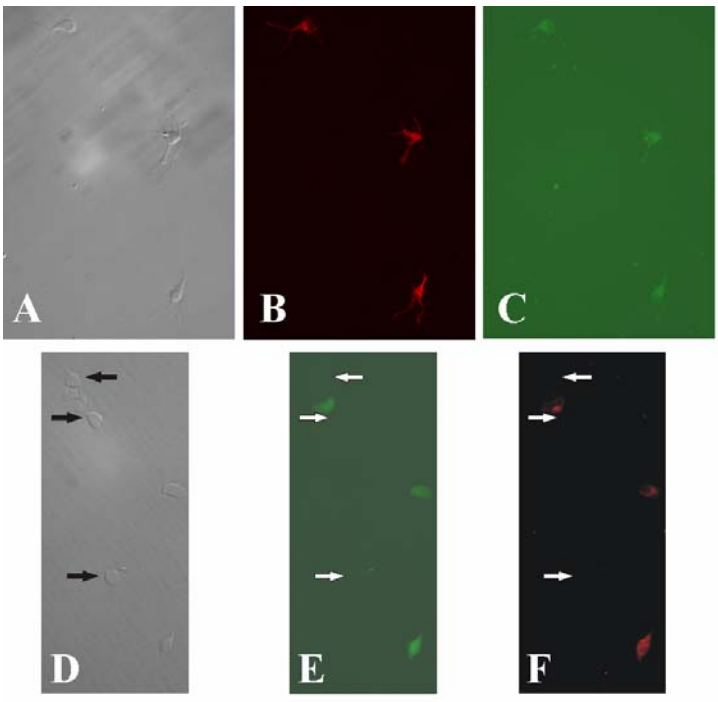

Figure 3.6. Kv1.4 immunostaining in cultured hippocampal astrocytes. A) DIC image of astrocytes in culture. B) GFAP and C) Kv1.4 fluorescence. Kv1.4 could only be detected under exposures 14X that of GFAP with additional image enhancement. D) DIC, E) GFP and F) Kv1.4 serve as the corresponding positive control in Kv1.4/GFP transfected HEK cells. Arrows denote untransfected Kv1.4 negative cells.

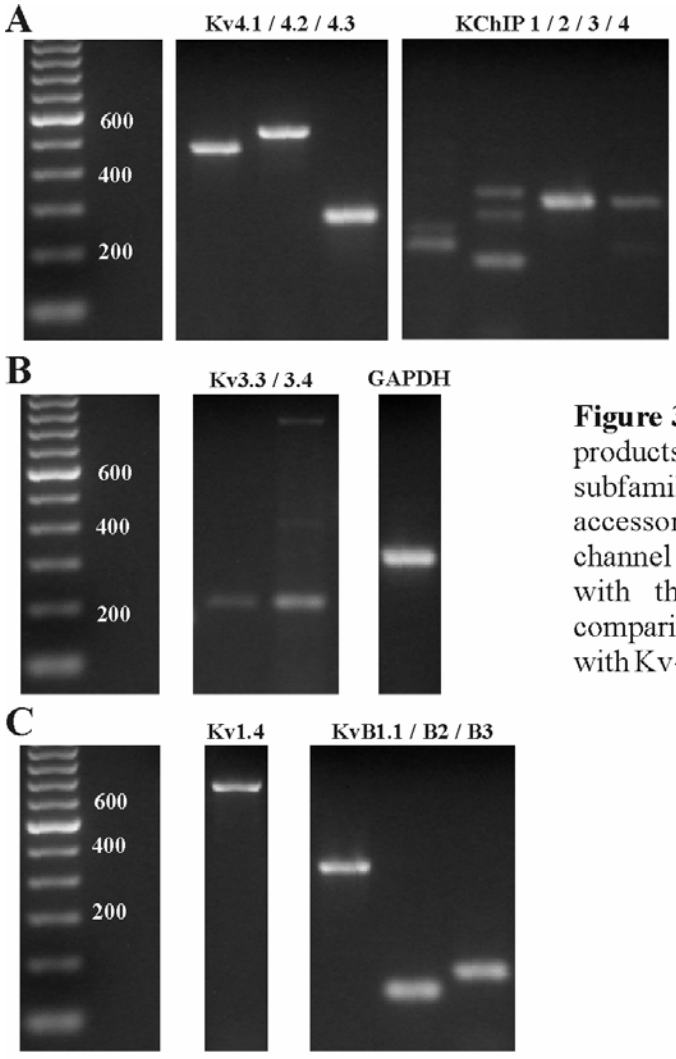

Figure 3.7. Hippocampal astrocyte RT-PCR mRNA products from 300 ng culture RNA. A) Kv4 *Shal* subfamily expression with potential cytoplasmic accessory subunits capable of modulating Kv4 channel kinetics. B) Kv3 *Shaw* subfamily expression with the ubiquitous cell enzyme GAPDH for comparison. C) Kv1 *Shaker* subfamily expression with Kv-alpha accessory subunit possibilities.

Shaw subfamily also proved successful (Fig. 3.7B), although with reduced intensity compared to *Shal* subfamily members and glyceraldehyde phosphate dehydrogenase used as a general cell marker for comparison (GAPDH; Fig. 3.7B right). Although immunocytochemical analysis did not provide significant evidence for the presence of Kv1.4, pharmacological data suggests ~5% of the A-currents may be due to *Shaker* related channel subunits. Therefore, expression of Kv1.4 from the Shaker family and the auxiliary β-subunit possibilities Kvβ1.1-1.3, Kvβ2.1 and Kvβ3.1 were examined as combinations of these α-subunits with β-subunits may constitute rapidly inactivating channels (Pongs et al. 1999; Heinemann et al. 1996; Manganas and Trimmer 2000). Interestingly, mRNA for Kv1.4 was found in these hippocampal cultures (Fig. 3.7C). In addition, the β-subunits Kvβ1.1, 2, and 3, but not Kvβ1.2 or 1.3 (not shown) were also found (Fig. 3.7C right). The β-subunits 1.1 and 3.1 are able to confer rapid inactivation onto several of the Kvα-subunits (Kwak et al. 1999a, b; Rettig et al. 1994), whereas the Kvβ2.1 appears to primarily regulate expression of channels at the membrane surface (Manganas and Trimmer 2000; Peri et al. 2001; Shi et al. 1996); although it has been shown to alter the activation and inactivation properties of the Kvα1.4 channel subunit (McCormack et al. 1995).

3.5 A-current kinetics are modulated by culture growth conditions

The most typical growth conditions used for primary culture of astrocytes consists of using 10% fetal bovine/calf serum (FBS/FCS) or 10% horse serum (HS) with DMEM. As FBS comes from developing fetuses and HS from mature adult horses, it seems reasonable to assume these sera contain differing levels of growth factors and/or cytokines that can influence proliferation and maturation processes. Consistent with this, it has been previously demonstrated that with use of the differing sera, astrocytic cell cultures can be manipulated to contain differing numbers of glial progenitor colonies following initial seeding (Federoff and Hall 1979), leading to substantially different confluent culture characteristics. With this in mind, whole-cell current patterns were compared under both FBS and HS growth conditions to address possible differences related to growth factor composition. Although no data was collected demonstrating cell culture growth rates in the two different sera, it is worth noting that cells grown in FBS typically reached confluence 2 days earlier than HS treated cells in sister cultures. Comparison of whole-cell voltage-isolated A-currents under the two culture conditions demonstrates that growth medium can lead to significantly different current patterns (Fig. 3.8). Astrocytes grown in 10% HS demonstrate significantly larger and more rapidly inactivating A-currents than cells grown in FBS (Fig. 3.8A and B, respectively). Interestingly, non-inactivating delayed rectifying (dr) currents (133 ± 16 vs. 138 ± 9 pA/pF; HS and FBS, respectively) and total outward potassium currents (334 ± 30 vs. 272 ± 21 pA/pF; HS and FBS, respectively) were not significantly different. The fact that the A-currents represent a larger percentage of total currents

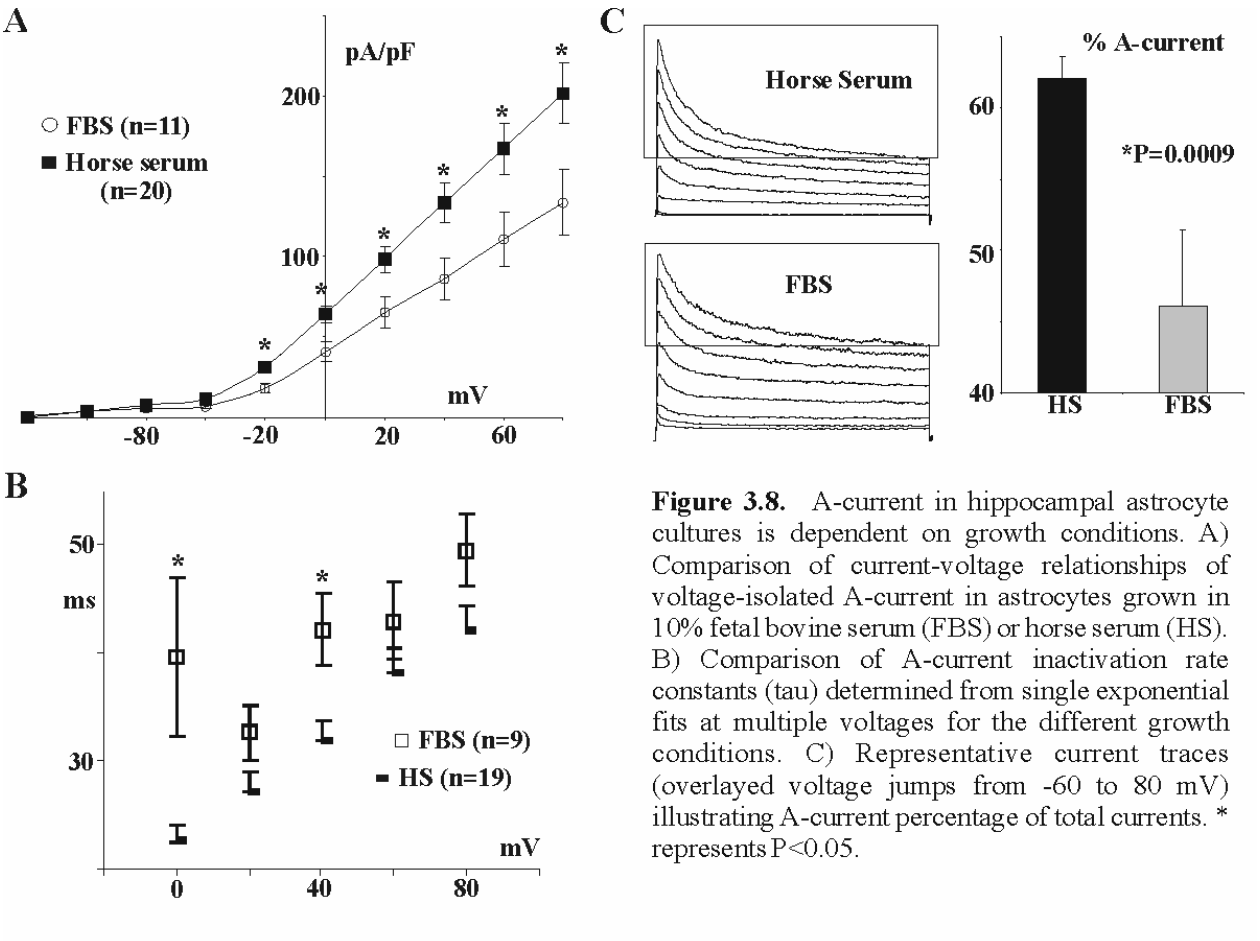

Figure 3.8. A-current in hippocampal astrocyte cultures is dependent on growth conditions. A) Comparison of current-voltage relationships of voltage-isolated A-current in astrocytes grown in 10% fetal bovine serum (FBS) or horse serum (HS). B) Comparison of A-current inactivation rate constants (tau) determined from single exponential fits at multiple voltages for the different growth conditions. C) Representative current traces (overlayed voltage jumps from -60 to 80 mV) illustrating A-current percentage of total currents. * represents $P<0.05$.

in HS treated cells than FBS treated cells (Fig. 3.8C) may be accounted for by the trend for total currents in horse serum to be larger than those in FBS. With only the A-current showing significantly different amplitudes and time-dependent kinetics, mRNA for possible subunits comprising A-currents were assessed under both growth conditions.

Modulation of potassium channel interacting protein (KChIP) mRNA expression is consistent with observed whole-cell current pattern differences under FBS or HS growth conditions. Qualitative analysis of mRNA expression of the different subunits known to result in A-currents under the different growth conditions did not demonstrate major differences (Fig. 3.9A). However, closer scrutiny demonstrates the lack of expression of the specific splice variants of KChIP1b and KChIP4a under FBS growth conditions (Fig. 3.9B). Although this finding would be much better assessed using single-cell quantitative PCR to correlate current pattern with mRNA expression, these findings are consistent with KChIP modulation of A-current amplitude and time-dependent kinetics (An et al. 2000; Holmqvist et al. 2001; Beck et al. 2002). Furthermore, in support of an accessory subunit difference being responsible for the difference in amplitudes and kinetics, 4-AP sensitive current was not significantly different under the two culture conditions (data not shown). As 4-AP acts on the channel pore, it represents corresponding density of α-subunits and demonstrates Kvα-subunit expression is not different, reinforcing the notion that the differences in current under the different culture conditions are likely due to accessory KChIP subunits.

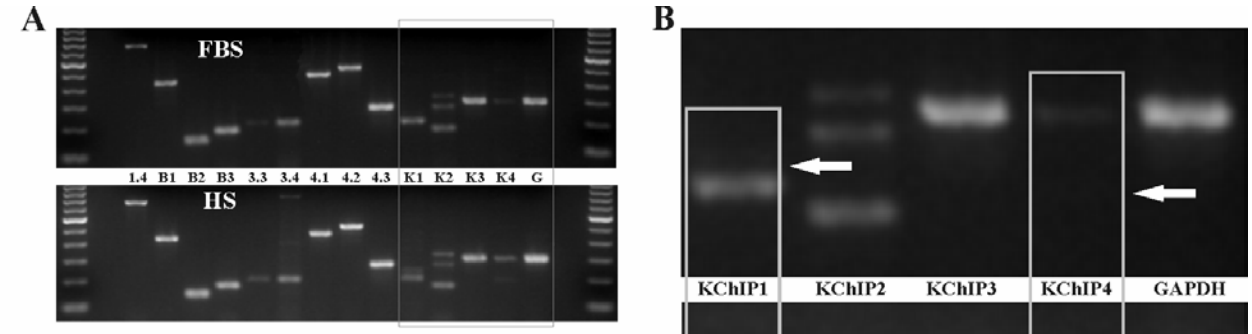

Figure 3.9. Hippocampal astrocyte RT-PCR mRNA products under FBS and HS culture conditions. A) Comparison of mRNA products of all alpha and beta subunits involved in A-current makeup. B) Magnification of the potassium channel interacting protein (KChIP) mRNA for closer inspection. Note the absence of KChIP1b and 4a (Arrows; see table 2.1 for band sizes) under FBS growth conditions. B - betasubunit; G- glyceraldehyde phosphate dehydrogenase (GAPDH); K- KChIP.

3.6 Summary and Discussion

This study is the first to provide a detailed analysis of the molecular identity of astrocytic inactivating A-type K^+ channel subunit expression. Pharmacological analysis of whole-cell A-currents in astrocytes demonstrated that ~70%, 10% and less than 5% of total A-currents are associated with Kv4, Kv3 and Kv1 channels, respectively (Fig. 3.1). The remaining 15% may possibly be explained as an incomplete block by TEA and/or 4-AP. Oxidation/reduction studies of N-terminal mediated rapid inactivation kinetics provide additional support for minimal contribution by Kv1 family members. Furthermore, ETYA pharmacology and kinetic analysis

provides novel evidence for a significant contribution of KChIP accessory proteins in the complexity of astrocytic A-current make-up (Figs. 3.2 and 3.3, respectively). This breakdown of electrophysiological expression is consistent with the Kv4 family showing bright ubiquitous staining in immunocytochemistry experiments (Fig. 3.5A) and the densest bands in PCR (Fig. 3.7A). The small contribution to inactivating A-currents by members of the Kv3 family is perhaps a result of targeted expression to astrocytic processes, where contribution to whole cell currents would be limited due to space clamp control issues (Fig. 3.5B). The targeted expression of specific A-channel subunits does, however, suggest that these channels serve a specific function. Additionally, modulation of A-current amplitude and kinetics (Fig. 3.8), possibly through expression of different KChIPs (Fig. 3.9), by different growth media also suggests a specific function for these channels in cell processes.

4.0 - ASTROCYTIC A-TYPE CHANNELS AND RAPID REPOLARIZATION

Although astrocytes have now been demonstrated to express multiple types of inactivating Kv channels as well as specifically target different Kv subfamily members to specific subcellular compartments, it is still not clear what role inactivating channels play in normal physiological function. Since astrocytes are known to be subjected to neuronal firing frequencies of up to 200 Hz in the stratum radiatum of the CA1 subfield of the hippocampus (Staba et al. 2002; Klausberger et al. 2003, 2004; Kunec and Bose 2003; Ponomarenko et al. 2003), high frequency trains of 0.5 ms current injections were used to assess whether A-type channels in astrocytes affect the rate of membrane repolarization similar to that of A-channels in neurons and cardiomyocytes. Furthermore, GABA and glutamate receptor-mediated membrane responses were assessed to help provide a physiological link to A-current function. Finally, a functional scenario is outlined.

4.1 Current-clamp studies suggest A-currents may limit membrane depolarization in response to high frequency membrane potential oscillations in astrocytes

Current injection studies show a distinct role for A-currents in shaping the repolarizing phase of the membrane voltage waveform (Fig. 4.1; Bordey and Sontheimer 1999). Consistent with previous studies, whole-cell current clamp evaluation of 20 ms 400 pA current injections demonstrate astrocytes have the ability to spike (Fig. 4.1; Sontheimer et al. 1992; Bordey and Sontheimer 1998a, b, 1999). Pharmacological analysis demonstrates that TEA sensitive K^+ currents impact the afterhyperpolarizations (AHP) but not the width of the waveform (Fig. 4.1A), whereas 4-AP has a dramatic effect on the width (Fig. 4.1B). This effect can be seen more clearly in the same cells as Figure 4.1A and B, but with a very short current injection allowing the spike to repolarize back to cell resting potential completely on its own (Fig. 4.1C and D, respectively). The slash marks on the depolarizing phase of Figure 4.1C and D indicate the time point at which the membrane was clamped back to 0 current, allowing visualization of spiking behavior. Application of 10 mM TEA, although causing a slight increase in amplitude, does not affect the repolarizing phase back to resting potential (Fig. 4.1C). On the other hand, 4 mM 4-AP clearly prolongs the repolarization phase back to resting potential (Fig. 4.1D). It is interesting to note the tracings in Figure 4.1C and D do not show AHPs compared to traces from the same cells in A and B, respectively. This is likely a result of the astrocyte resting membrane potential being highly negative close to the equilibrium potential of K^+. In support of this possibility, cells with a slightly depolarized resting potential (-40 to -47 mV; n = 5) always displayed an AHP with similar current injection to that shown in Figure 4.1C and D (data not shown).

Astrocyte membrane potentials were followed under high frequency current injection conditions in order to evaluate their ability to maintain their resting membrane potential and to respond to individual stimuli. Hippocampal neurons have been shown to fire at frequencies of up to 200 Hz (Staba et al. 2002; Klausberger et al. 2003, 2004; Kunec and Bose 2003; Ponomarenko

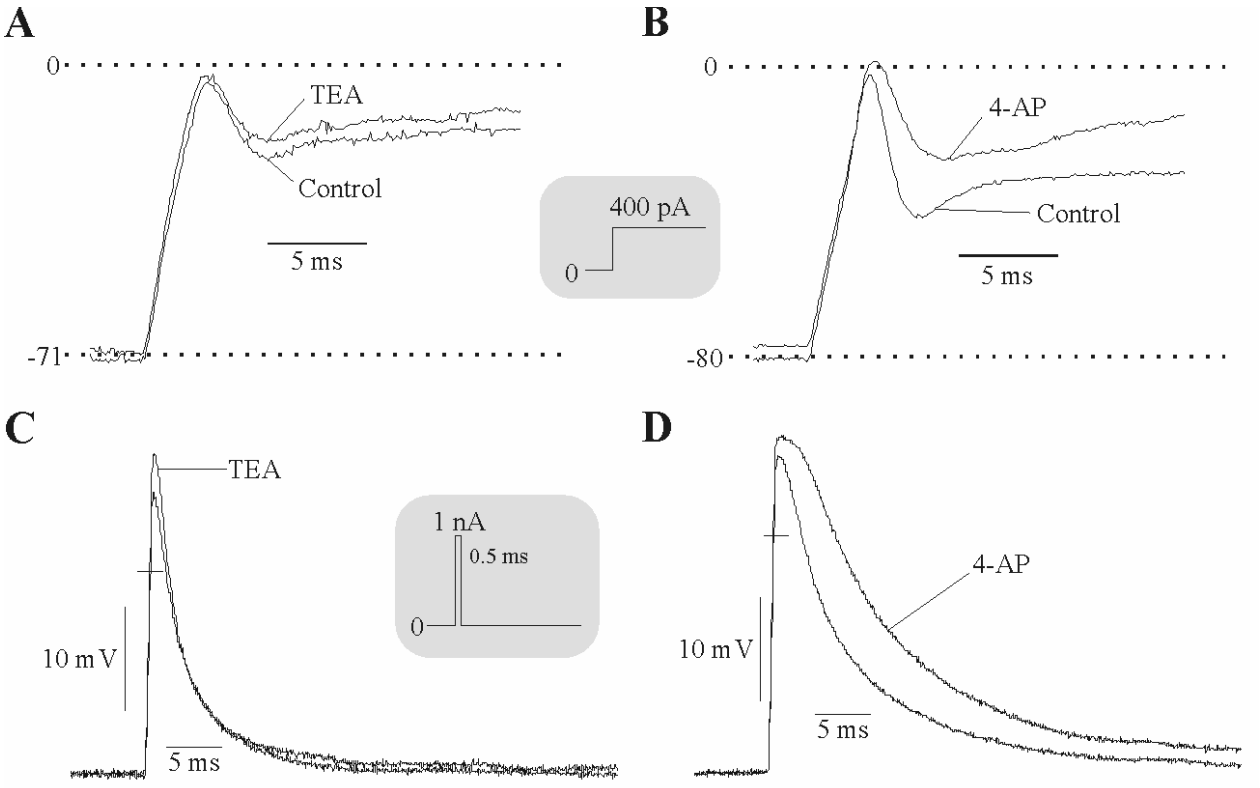

Figure 4.1. Pharmacological impact of TEA and 4-AP on depolarizing waveforms in response to current injections. A) and B) are examples of current clamp waveforms in response to the current injection pattern illustrated in shaded inset. C) and D) Modification of the current injection protocol (shaded inset) allowed unhindered demonstration of spiking and repolarization of the same astrocytes illustrated in A and B, respectively. The hash mark on the depolarizing phase of the waveform indicates the time point at which the current was clamped back to 0.

et al. 2003). Therefore, astrocytes under current-clamp control were subjected to current injections at 100 and 200 Hz before and after administration of either 10 mM TEA or 4 mM 4-AP to assess the roles of delayed and A-type current in membrane responses (Fig. 4.2). Aside from the small depolarizing effect of TEA on resting membrane potential (Fig. 4.2A), TEA did not appear to dramatically alter the astrocytes ability to respond to subsequent stimuli at high frequency as evident when the current traces are overlaid (Fig. 4.2A bottom). In contrast, 4-AP had a dramatic effect on frequency oscillations (Fig. 4.2B). The same prolongation of the repolarization phase seen in Figure 4.1B results in summation leading to a more rapid and sustained membrane depolarization without altering the amplitude of individual spikes (Fig. 4.2B bottom).

4.2 Do astrocytes experience membrane depolarizations capable of stimulating inactivating A-type currents?

The real question as to the role of A-currents in astrocytes is whether or not astrocytes ever experience membrane depolarizations that are both rapid and sizeable enough to activate these rapidly inactivating Kv currents. With astrocytic resting membrane potentials being highly negative (-80 to -95 mV; Ballanyi et al. 1987; Sontheimer and Waxman 1993; McKhann II et al.

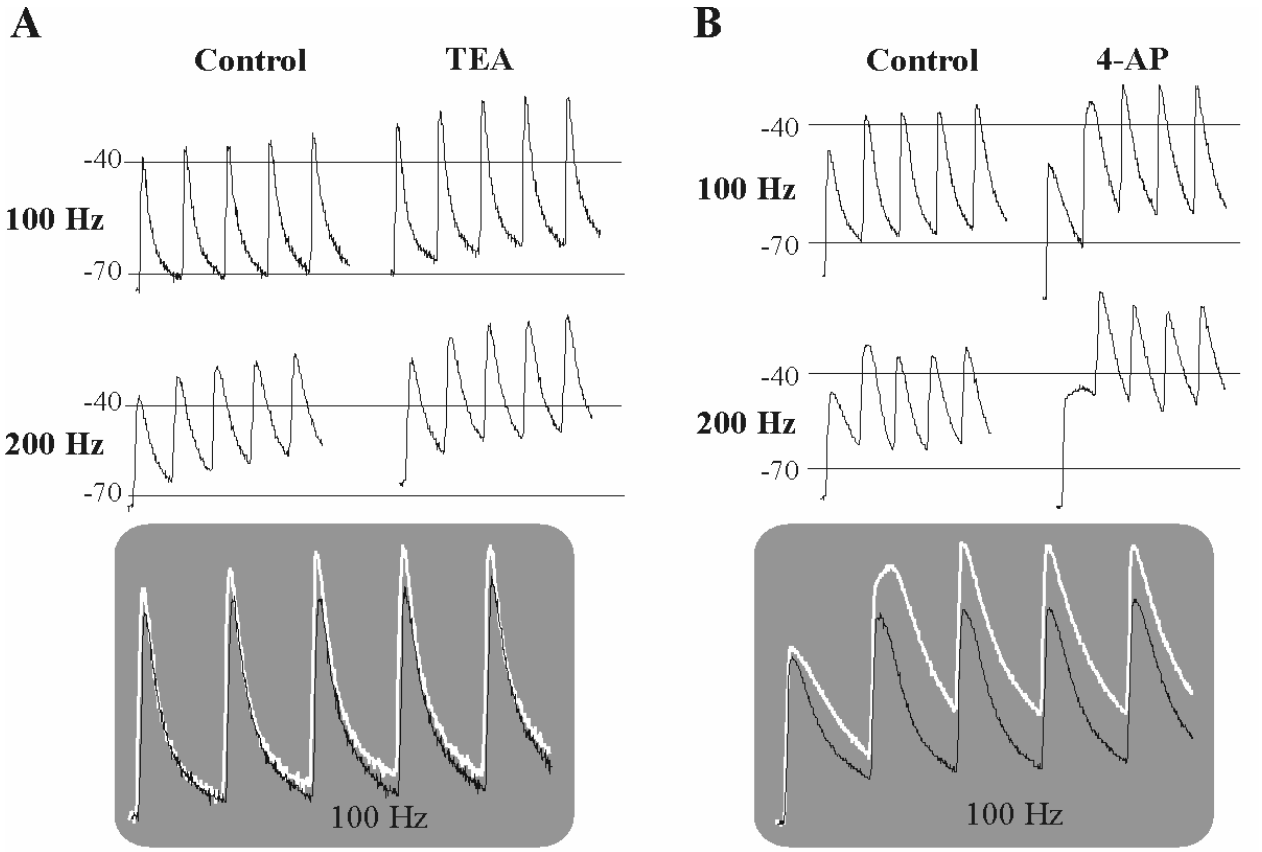

Figure 4.2. A-currents enable high frequency membrane voltage oscillations in astrocytes. The same two cells as illustrated in Fig. 4.1 were subjected to high frequency current injections like that in Fig. 4.1C and D. A) and B) Identical waveforms in the presence and absence of 10 mM TEA (A) or 4 mM 4-AP (B) are illustrated for comparison. The two waveforms in response to 100 Hz current injection were overlaid for more direct comparison of effect of pharmacological agent on waveform summation (bottom shaded inset).

1997) and the fact that astrocytes typically express both large inwardly and outwardly rectifying potassium channels, it is unlikely that membrane responses reach much beyond -20 mV. Based on A-current voltage kinetics, an action potential-like rapid depolarization that can depolarize the membrane to above 0 mV in a couple of milliseconds would be required to activate this current. This, indeed, is what happens with the neuronal action potential where A-currents play a significant role in rate of repolarization. The $GABA_A$ agonist muscimol was applied in an attempt to correlate membrane responses with an endogenous ligand (Fig. 4.3). Although the representative cell shown in Figure 4.3 had sizeable A-currents (shaded inset), the response to a short 5 ms pulse of muscimol resulted in a membrane oscillation that took longer than 5 seconds to repolarize to baseline levels (Fig. 4.3A) compared to the ultra rapid repolarization seen in response to current injections (Figs. 4.1 and 4.2). The repolarization following application of muscimol in these studies is most likely due to inwardly rectifying K^+ channels and Na^+/K^+ ATPase activity as the membrane potential only reached slightly above -40 mV, which is insufficient to activate significant outward Kv currents. However, it is worth noting the lack of the slow glial 'spike' with muscimol application compared to current injection (400 pA; Fig. 4.3A). The glial 'spike', therefore, may be the key to membrane potentials sufficient to activate A-currents for rapid repolarization. It is clear that muscimol in this study, as well as glutamate

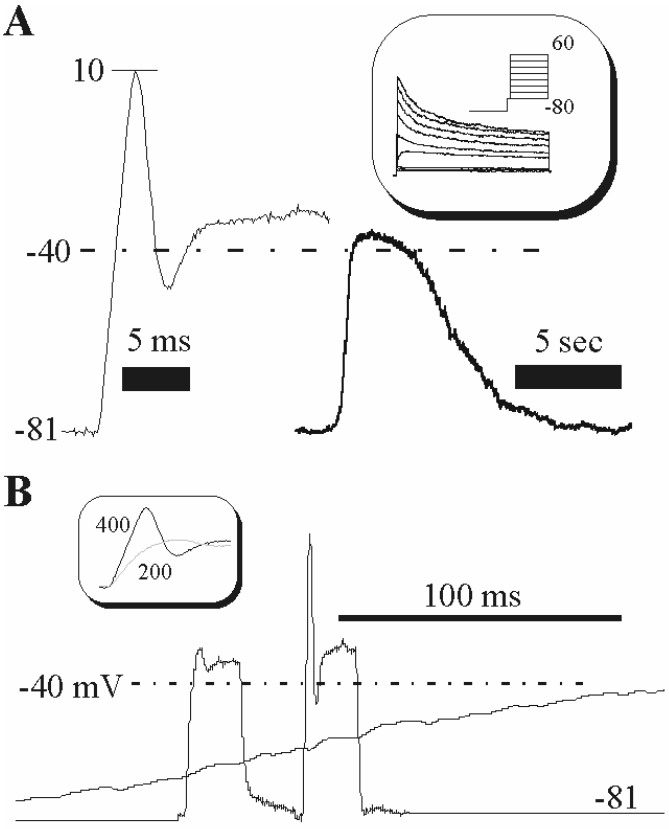

Figure 4.3. A representative cell demonstrating $GABA_A$ receptor-mediated membrane responses in cultured astrocytes. A) Comparison of a 20 ms 400 pA square current pulse with a 5 ms muscimol application in current-clamp mode. Voltage-clamped currents in response to a series of voltage jumps are illustrated in the shaded inset. Note the dramatically different time scale bars. B) Same voltage traces as in A, but displayed on the same time scale axis. The additional 200 pA current injection trace was added to help illustrate the importance of the rate of depolarization on the Na^+-mediated glial 'spike' under the culture conditions in this study.

and GABA agonists in other studies *in situ* (Jabs et al. 1994; Borges and Kettenman 1995; Seifert and Steinhauser 1995; Robert and Magistretti 1997; Bekar et al. 1999; Bekar and Walz 1999; Schroder et al. 2002) are able to activate large membrane conductances capable of reaching threshold for activation of glial Na^+ channels for 'spike' generation. However, responses in this study demonstrate that the rate of depolarization is crucial as the Na^+ channels (A-channels also) move into the inactivated state with slow depolarizations (Fig. 4.3A and B; note time scale). The lack of a rapid muscimol depolarization in this study is due to the time resolution of the perfusion system used. Many studies have achieved rapid receptor responses (Seifert and Steinhauser 1995; Matthias et al. 2003) that could be able to elicit 'spiking' with subsequent A-current rapid repolarization. Matthias et al. (2003), using a fast pneumatically controlled application system, achieved very rapid current responses to 1mM glutamate (Fig. 4.4 inset) better simulating synaptic-like events. Comparing this response with the muscimol voltage-clamped current response from the same cell used in Figure 4.3 (Fig. 4.4 left), it appears that one could expect involvement of the glial 'spike' in amplifying the depolarizing response to glutamate as well as enabling A-current (and delayed-current) mediated rapid repolarization. Thus, it appears that significant A-current activation may be dependent on the slow glial 'spike'. The question then becomes: Do astrocytes exhibit the action potential-like 'spike' under physiological conditions?

4.3 GABA and glutamate receptor responses in astrocytes may promote rapid depolarization with subsequent A-current activation.

GABA and glutamate are the two major endogenous neurotransmitters acting on astrocytes in the hippocampus. Interestingly, they both appear to lead to a secondary block of Kv currents mediated via changes in intracellular Na^+ and Cl^- for glutamate and GABA, respectively (Robert

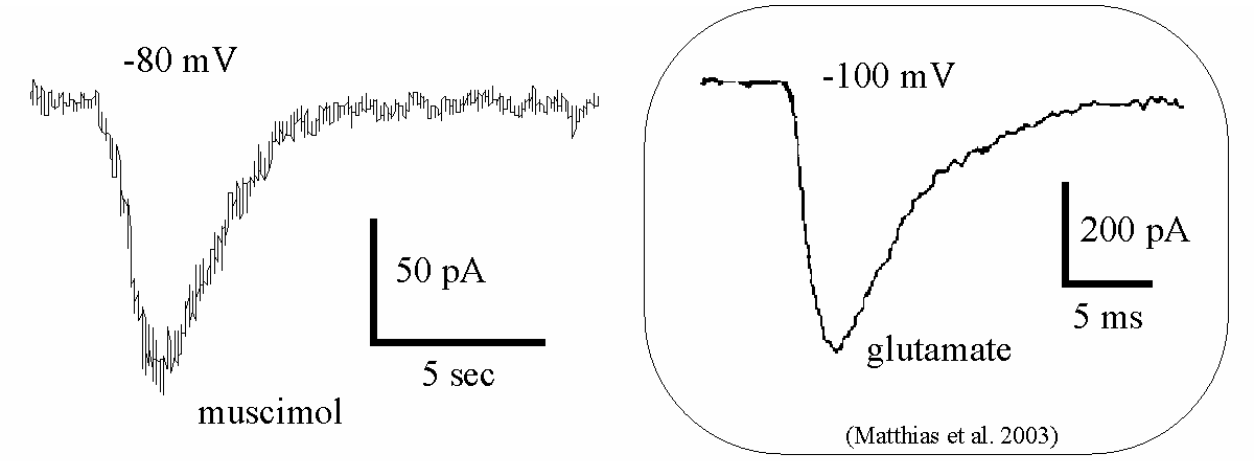

Figure 4.4. Comparison of a voltage-clamped current response to 200 uM muscimol (same cell as Fig 4.3) with a current response to 1 mM glutamate (inset; taken from Matthias et al. 2003). Note the differences in the time and amplitude scale bars.

and Magistretti, 1997; Bekar and Walz, 1999; Bekar et al. 1999). Examination of the respective receptor-mediated effects on the A-type and delayed-type outwardly rectifying potassium channels using a voltage isolation voltage-jump protocol (Fig. 4.5A) demonstrated a more selective block by the $GABA_A$ agonist muscimol of A-type conductance compared to the equal block of both outward conductances by the glutamate agonist kainate (Fig. 4.5). By comparing the percentage block of each of the A-type and delayed-type Kv currents normalized to the corresponding kainate or muscimol receptor current amplitudes, one can see that the kainate effect is more sensitive and indiscriminate compared to the more selective muscimol effect (Fig. 4.5D, E, F). As there is a differential block of the two major types of outward Kv currents, this may lead to radically different membrane responses under high frequency stimulation with the respective excitatory and inhibitory neurotransmitters.

4.4 Summary and Discussion

This study demonstrates a role for astrocytic A-current in repolarization of large membrane voltage oscillations, possibly allowing astrocytes to respond to high frequency synaptic-like events. However, it remains to be established whether astrocytes ever see membrane depolarizations large enough to activate these currents endogenously. The glial 'spike' phenomenon associated with astrocytes under various pathological and culture conditions is an enticing mechanism for speculation as to potential activation of these A-currents. To date however, this glial 'spike' has never been demonstrated under physiological conditions. Data presented in this study using cultured astrocytes suggest that in response to rapid glutamate or GABA receptor activation, it may be possible to elicit this action potential-like 'spike' activating A- and delayed-current repolarization (which we were unable to simulate in this study). The major hurdle to overcome is the lack of 'spiking' behavior found in adult astrocytes *in situ*. It is thought that the small Na^+/K^+ (0.1-0.3; Sontheimer et al. 1991; Sontheimer et al. 1994; Sontheimer 1994; Bordey and Sontheimer 1998a, b) ratio in astrocytes is responsible for this lack of 'excitability' given that blockade of potassium currents with 4-AP (Bordey and Sontheimer 1999) or low concentrations of Ba^+ (Bordey and Sontheimer 1998b) bring this ratio closer to 1 and, then, allow 'spiking' behavior. Interestingly, this and other studies demonstrate both GABA

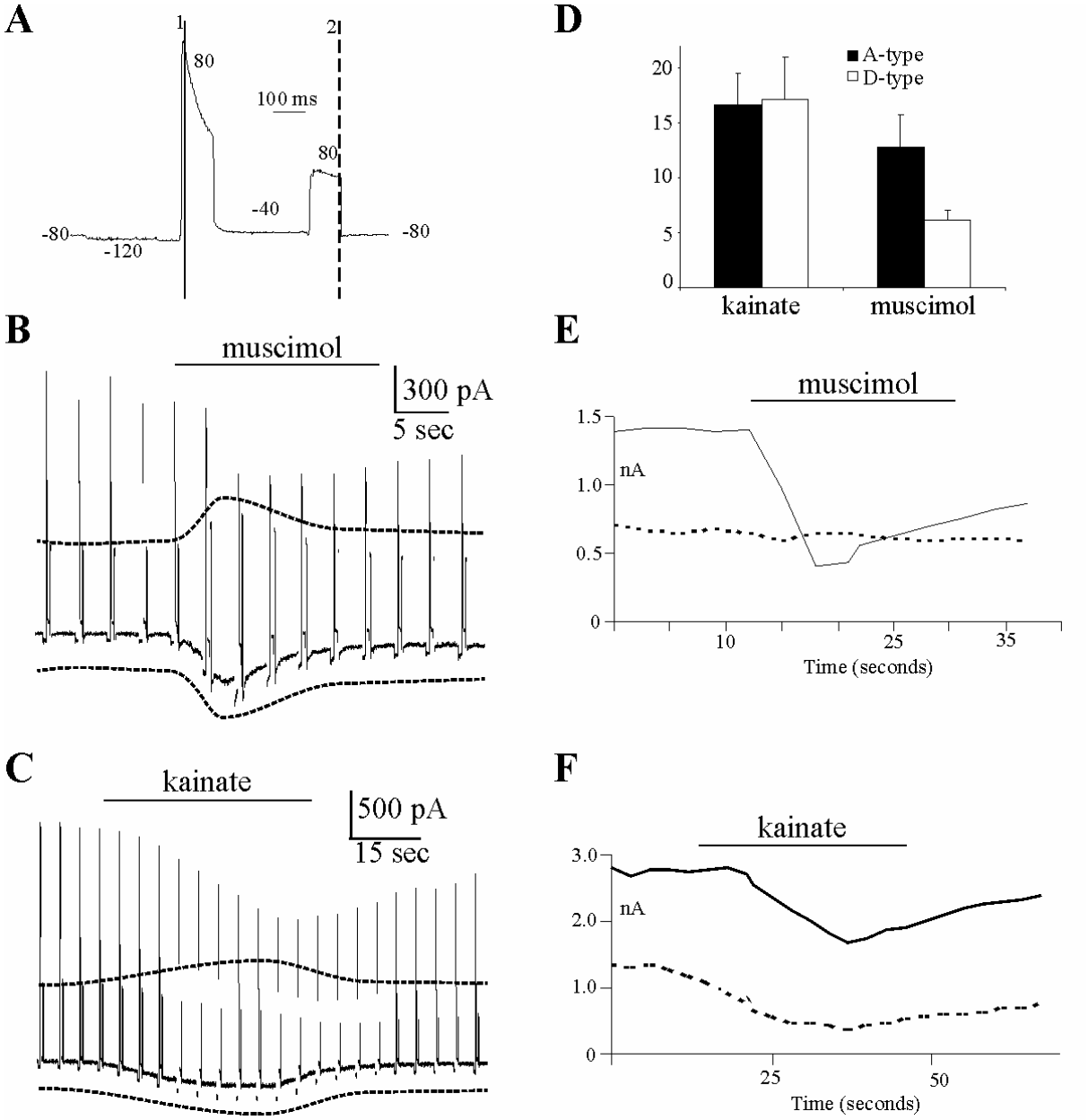

Figure 4.5. GABA and glutamate ionotropic receptor activation blocks outwardly rectifying Kv currents differently. A) Voltage-jump protocol used to isolate receptor-mediated effects on A-type and delayed-type Kv currents. B) and C) Same voltage protocol as shown in A repeated every 5 seconds before, during and after receptor agonist administration. As both muscimol and kainate have reversal potentials of ~0 mV, dotted lines are added to illustrate the expected amplitudes of the delayed-type Kv currents at 80 mV (mirror image of receptor response at -80 mV). Effects of receptor agonists on A-type current is obtained by subtracting the delayed-type current from the peak total current whereas delayed-type current is obtained by subtracting delayed current from expected current (dotted line). The percentage decrease of the two current types normalized to receptor current amplitudes are compared in D. E) and F) A-type (solid; line 1 in A) and delayed-type (dotted; line 2 in A) current amplitude plotted over time before, during and after receptor administration. E and F correspond to cell traces in B and C, respectively.

and glutamate receptor mediated secondary block of outward potassium conductances. In addition, it has recently been shown that glutamate can block inward potassium currents as well (Schroder et al. 2002). In light of these findings, it is tempting to postulate that these effects serve to increase the Na^+/K^+ ratio, creating a scenario where the astrocyte may begin to show 'spiking' behavior and, thus, A-current mediated rapid repolarization. In the confines of a synaptic cleft or the small extracellular space in the complex CNS, it may be possible for high frequency glutamate or GABA mediated synaptic events to, initially, depolarize astrocytes with subsequent K^+ conductance decrease that, with additional events, lead to receptor-mediated depolarizations augmented by the small 'spiking' behavior recruiting both A- and delayed-current for rapid repolarization.

5.0 - INTRACELLULAR ANION CONCENTRATION MODULATES KV CHANNELS

In the previous chapter, it was shown that astrocytic voltage-gated outward K^+ currents are linked to ionotropic transmitter responses of glutamate and GABA. Stimulation of GABA and glutamate ionotropic receptors has been shown to have two distinct actions in astrocytes both *in situ* and *in vitro*: receptor channel mediated current with a concomitant block of outward K^+ currents shown to be dependent on receptor current (Jabs et al. 1994; Robert and Magistretti 1997; Bekar and Walz 1999; Bekar et al. 1999). In the case of kainate receptor-mediated Na^+ influx, it is thought that Na^+ competes with K^+ for entry into the K^+ channel pore at highly depolarized potentials, thus blocking this current (Borges and Kettenmann 1995; Robert and Magistretti 1997). For the $GABA_A$ receptor, it is known that the block is dependent on changes in intracellular Cl^- concentration related to Cl^- efflux (Bekar and Walz 1999), but the mechanism remains to be determined. In this study, the mechanism of anion-mediated block is investigated using both Cl^- and I^- at multiple concentrations. In addition, the block is shown to be related to anion effects on voltage-gating and possibly a cytoskeletal interaction.

5.1 Muscimol-mediated effects are dependent on intracellular Cl^- concentration

It has been previously established that the muscimol receptor response requires a Cl^- flux through the channel pore to affect K^+ outward currents (Bekar and Walz 1999). In order to delineate a possible direct effect of Cl^- on K^+ channels, whole cell currents were measured with four different pipette (intracellular) Cl^- concentrations of 138 (n=56), 80 (n=10), 40 (n=26), and 20 mM (n=14). Whole cell current-voltage analysis under these conditions demonstrated that K^+ channels were affected by differing Cl^- concentrations (in the pipette) alone. A-type K^+ currents under conditions of 20, 40, and 80 mM intracellular Cl^- are approximately half that of 138 mM Cl^-, showing a significant difference ($P<0.05$) at voltage steps more depolarized than -40 mV (Fig. 5.1A, left). The delayed type current did not show a significant difference between the four concentrations at highly depolarized potentials, but did show significantly lower currents at -20 mV under 20 and 40 mM concentrations compared to 138 mM; and 0 mV under 20 mM conditions compared to 138 mM (Fig. 5.1A, right). Two-way statistical analysis of both the A-type and delayed-type K^+ currents under the four different intracellular Cl^- concentrations demonstrated a significant ($P<0.001$) Cl^- concentration-dependent effect on the A-type current only.

With application of muscimol under each concentration, the block of both outward K^+ currents was determined using the same voltage jump protocol shown in Figure 4.5A. The % block of each current was normalized (divided by) to receptor current density for comparison. The block of the A-type current showed a significant concentration-dependent effect, whereas there was no significant block of the delayed-type current at any concentration (Fig. 5.1B). Similar to the effects of concentration on whole cell K^+ currents, two-way analysis demonstrated a significant selective effect of Cl^- concentration on muscimol-mediated block of the A-type current only ($P<0.001$). In contrast, there was no significant effect of the concentration of Cl^- on the block of K^+ currents mediated by kainate (Fig. 5.1B, inset). This result serves to verify that

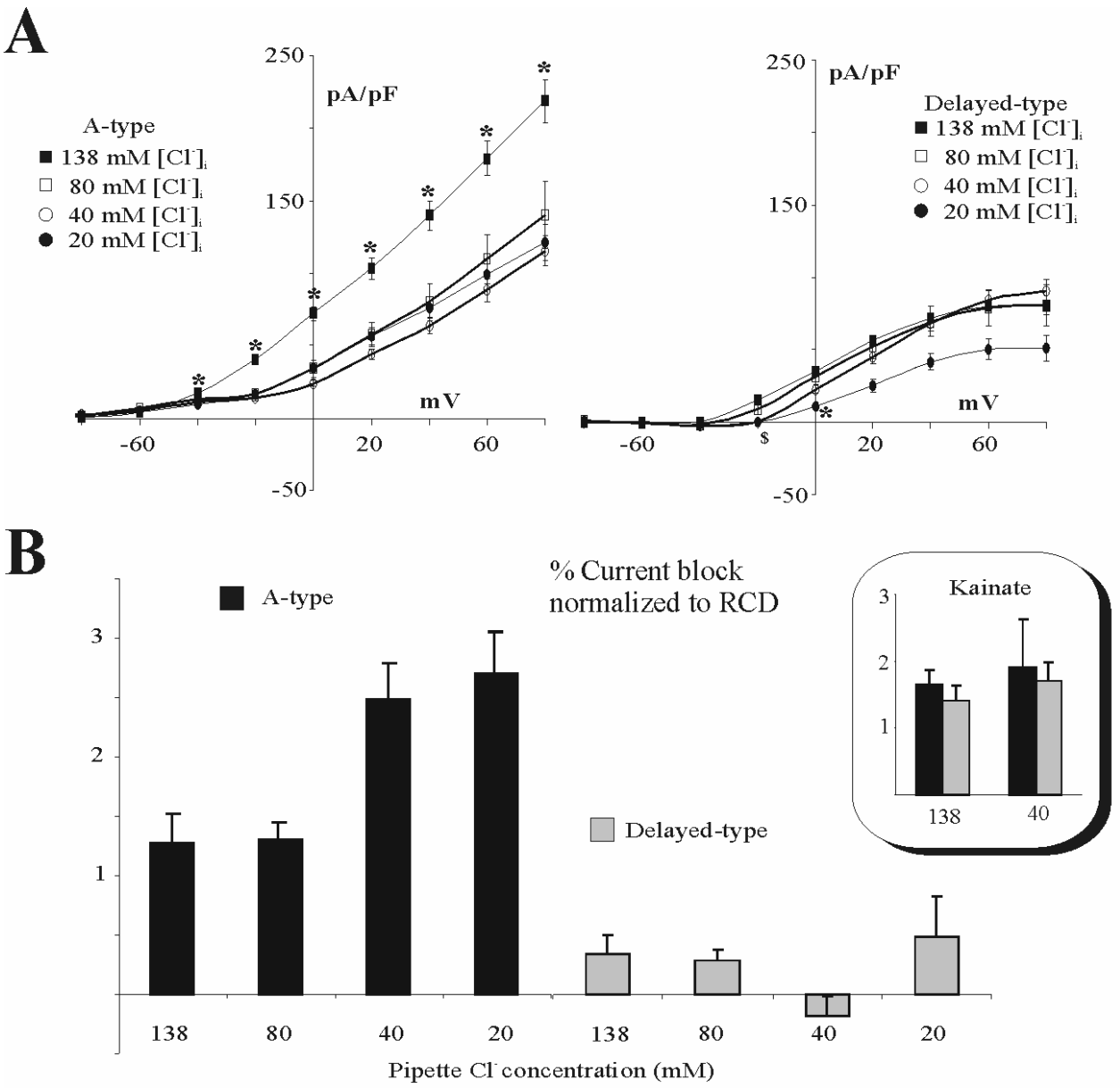

Figure 5.1. Chloride concentration-dependent effect on voltage-gated K^+ currents. A) Current-voltage relationship of A-type (left) and delayed-type (right) K^+ outward currents under four different intracellular Cl^- concentrations. Asterisk indicates a significance of $P < 0.05$ from all other concentrations. Dollar symbol indicates that currents at 20 and 40 mM are both significantly different than currents at 80 and 138 mM. B) Demonstration of the effect of rapid Cl^- effluxes across the membrane elicited by the $GABA_A$ agonist muscimol. Percentage block of A-type (black bars) and delayed-type (shaded bars) K^+ currents normalized to muscimol receptor current density for the four different intracellular Cl^- concentrations. Note the concentration-dependent effect on the A-type block only. Parallel experiments conducted with kainate (inset) demonstrate a nondiscriminating block of both K^+ currents under both Cl^- concentration conditions.

the block is dependent on changes in intracellular Cl^- concentration in response to $GABA_A$ channel activation, even though the intracellular Cl^- is reasonably clamped by dialysis with the pipette solution.

5.2 Altered affinity characteristics with iodide replacement

Iodide from the halide family was chosen to replace Cl^- because it has a lower charge density and therefore follows the lyotropic or Hofmeister anion series with relation to membrane/water surface potential, altering anion interaction with larger charged molecules (Dani et al. 1983; MacKinnon et al. 1989). Additional support was found for selective modulation of A-type channels by anions in experiments where I^- replaced Cl^- at intracellular concentrations of 130 and 30 mM. These experiments demonstrated similar characteristics to those of Cl^- but with a shift in the sensitive range to lower anion concentrations. This corresponds to the predicted increased ease of I^- approach to the water/membrane interface, not requiring as large a concentration/diffusion gradient as that of Cl^-. At symmetrical 130 mM I^- concentrations, there appeared to be no selective block of the outward K^+ currents in response to muscimol application (Fig. 5.2A, 130 I^-). However, when the intracellular I^- concentration was reduced from 130 to 30 mM, block of the A-type current was comparable to that of muscimol in 138 and 80 mM intracellular Cl^- (Fig. 5.2A, 30 I^- compared to 138 Cl^-). The block of the K^+ currents shows an identical pattern with the two anion species but with an apparent shift in sensitive concentration range (Fig. 5.2A).

Whole cell currents displayed a similar pattern to that of the different Cl^- concentrations with the effect on the A-current showing a greater spread (Fig. 5.2B). The A-type current was significantly lower at 30 mM I^- concentration from -40 mV and depolarized compared to that at 130 mM. The delayed-type current only showed a significant difference at 20 and 40 mV (Fig. 5.2B right) between the two concentrations. Again, both the muscimol-mediated block and the whole cell current patterns, in I^- containing solutions, showed a selective anion concentration dependent effect on the A-type current only. Interestingly, when K^+ currents in I^- are compared to those in Cl^- containing solutions, the delayed outward current in I^- was significantly larger (Fig. 5.2C right), whereas A-type currents were not affected (Fig. 5.2C left). This is likely a result of the increased negative charges lining the membrane surface (because of increased ease of approach) increasing corresponding positive charges leading to an increased cation conductance.

5.3 Muscimol-mediated effects under gramicidin perforated patch conditions

With the seeming dependence of K^+ outward currents on intracellular anion concentrations it was considered necessary to evaluate $GABA_A$ responses under more physiological conditions. With the use of the cation permeable antibiotic gramicidin it was possible to study the $GABA_A$ response without experimentally altering the intracellular Cl^- concentration. A total of 13 cells were patched using the gramicidin perforated patch method with an average membrane potential of -73 ± 3.9 mV. Current-voltage curves of both the A-type and delayed-type outward rectifying K^+ currents are consistent with the respective current-voltage curves under 20-80 mM intracellular Cl^- concentrations (Fig. 5.3A). Given that muscimol activates the $GABA_A$ Cl^- receptor channel, muscimol application to astrocytes under perforated patch control can be used to determine the intracellular Cl^- concentration by determining the reversal potential of the receptor current. In order to eliminate secondary effects on K^+ current, 10 mM barium was added

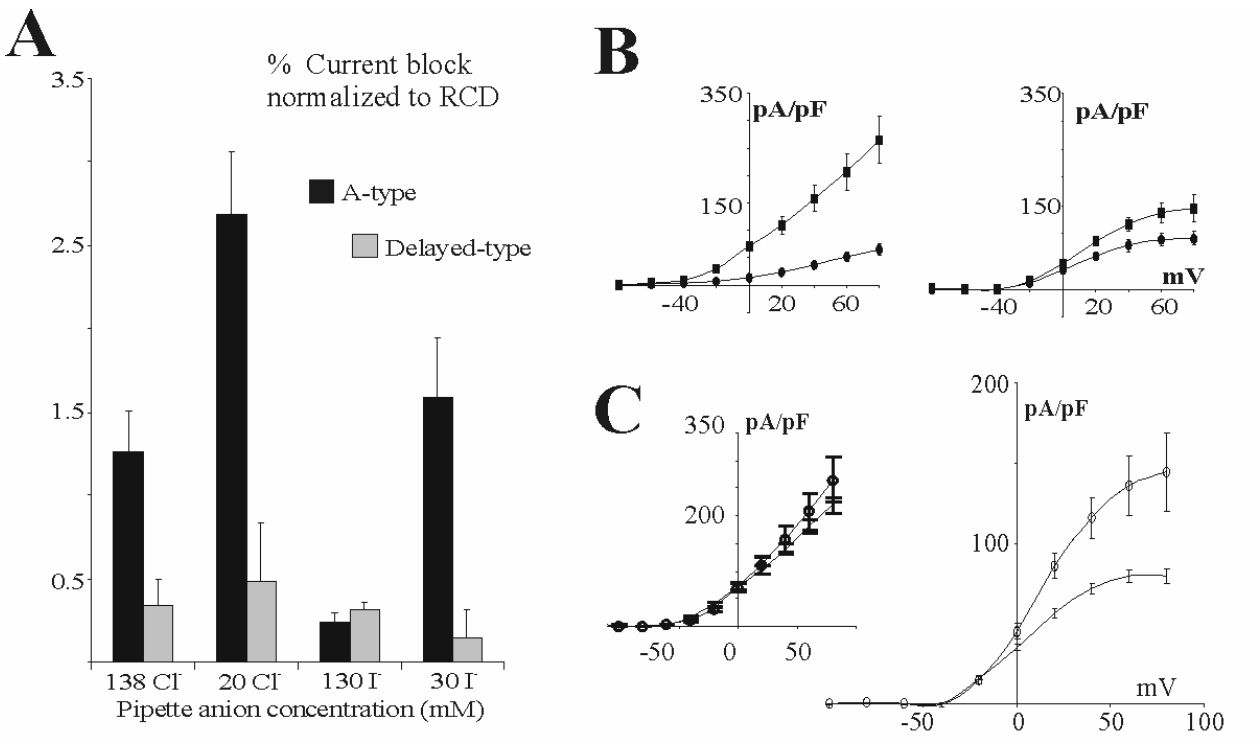

Figure 5.2. Chloride replacement experiments support a selective anion-mediated modulation of A-type K^+ currents. A)Percentage block of A-type (black bars) and delayed-type (shaded bars) K^+ currents normalized to muscimol receptor current density for two different Cl^- concentration experiments compared to corresponding I^- replacement experiments. Note both anions display a concentration-dependent effect on A-type current only. Also note the shifted concentration response under I^- replacement conditions. B) Current-voltage relationships for A-type (left) and delayed-type (right) currents under 130 (squares) and 30 mM (circles) I^- conditions. Note the concentration-dependent effect on A-type current. C) Comparison of A-type (left) and delayed-type (right) current densities in both I^- (open circles, 130 mM) and Cl^- (line, 138 mM). The delayed current density in I^--containing solutions was significantly larger than in Cl^-.

to the perfusate to block both outward and inward K^+ currents and a voltage ramp protocol was applied every 3 seconds before, during, and after muscimol application (Fig. 5.3B). By subtracting a voltage ramp prior to muscimol from one during muscimol application one can plot current voltage receptor response. The reversal potential for the receptor current ranged from -24 to -48 mV and averaged -41 ± 2.3 mV (n = 10, Fig. 5.3C). Given the known extracellular Cl^- concentration of 137.5 mM and use of the Nernst equation, interpolated reversal potentials predict intracellular Cl^- concentrations ranging from 22 to 55 mM and averaged 29 ± 3.2 mM (n = 10). Analyzing the block of outward A-type currents under the more physiological perforated patch method demonstrated a block, once normalized, not significantly different to that in 20 and 40 mM intracellular Cl^- whole cell experiments (Fig. 5.3D), consistent with the average calculated intracellular Cl^- concentration of 29 mM. This is consistent with 31 to 50 mM found in radioactive Cl^- efflux experiments (Kimelberg et al. 1979; Kimelberg 1981; Walz and Hertz 1983) and 20 to 40 mM found in cultured astrocytes using Cl^--sensitive microelectrodes (Kettenman et al. 1987). However, the methods used in these experiments likely underestimated

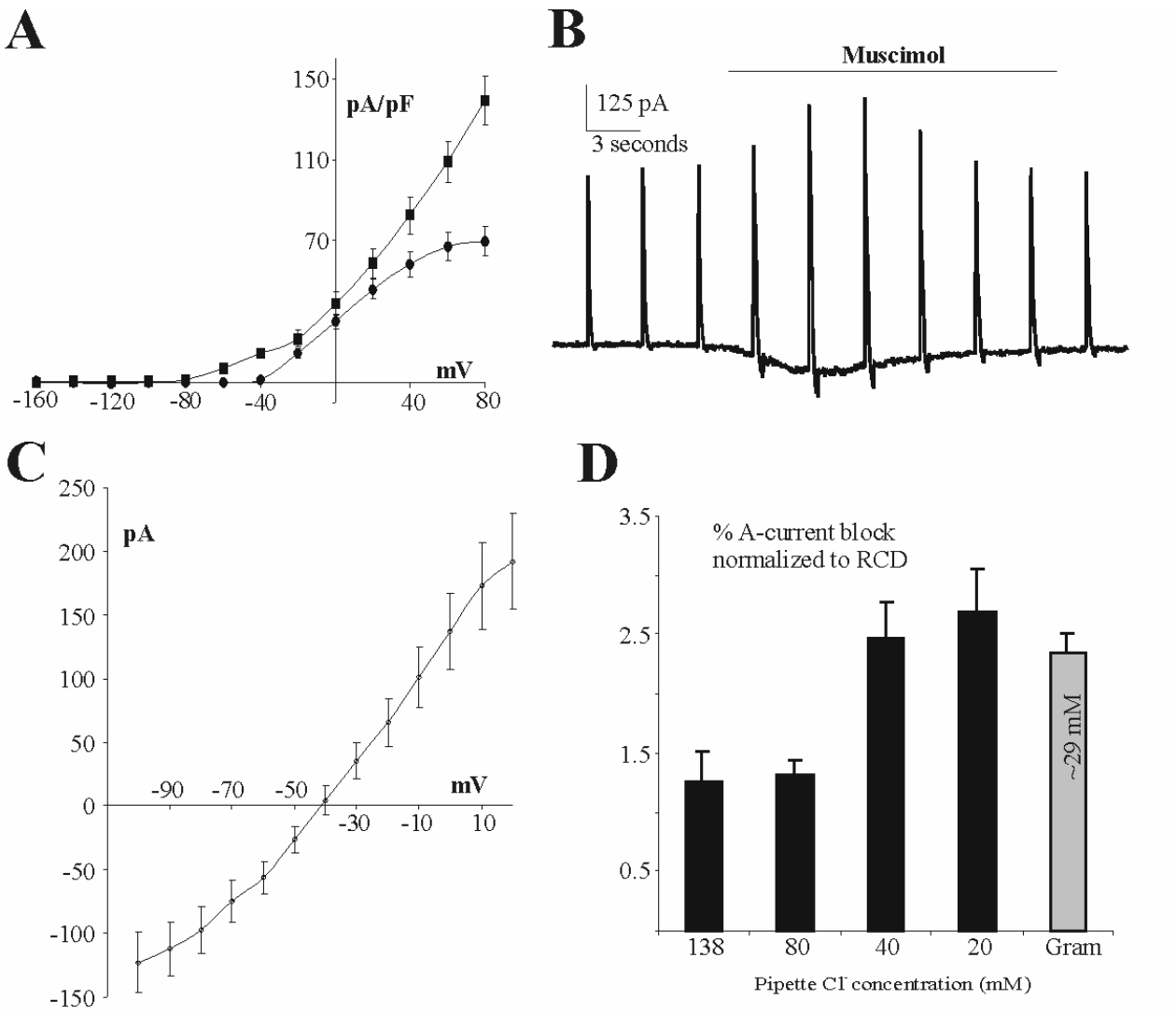

Figure 5.3. Gramicidin perforated patch experiments. A) Both A-type (squares) and delayed-type (circles) current densities are consistent (not significantly different) with corresponding whole cell currents under 20-80 mM intracellular Cl^- conditions (compare Fig. 5.1A). B) Application of voltage ramps (+80 mV to -160 mV, 2.5 ms) every 3 seconds in the presence of 10 mM Ba^{2+} (block all three K^+ currents, see results) allowed for estimation of the $GABA_A$ receptor reversal. C) The receptor response reversed at 41 +- 2.3 mV (n = 10). D) The block of the A-type current in response to muscimol application in perforated patch experiments is comparable to that under whole cell experiments with 20 and 40 mM intracellular Cl^- conditions, which is consistent with the estimated intracellular Cl^- concentration.

Cl^- concentration given that when the $GABA_A$ receptor opens, there is an efflux of intracellular Cl^-, thereby depleting remaining concentrations.

5.4 Chloride-dependent effects in astrocytes are mediated through effects on voltage-gating

Steady-state activation (Fig. 5.4A), but not inactivation (Fig. 5.4B) of the A-type outward K^+ current showed a significant depolarizing shift ($V_{1/2}$, -9.2 ± 2.19 to 21 ± 4.77 mV) when comparing intracellular Cl^- concentrations of 138 mM (n = 21) and 20 mM (n = 14). In contrast, comparison of delayed-type K^+ current steady-state kinetics under the two intracellular Cl^-

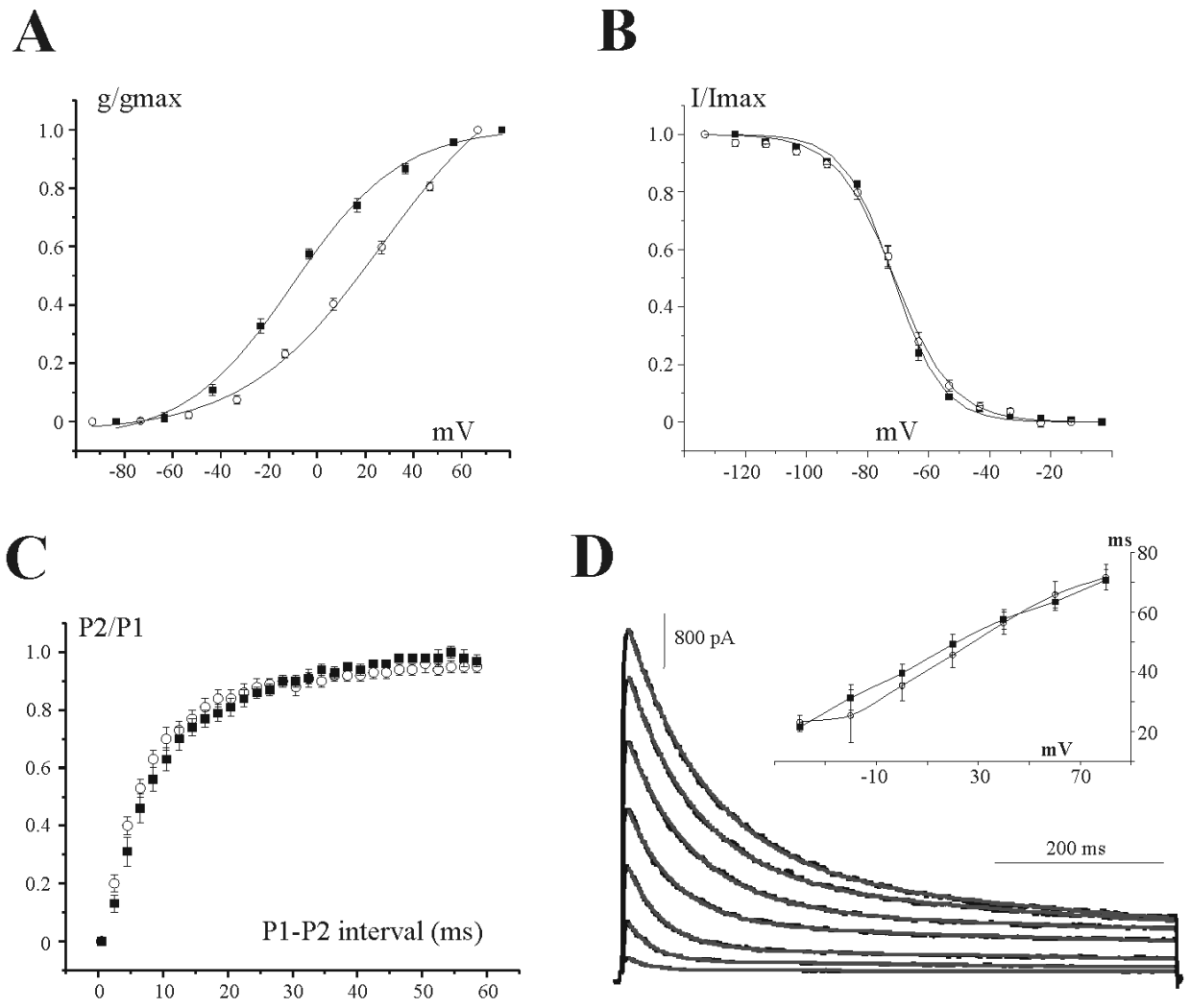

Figure 5.4. Activation, inactivation and reactivation kinetics of the A-type K^+ current under 138 and 20 mM intracellular Cl^- conditions. A) Steady state inactivation and B) activation curves of A-type currents under 138 (squares) and 20 mM (circles). Data fit to Boltzmann equation for determination of ½ inactivation or activation constants. C) Reactivation kinetics of A-type currents. A twin depolarizing pulse protocol was applied from a holding of -120 mV to +80 mV with increasing inter pulse intervals (P1-P2 interval). Time constants of reactivation under 20 mM (open circles) intracellular Cl^- were not significantly different from time constants under 138 mM conditions (solid squares). D) Time constants of current decay (inactivation) are plotted against voltage for 20 (open circles) and 138 mM (solid squares) Cl^- internal solutions. Time constants were derived from single exponential curve fitting of currents obtained by the 400 ms voltage jump protocol displayed.

concentration conditions failed to illustrate a significant change (data not shown). Although Cl^- concentration appeared to affect activation of A-type currents specifically, it did not affect reactivation kinetics or time constants of inactivation. Reactivation protocols demonstrated very similar patterns with time constants of reactivation of 7.68 ± 0.55 ms in 20 mM (n = 6) and 10.15 ± 1.07 ms in 138 mM (n = 8; $P = 0.07$) intracellular Cl^- when fitting the data to a single exponential function (Fig. 5.4C). Inactivation time constants, fit to single exponential functions, were also not significantly different under 138 and 20 mM Cl^- concentration conditions at several

voltages (Fig. 5.4D). Together, these data suggest that Cl^- mediates its effects on A-type channels by altering the voltage of activation.

5.5 Unlike astrocytes, Kv current kinetics in HEK293 cells are not $[Cl^-]_i$-sensitive

In order to examine the effects of $[Cl^-]_i$ on Kv channels more closely, individual Kv channels were assessed in HEK293 cells. The Kv1.4 and Kv4.2 channel expression both resulted in sizeable A-type inactivating current patterns, whereas the Kv1.5 channel resulted in delayed-type non-inactivating currents (Fig. 5.5). Steady-state channel kinetics were evaluated under high Cl^- and low Cl^- conditions for each channel in order to verify results found in cultured astrocytes. Interestingly however, intracellular Cl^- was found to have no impact on Kv1.4, Kv1.5 or Kv4.2 (Fig. 5.5, Table 5.1).

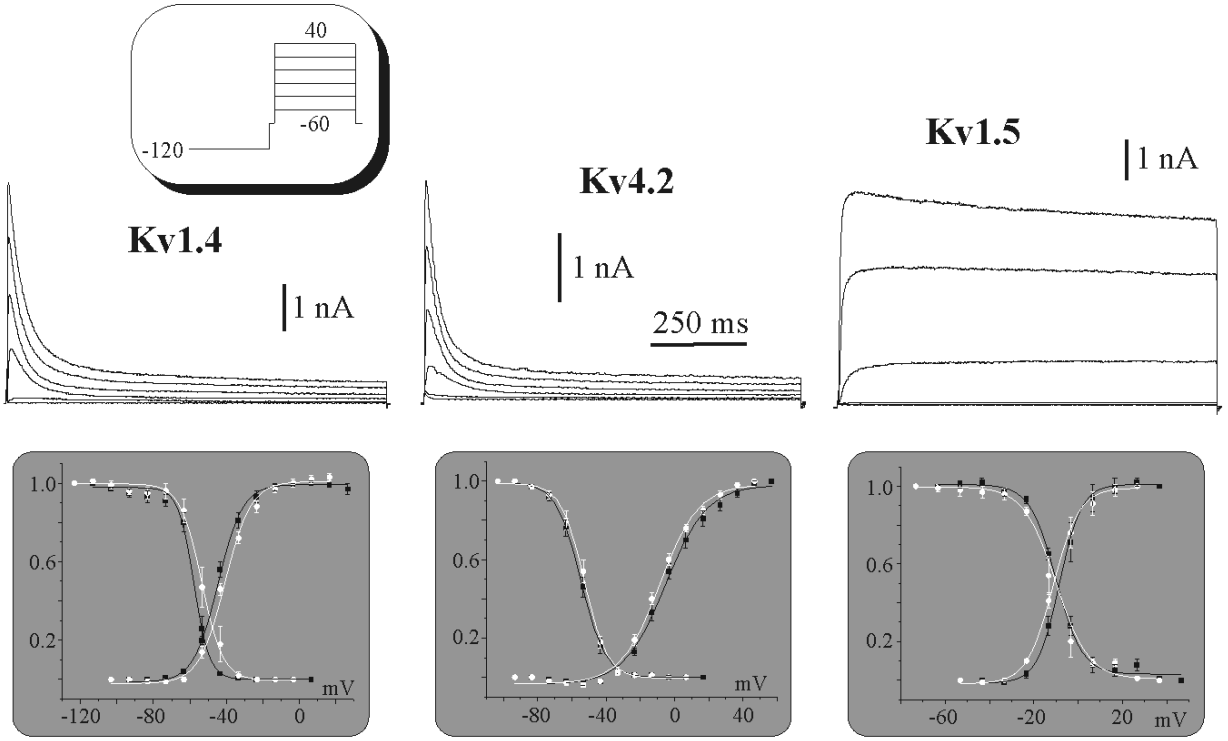

Figure 5.5. Kv channels expressed in HEK293 cells do not show significant sensitivity to intracellular chloride. The top three current tracings are representative examples of Kv1.4, Kv4.2 and Kv1.5 channels in response to voltage commands from -60 to 40 mV in 20 mV increments as displayed in shaded inset. Normalized steady-state inactivation and activation kinetics are displayed in the shaded box for each channel. Kinetics are displayed for both high Cl^- (138 mM; black) and low Cl^- (20 mM; white) internal solutions for comparison.

5.6 Cytoskeletal disruption in HEK cells unmasks a $[Cl^-]_i$-dependent hyperpolarizing shift in Kv current kinetics

Since it has been previously demonstrated that Kv channels bind to the cytoskeleton in HEK293 cells (Maruoka et al. 2000; Cukovic et al. 2001; Wang et al. 2004), perhaps differential cytoskeletal interaction in this kidney cell line is responsible for the lack of a Cl^--sensitive effect

Table 5.1. Steady-state 50% ($V_{1/2}$) channel kinetics

	Activation		Inactivation	
	High $[Cl^-]_i$	Low $[Cl^-]_i$	High $[Cl^-]_i$	Low $[Cl^-]_i$
Kv4.2	**-4.67** +/- 1.80 (10)	**-8.71** +/- 1.25 (8)	**-54.65** +/- 1.38 (9)	**-53.25** +/- 1.85 (9)
Kv1.5	**-7.68** +/- 1.47 (6)	**-10.20** +/- 1.56 (5)	**-9.77** +/- 0.97 (6)	**-11.99** +/- 2.24 (3)
Kv1.4	**-43.25** +/- 0.86 (27)	**-40.64** +/- 0.98 (19)	**-57.17** +/- 1.14 (15)	**-52.81** +/- 2.45 (12)
Kv1.4 CytoD	**-45.89** +/- 0.65 (11)	**-50.23** * +/- 2.02 (8)	**-57.77** +/- 0.99 (9)	**-67.63** * +/- 2.70 (5)
Kv1.4 CytoD Phall		**-37.44** +/- 2.36 (5)		**-55.80** +/- 2.04 (8)
Kv4.2 CytoD		**-27.24** * +/- 2.93 (3)		**-74.33** * +/- 2.56 (3)

Numbers in brackets represent number of cells. * indicates significant difference ($P < 0.05$) compared to the same channel without pharmacological manipulation within the same column (same Cl^- conditions).

compared to astrocytes. Upon disruption of the cytoskeleton in Kv channel expressing HEK293 cells, a hyperpolarizing shift in steady-state kinetics can be seen only at low intracellular Cl^- concentrations (Fig. 5.6; Table 5.1). In contrast to the depolarizing shift seen in activation kinetics in astrocytes, this corresponds to a hyperpolarizing shift in kinetics from high Cl^- to low Cl^- internal solutions. Although this effect in HEK cells is opposite to what is seen in astrocytes, it does demonstrate that both cytoskeletal interaction and anion concentration can have an impact on channel structure and subsequent gating kinetics. It should also be highlighted, as in Chapter 3, that astrocytic A-currents are highly complex and most likely involve additional cytoplasmic subunits (KChIPs) that are known to impact channel kinetics in a manner apart from conditions demonstrated above.

5.7 Astrocytic cytoskeletal disruption affects muscimol-mediated Kv current block

Due to the fact that a $[Cl^-]_i$ effect is only seen in HEK293 cells after cytoskeletal disruption, is it possible that cytoskeletal dynamics play a role in the selective chloride-dependent effect on inactivating Kv currents in cultured astrocytes? Comparison of the $GABA_A$-mediated block of

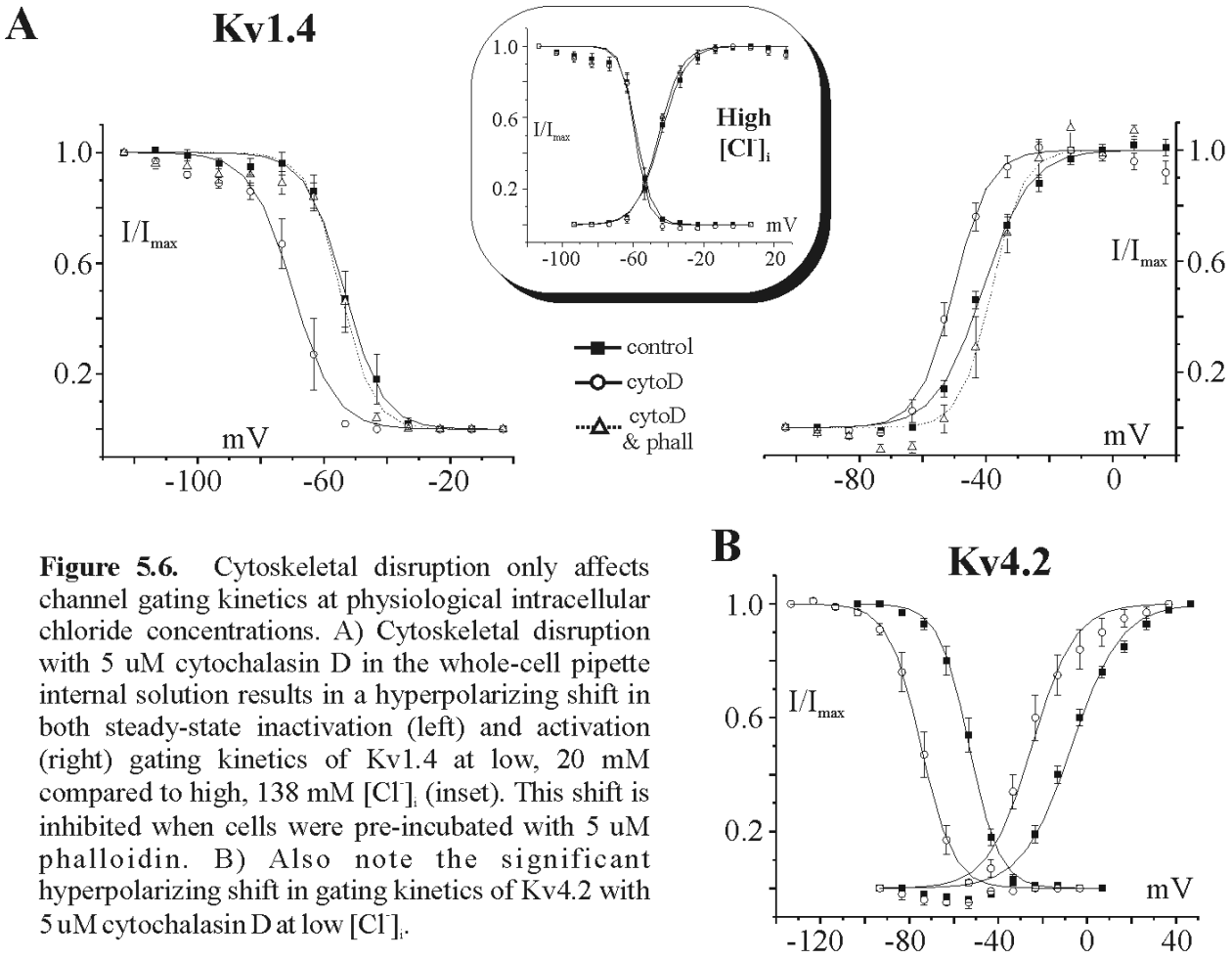

Figure 5.6. Cytoskeletal disruption only affects channel gating kinetics at physiological intracellular chloride concentrations. A) Cytoskeletal disruption with 5 uM cytochalasin D in the whole-cell pipette internal solution results in a hyperpolarizing shift in both steady-state inactivation (left) and activation (right) gating kinetics of Kv1.4 at low, 20 mM compared to high, 138 mM $[Cl^-]_i$ (inset). This shift is inhibited when cells were pre-incubated with 5 uM phalloidin. B) Also note the significant hyperpolarizing shift in gating kinetics of Kv4.2 with 5 uM cytochalasin D at low $[Cl^-]_i$.

Kv currents in astrocytes under conditions of cytoskeleton disruption (n = 9) with controls (n = 12) demonstrated a complete loss of selectivity (Fig. 5.7A). In addition, when normalized to the increased $GABA_A$ receptor current density under cytoskeletal disruptive conditions (Fig. 5.7B inset), it appears that the sensitivity of the $GABA_A$-mediated block is also reduced (Fig. 5.7B). Therefore, it appears that the chloride-dependent effect on Kv currents in astrocytes may involve cytoskeletal protein-protein interactions. However, it can not be ruled out that cytoskeletal disruption in astrocytes merely disassociates specific Kv channel subtype localization with the $GABA_A$ receptor. This mislocalization could explain loss of selectivity of the response and, by shifting microdomains of $[Cl^-]_i$ changes away from Kv channels in general, would impact the sensitivity of the response as well.

5.8 Summary and Discussion

This study demonstrates that the reduction of inactivating A-type Kv currents in astrocytes as a result of $GABA_A$ receptor activation is dependent on direct action of intracellular anion concentrations on the Kv channel structure. Iodide replacement shifted sensitivity of the effect consistent with physical differences in charge density and mobility compared to chloride. These studies further demonstrate that the effect in astrocytes is highly selective to steady-state activation kinetics of A-type channels specifically, suggesting that anion concentration impacts voltage-sensing/gating ability. Examination of individual Kv channel subunits expressed in

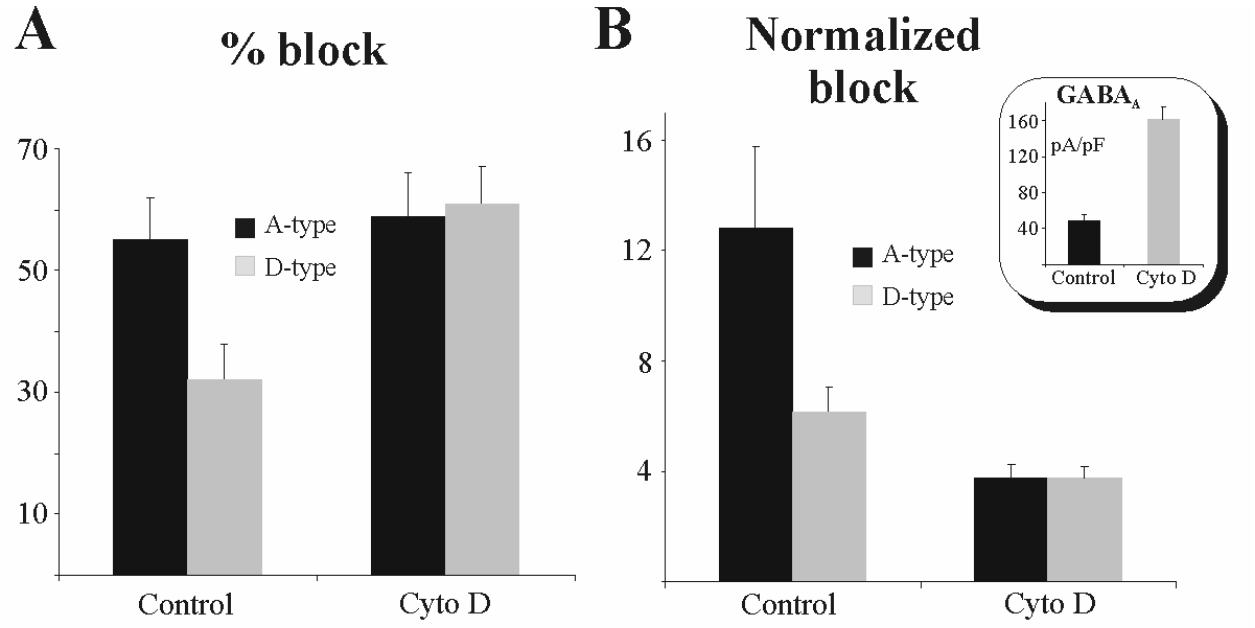

Figure 5.7. Selectivity and sensitivity of muscimol-mediated block of Kv currents is lost following cytoskeletal disruption. A) With the addition of 5 uM cytochalasin D in the whole-cell pipette solution, the selective effect on A-type current block is lost. B) With normalization of the % block to the $GABA_A$ receptor current density ($GABA_A$ density increases with cytoskeletal disruption; inset) because the block is dependent on Cl^- efflux through the $GABA_A$ channel, a significant decrease is seen in the sensitivity of the Kv currents to changes in $[Cl^-]_i$.

isolation in the HEK293 cell expression system also demonstrated a very interesting cytoskeletal involvement in channel kinetics and chloride-sensitivity. Re-examination of chloride-dependent effects in astrocytes under cytoskeletal disruptive conditions supports this contention, as both selectivity and sensitivity to chloride are lost with cytoskeletal disruption.

6.0 - GENERAL DISCUSSION

6.1 Complex inactivating potassium channel expression in cultured astrocytes

These studies are the first and only to provide a detailed breakdown of the molecular identity of astrocytic inactivating A-type K^+ channels. Despite many studies having looked at the electrophysiological current profiles of astrocytes *in situ* (Bordey and Sontheimer 1997, 2000) or in acutely isolated astrocyte preparations (Zhou and Kimelberg 2000; Schools et al. 2003), there have yet to be attempts to elucidate the specific molecular counterparts of these currents, inactivating A-type currents in particular. Although astrocytic current patterns differ depending on stage of development (Bordey and Sontheimer 1997) or location in the brain (Bordey and Sontheimer 2000) suggesting these current patterns are modulated by their environment, current profiles in culture are consistent with expression patterns seen *in situ.* In some cases, cultured astrocytes have even been used to examine the impact of injury on these current profiles (MacFarlane and Sontheimer 1997). For these reasons, and the fact that culture models are much more amenable to experimentation, hippocampal astrocyte cultures were used throughout this thesis to provide a first look at inactivating potassium channel complexity.

6.1.1 Complex inactivating potassium channel expression in cultured astrocytes

It was found that the Kv4 *Shal* subfamily is responsible for the majority of A-current in astrocytes using electrophysiological kinetics and pharmacology, immunocytochemistry, and RT-PCR. Electrophysiological analysis demonstrated that ~70%, 10% and less than 5% of total A-currents are comprised of Kv4, Kv3 and Kv1 channels, respectively (Fig. 3.1). Novel evidence for KChIP contribution to astrocytic A-current complexity was also found (Fig. 3.2 and 3.3). The electrophysiological evidence is consistent with the lack of significant redox effects on inactivation (Fig. 3.4) and that Kv4.3 shows bright ubiquitous staining in immunocytochemical experiments (Fig. 3.5B) and the densest bands in PCR (Fig. 3.7A). The small contribution by the Kv3 family is perhaps a result of targeted expression to the processes, where contribution to whole cell currents is limited due to space clamp control issues (Fig 3.4A).

Although Kv1.4 immunostaining could not be confidently demonstrated above background levels in cultured stellate astrocytes (Fig. 3.6A-C), PCR results demonstrate the presence of Kv1.4 mRNA (Fig. 3.7C). Interestingly, the accessory subunits Kvβ1.1 and Kvβ3.1, which contain an inactivating N-terminal ball domain, were also demonstrated to be present by RT-PCR. Kv1.4 mRNA in these heterogeneous cultures may be a result of small contaminating populations of microglia, endothelial cells and/or fibroblasts. Alternatively, it may be that the density is very low in astrocytes and the channels may be targeted, as in neurons, to astrocytic endfeet terminals (discussed in section 6.1.2). Kv1.4 subunits may also form heteromultimers with Kv1.1 or 1.2 subunits (Sheng et al. 1993; Monaghan et al. 2001) diluting immunopuncta, making positive staining above background very difficult. In any case, in stellate astrocytic voltage-clamp studies, Kv1 family contribution to A-currents appears to be minimal (≤ 5%; Fig. 3.1D), probably due to targeting to distal cell processes resulting in space clamp issues similar to the Kv3 subfamily.

The apparent targeted expression of specific A-channel subunits in these culture studies may be due to inherent targeting sequences or accessory β-subunits of the different subfamily α-subunits. However, under different serum conditions in culture, differences in A-current expression patterns can be found (Fig. 3.8) that correspond to small differences in KChIP mRNA expression as determined by RT-PCR (Fig. 3.9). This suggests that, on top of possible sequence or accessory subunit targeting of the different Kvα-subunits, environment (growth factors and cytokines) may play a role in modulating accessory subunit expression with subsequent effects on current profiles. The ability of environmental signals to modulate these currents is good evidence supporting the view that these channels serve a physiological function that still remains to be determined.

6.1.2 Does channel localization provide insight to function?

The three different Kv families involved in creating A-type inactivating potassium currents differ in their kinetics and therefore function. Targeted localization of these Kvα-subunits in neurons is a testament to this fact (for review see: Trimmer and Rhodes 2004). Neurons target Kv1.4 primarily to terminals (Sheng et al. 1992, 1993; Monaghan et al. 2001), Kv4.2 to somata and dendrites (Sheng et al. 1992; Song et al. 1998; Rhodes et al. 2004; Shibasaki et al. 2004) and Kv3.4 is located in the axosomatic compartment (Veh et al. 1995; Riazanski et al. 2001). Rationale behind such targeting can be seen when considering channel gating kinetics in the framework of neuronal function. Kv4.2 activates at subthreshold potentials limiting excitability and amplitude of action potentials as well as, with its rapid reactivation kinetics, allowing rapid firing capability making it ideally suited for somal temporal summation from multiple action potentials coming in from a single dendrite. Kv3.4, sharing similar rapid reactivation kinetics, allows rapid firing of action potentials (Lien and Jonas 2003; Shevchenko et al. 2004). However, activation of Kv3.4 is much more depolarized, making it less suited for controlling excitability but allowing for much larger action potential amplitudes, which might seem appropriate in or adjacent to the axon hillock. Kv1.4 demonstrates subthreshold activation similar to that of Kv4.2, but has much slower reactivation kinetics. The slow reactivation kinetics of Kv1.4 can lead to use-dependent accumulation of inactivation (Geiger and Jonas 2000; Shimizu et al. 2002). As Kv1.4 is located in nerve terminals, this means that in response to high frequency trains of action potentials, Kv1.4 would accumulate in the inactivated state allowing larger terminal depolarizations for increased neurotransmitter release (Geiger and Jonas 2000; Monaghan et al. 2001).

Although the function of A-channels in astrocytes is yet to be determined, they too appear to be targeted to specific subcellular locations (see Fig. 6.1 for comparison of proposed A-type Kv expression patterns in astrocytes compared to neurons). The Kv3.4 channel appears to be primarily targeted to astrocytic cell processes in the culture model used in this study, consistent with Kv3.4 found in the axosomatic compartment of neurons (Fig. 6.1). The fact that targeting of Kv3.4 occurs in culture may suggest this is a mechanism independent of environment or activity and more dependent on an inherent channel targeting sequence like that seen for Kv1 channels (Li et al. 2000) and Kv4 channels (Rivera et al. 2003). If this is the case, then localized expression patterns *in vitro* may represent expression patterns in astrocytes *in vivo*. Although Kv1.4 immunostaining was found to be very weak close to background, RT-PCR for Kv1.4 as well as Kvβ1.1 and 1.3 accessory subunits supports the notion that the *Shaker* Kv1 subfamily contributes to inactivating A-current in astrocytes. However, if they are present, the lack of significant oxidizing effects on A-current (Fig. 3.4) and only a small (<5%) open-state

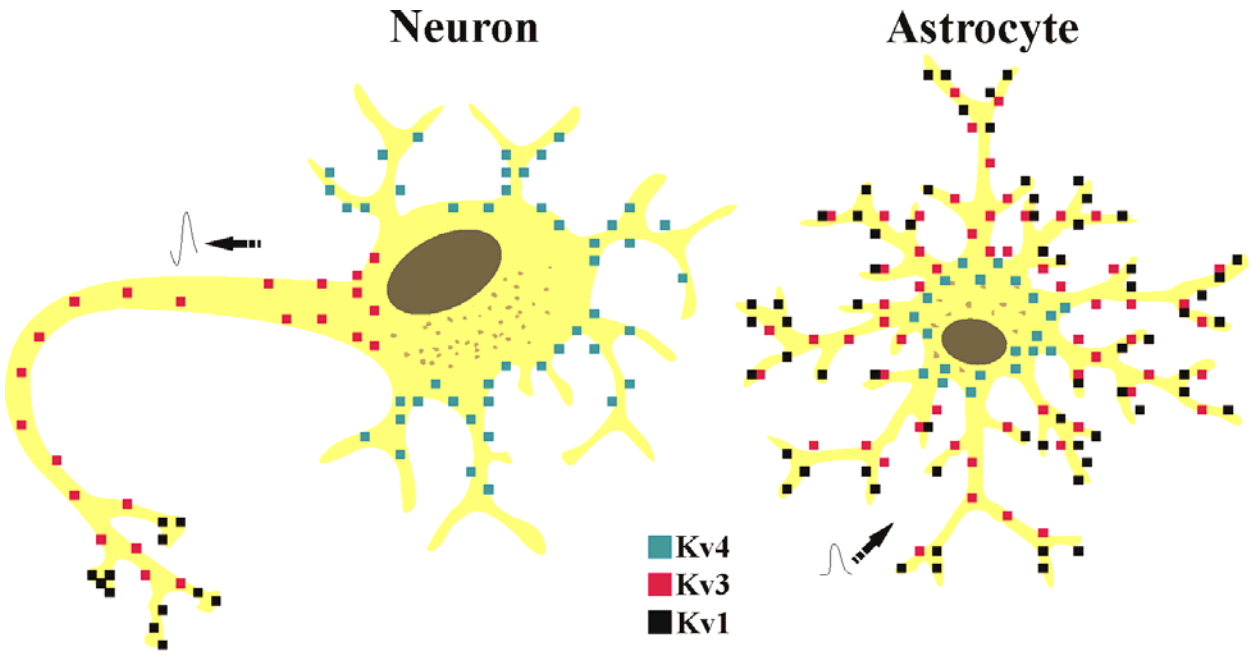

Figure 6.1. Schematic representation of inactivating A-type Kv channel localization in a neuron versus an astrocyte. Note the proposed distribution of Kv1 and Kv3 subunits in astrocytic processes to most closely resemble distribution of A-type channels in neuronal axons as opposed to dendrites. This may facilitate propagation and maintenance of signal amplitude from distal processes to the glial cell soma.

pharmacological block (Fig. 3.1) suggest that Kv1 family channels are not under adequate space-clamp control, possibly meaning they are located very distant in the cell processes as they are in neuronal synaptic terminals (Fig. 6.1). *Shal* Kv4.3 subfamily localization to both the soma and processes in this study are consistent with Kv4 channel distribution in soma and dendrites of neurons. However, it is interesting to note that in CA1 neurons, Kv4 density increases in the dendrites with distance from the soma (Hoffman et al. 1997). As density of the Kv4 channel family is highly associated with the accessory KChIP expression, specific localization or targeting may also be. In support of this, Rhodes et al. (2004) demonstrated a differential distribution of KChIPs and Kv4 subunits throughout the hippocampus that appears consistent with the possibility that Kv4 expression pattern is related to expression of the different KChIPs. In the present studies, although RT-PCR demonstrated mRNA for all three Kv4 subfamily members, immunochemistry was only performed on Kv4.3. Kv4.3 expression in the hippocampus is very distinctive, with no expression in CA1 and prominent expression in CA3 and dentate gyrus. Furthermore, KChIP1 is only found in Kv4.3 expressing cells and appears to be primarily restricted to large interneurons (Rhodes et al. 2004). In contrast to an increase in Kv4 density along the distance of the dendrites in neurons (Hoffman et al. 1997), it appears that Kv4.3 density in astrocyte processes is much lower than in the soma. It would be interesting to determine Kv4.1 and 4.2 distributions along astrocytic processes to better correlate localization with that seen in hippocampal neurons.

Keeping in mind that Kv4.1 and 4.2 channels were not assessed in immunochemistry experiments, results with Kv3.4 and Kv4.3 appear to demonstrate astrocyte localization consistent with astrocyte processes most closely resembling axonal rather than dendritic patterns (Fig. 6.1). As mentioned earlier, Kv3.4 allows rapid membrane voltage oscillations but, unlike Kv4 channels, would allow larger oscillations due to its delayed activation kinetics. Also, Kv1.4

use-dependent kinetics allow repetitive signals to be amplified. I suggest that in contrast to the propagation of membrane responses towards axon terminals in neurons, this pattern of channel expression may allow larger membrane oscillations in astrocytic processes in order to better ensure spread of membrane responses toward the cell soma, given the increased conduction resistance and lack of myelin in thin astrocytic processes. This hypothesis is also consistent with sodium channel immunocytochemical localization in soma and processes of stellate spinal cord astrocytes in culture (Reese and Caldwell 1999). This distribution pattern may also be useful in propagating membrane responses from astrocyte to astrocyte through the glial syncytium. The larger density of Kv4.3 channel localization in the soma may serve to blunt incoming signals requiring some form of membrane summation in order to maintain the response through to another cell process. It may also be that electrical signals propagated down astrocytic cell processes to the soma enable adequate somal Ca^{2+} elevations for propagation through the syncytium. Clearly, much work needs to be done to clarify these possibilities *in situ* or *in vivo*. Whatever the case may be, it appears that the complex astrocytic voltage-gated channel expression may enable some form of signal processing similar to that which occurs in neurons.

6.1.3 KChIPs: A-type Kv channel calcium sensors?

Given the implications for calcium waves and oscillations in astrocytes, it is not surprising to find evidence for astrocyte expression of KChIPs (Figs. 3.2, 3.7) from the larger neuronal calcium sensor-recoverin gene subfamily (An et al. 2000). KChIPs contain four EF-hand-like motifs (An et al. 2000) suggesting they may provide Ca^{2+} sensitivity to the A-type Kv4 channel family. KChIPs 1-3 as well as frequenin (also known as neuronal calcium sensor 1; NCS-1) from the same gene subfamily have been shown to localize and modulate Kv4.2 currents in a Ca^{2+}-dependent manner (An et al. 2000; Nakamura et al. 2001) with increasing Ca^{2+} levels prolonging the rate and increasing recovery of Kv4 inactivation. Interestingly, mutation of the EF-hand domains in KChIP1 failed to interrupt association with Kv4.2, but did inhibit modulatory effects (An et al. 2000), suggesting Ca^{2+}-binding is crucial to KChIP modulation of Kv4 channel kinetics. Also of interest is that KChIP4, in contrast to the other modulatory subunits, contains a K^{+}-channel inactivation suppressor (KIS) domain which effectively converts Kv4 inactivating channels into non-inactivating delayed-type channels (Holmqvist et al. 2002). Thus, at present there appear to be four different KChIP genes with a total of eight different splice variants among these, which are capable of modulating Kv4 channel currents in, often times, very different ways. For example, of the three KChIP2 splice variants 2a, 2b and 2c, the two longer isoforms 2a and 2b contain palmitoylation sites that have been shown to enhance plasma membrane localization (Takimoto et al. 2002). KChIP2c expression does not. Furthermore, KChIP1 has been shown to affect Kv4.1 and 4.2 differently (Nakamura et al. 2001) dependent on differences in Kv4 N-terminals. Thus, interaction of KChIPs with Kv4 channels is highly complex and can result in enormous diversity in current profiles. In addition to KChIPs, there are several other accessory proteins capable of modulating Kv4 channel currents (frequenin, Nakamura et al. 2001; CD26-related DPPX, Nadal et al. 2003; MiRPs, Abbott et al. 2001 and Zhang et al. 2001; PSD-95, Wong et al. 2002; Kvβ, Yang et al. 2001; KChAP/Kvβ1.2, Kuryshev et al. 2001; filamin, Petrecca et al. 2000). Of these, the CD26-related dipeptidyl aminopeptidase-like protein DPPX is a potential candidate, in addition to the KChIPs investigated in these studies, for the more rapid recovery from inactivation of astrocytic A-currents compared to Kv4.2 expressed alone in HEK293 cells. Also, the known interactions of Kv4 channels with PSD-95 and filamin provide a link to cytoskeletal localization and clustering. Although there are many possible accessory

subunits capable of modulating Kv4 currents, the expression of KChIP mRNA in the present studies suggests that at least part of the astrocytic A-current may be Ca^{2+}-sensitive. In addition to a possible KChIP role in localization and expression of A-current, Ca^{2+}-sensitivity may serve a negative feedback role to allow an increase in outward K^+ flux for increased repolarization under high activity conditions. Furthermore, KChIP sensitivity to physiological concentrations of arachidonic acid in astrocytes provides an additional link to synaptic plasticity events, as AA is thought to play a major role in long-term potentiation (Chen et al. 2002; Kondo et al. 2002; Ramakers and Storm 2002).

6.1.4 Endogenous hippocampal neuronal firing frequency is consistent with astrocytic signaling capability

The hippocampus is heavily involved in encoding, consolidating and retrieving information by means of frequency dependent network oscillations. Theta oscillations (4-10 Hz) of hippocampal pyramidal cells and interneurons occur during exploratory behaviors and rapid eye movement (REM) sleep, whereas sharp-wave firing of CA3 pyramidal neurons is associated with high frequency (120-200 Hz) ripples in CA1 dendritic fields during consummatory behaviors and slow-wave sleep (Kunec and Bose 2003; Ponomarenko et al. 2003; Klausberger et al. 2003, 2004). Burst firing may be required to induce synaptic modifications in hippocampal circuits as well as projections to neocortical targets that participate in memory consolidation (Buzsaki et al. 1987; Staba et al. 2002). Interestingly, astrocytic Ca^{2+} oscillations and possibly syncytial Ca^{2+} waves thought to play a role in long-term potentiation and modification of synaptic connections (Dani et al. 1992; Porter and McCarthy 1996; Kang et al. 1998; Liu et al. 2004; Nagai et al. 2004) appear to be augmented under conditions of neuronal bursting behaviour (Latour et al. 2001; Hirase et al. 2004). Therefore, not only does it appear that astrocytes are subjected to high frequency stimulation, but astrocytes may be a key component in the remodeling and strengthening of synaptic connections. The question left unanswered is whether astrocytes respond to these high frequencies with high frequency membrane oscillations or with only a large blunted depolarization resulting in Ca^{2+} signaling.

6.1.5 Perspectives and limitations: Could the slow glial 'spike' serve to activate A-currents for increased rate of repolarization?

Although astrocytes appear to be subjected to high frequency neuronal activity and are able to respond to both GABA and glutamate in the hippocampus, large, rapid (ms) NT-mediated depolarizations above ~-50 mV would be required in order to allow A-current-mediated repolarization. With a resting membrane potential between -70 and -90 mV, it may be unphysiological to expect depolarizations much above this threshold level in response to GABA or glutamate. With a depolarization insufficient to reach threshold for voltage-gated channels the repolarization phase would be dependent on the lower inwardly rectifying K^+ channel density and the Na^+/K^+ pump, resulting in a comparatively slower repolarization. However, given that astrocytes in this study as well as spinal cord cultures (Sontheimer et al. 1992), spinal cord slices (Bordey and Sontheimer 1999), gliomas (Patt et al. 1996; Labrakakis et al. 1997, 1998; Bordey and Sontheimer 1998a) and glial cells associated with epileptic seizure foci (Bordey and Sontheimer 1998b) demonstrate a slow glial 'spike', A-currents may subsequently be activated in response to rapid NT-depolarization with a concomitant glial 'spike', which typically depolarizes cells up to -20 or 0 mV, well above threshold for activation of A-currents (Fig. 4.1). The lack of

this slow glial 'spike' in the majority of mature astrocytes is thought to be a result of significant inward rectifying K^+ channels as glial cells begin to demonstrate 'spike' phenomena when inward K^+ currents are blocked with low concentrations of Ba^{2+} (Bordey and Sontheimer 1998a, 1999). Interestingly, glutamate (AMPA) receptor activation in mouse hippocampal CA1 astrocytes demonstrates a concomitant block of inwardly rectifying K^+ currents (Schroder et al. 2002) thought to be mediated by increases in intracellular Na^+. Together, this suggests that in the confines of the synaptic cleft or small extracellular environment, rapid glutamatergic synapse activity (<3 ms; Seifert and Steinhauser 1995; Matthias et al. 2003) with block of inwardly rectifying K^+ currents may, at high frequency, lead to the development of a slow glial 'spike' similar to that seen in Figure 4.1A and B, with subsequent A-current and delayed current activation for rapid repolarization. Therefore, it may be that the glial 'spike' plays a role in potentiating and accelerating NT-mediated membrane oscillations, enabling astrocytic membrane responses to better mirror synaptic events (Fig. 6.2). Support for this will undoubtedly need to come from studies in live animals or acutely isolated slice preparations where functional synapses remain intact. One must remember, as noted earlier regarding channel localization, a possibility for lack of the glial 'spike' *in situ* could be due to localization of Na^+ and K^+ channels to distant processes where spiking may not be seen as a result of space-clamp control issues. Dual electrophysiological recordings and/or multi-photon confocal imaging techniques provide the resolution required to observe astrocyte membrane responses to synaptic or axonal firing events, with perhaps the additional ability to correlate astrocyte membrane responses using voltage-sensitive dyes with calcium signaling.

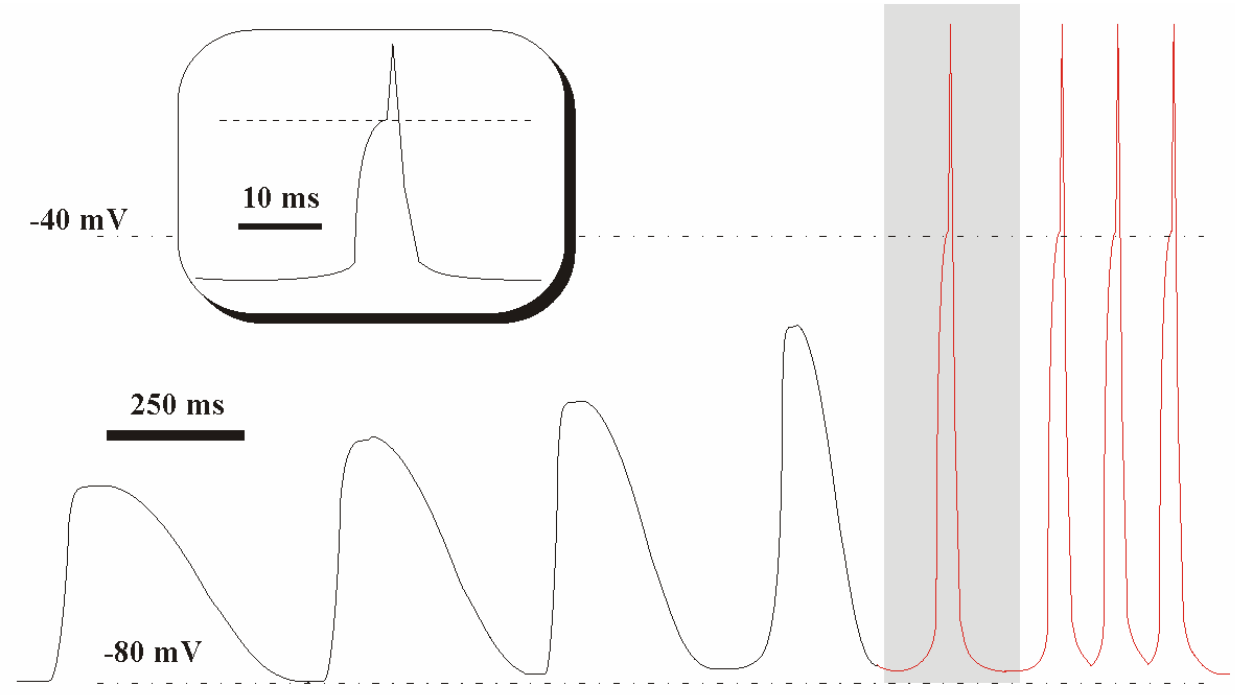

Figure 6.2. Hypothetical representation of increasing frequency of synaptic glutamatergic responses in a glial cell process. With subsequent glutamate responses leading to increasing amplitude of depolarizations, due to secondary longer lasting effects on reducing K^+ conductance, threshold for voltage-gated Na^+ and both inactivating and non-inactivating Kv channels may be reached enabling rapid repolarization for even higher frequency responses. The inset is an expanded time scale view of the lightly shaded membrane response.

6.2 Towards understanding the mechanisms behind anion-mediated alterations in Kv channel gating

Chloride is the most abundant biologically available anion in cells. Work originally carried out in skeletal muscle and erythrocytes led to chloride being regarded as having a thermodynamically passive and unspecialized role. However, over time it was discovered that chloride is used by transport systems as the neutralizing co-ion for cations and as a counter-ion in anion exchange mechanisms. Furthermore, in contrast to all other biological ions, chloride resting concentration shows considerable variation among different mammalian cell types, ranging from 3 mM in skeletal muscle to values as high as 40-50 mM in smooth and cardiac muscle (Chipperfield and Harper 2000). Glial cells in the brain also demonstrate variable intracellular chloride concentrations ranging from 29 to 46 mM (Kimelberg 1981; Kettenmann et al. 1987; Walz and Mukerji 1988; Bevensee et al. 1997; Bekar and Walz 2002) in astrocytes compared to 2-3 mM accumulation above a passive distribution of ~10 mM in oligodendrocytes (Hoppe and Kettenmann, 1989). In addition to variable concentrations in different cell types, chloride equilibrium can change throughout the lifespan of the cell. Neurons in the hippocampus have an intracellular chloride concentration with a depolarizing equilibrium potential during the first two weeks of development that later becomes hyperpolarizing (Cherubini et al. 1991). The wide range of chloride equilibrium potentials found among the different cell types suggests that chloride may play a functional role in cellular signaling processes.

Evidence is accumulating for a role of intracellular chloride concentration in modulation of ion channels and other cellular processes.

- Calcium-activated, non-selective cation channels in lung epithelium show an increased open probability to decreased intracellular chloride concentration (Tohda et al. 1994).
- In intralobular duct cells of mouse salivary glands, increased intracellular chloride concentration resulted in an increase in sodium conductance (Dinudom et al. 1993).
- In shark rectal gland a reduction in $[Cl^-]_i$ activates the Na-K-Cl cotransporter whereas an increase in $[Cl^-]_i$ blocks activation (Lytle and Forbush 1996). This mechanism is based on a direct interaction of chloride with regulatory phosphorylation of the transporter.
- Chloride has a stimulatory effect on CFTR activation, independent of its regulation by cAMP (Wang et al. 1993).
- Anions like Cl^- from the halide series have been shown to alter affinity of G-protein βγ-subunit binding with the α-subunit in various cell types (Higashijima et al. 1987; Lenz et al. 1997).
- In an early study, Adams and Oxford (1983) showed that inorganic anions could modify a delayed rectifying K^+ channel gating mechanism in squid giant axons.
- Others have shown that Cl^- exerts an allosteric-like effect that does not depend on binding, but to neutralization of electrostatic repulsion of positive charges in the hemoglobin-binding cavity (Perutz et al. 1994).
- Reduction of intracellular chloride concentration by 10 mM in photoreceptors of salamander retina significantly decreased L-type-like calcium currents and synaptic transmission (Thoreson et al. 1997), as well as reduced delayed outward rectifying and inward rectifying potassium currents (Thoreson and Stella 2000).
- Anions affect hydrophobic interactions in peptides through charge screening that can alter 3-dimensional conformation (Jelesarov et al. 1998).

Although chloride is implicated in many cellular processes, a physiologically significant role of this ion as an intracellular modulator of channel function has not been convincingly demonstrated. Nevertheless, the studies showing chloride-dependent effects provide a rationale for further investigation of a potentially novel role for chloride ions in modulation of cellular functions.

The $GABA_A$-mediated block of outward K^+ currents in astrocytes is found both *in situ* and *in vitro* (Bekar et al. 1999). The experiments described here are the first to demonstrate a selective effect of Cl^- on inactivating A-type outward K^+ currents in animal cells. The Cl^- specific effect is a physiological response to $GABA_A$ receptor activation and opening of the Cl^- channel pore (Bekar and Walz 1999). Although a similar but non-selective block of both voltage-gated outward K^+ currents (inactivating A-type and delayed-type) is mediated via Na^+ entry through the kainate subtype of the glutamate ionotropic receptor (Robert and Magistretti 1997), it is not clear how anion concentration can impact cation channel (Kv) properties. The experiments in this thesis, consistent with effects on voltage-gated Ca^{2+} channels in salamander retina (Thoreson and Stella 2000), demonstrate that anion concentration directly affects channel gating through a process that is related to the anions' lyotropic or Hofmeister physical characteristics (described in more detail in section 6.2.3).

6.2.1 Muscimol-mediated effects on Kv currents are dependent on intracellular anion concentration

In support of a Cl^- specific mechanism, the muscimol-mediated block of K^+ conductance showed Cl^- concentration dependent effects on the inactivating A-type channel specifically. Furthermore, the block appears most sensitive at the lower intracellular Cl^- concentrations (Fig. 5.1B; 20-40 mM), consistent with the estimated average intracellular Cl^- concentration of 29 mM obtained from experiments using the more physiological gramicidin perforated patch configuration. However, the Cl^- concentration range most sensitive to muscimol appears to be inconsistent with the concentration range affecting A-type currents under static Cl^- whole cell conditions (Fig. 5.1A; 138-80 mM). This discrepancy cannot be explained, but the change in concentration itself may be more important than the actual equilibrated concentration. Nevertheless, statistical analysis of K^+ currents under static Cl^- concentrations still supports a Cl^- concentration effect on the A-type current only. Additional support for a Cl^- specific effect was demonstrated using anion substitution experiments where I^- replaced Cl^- (Fig. 5.2). Iodide displayed similar effects on K^+ currents to that of Cl^-, although with altered affinity characteristics that are probably related to differences in charge density between the two anion species (Discussed in section 6.2.3; Dani et al. 1983; MacKinnon et al. 1989). Gramicidin experiments confirm that the effect on A-type current occurs at physiological Cl^- concentrations, and also demonstrate the insignificance of pipette Cl^- concentration dialysis. The effective block of the A-type current in response to muscimol under gramicidin perforated patch (no dialysis) is not significantly different than the block under whole cell (Cl^- dialysis) conditions (Fig. 5.3D). This suggests that the change in Cl^- concentration is highly localized to the channel region and is largely unaffected by Cl^- from the patch pipette.

The above-mentioned Cl^--mediated effects logically lead to the question: What physiological or pathological internal Cl^- concentration changes do astrocytes experience? As previously stated, Cl^- effects on K^+ currents are most pronounced at physiological Cl^- concentrations. A decrease in intracellular Cl^- concentration occurs in astrocytes as a result of GABA receptor channel activation (Bekar et al. 1999; Bekar and Walz 1999). Increases in

intracellular Cl^- are most likely associated with increases of intracellular KCl as a result of exposure to various amounts of excess extracellular K^+ (Walz 2000). The largest exposure would occur during waves of spreading depression, when the extracellular K^+ concentration can be as high as 80 mM (Irwin and Walz 1999). Simulating such situations in cell culture with radioactive analysis of water and Cl^- movements led to an estimated increase in Cl^- concentration of 40-50 mM within 2 minutes (Walz 1987; Walz and Mukerji 1988). Smaller internal Cl^- concentration changes are sure to occur during physiological spatial buffering and siphoning activities.

As mentioned in the introduction to section 6.2, several studies using various preparations have shown Cl^- concentration-dependent effects. The three studies most pertinent to the work in this thesis were those by Perutz et al. (1994), Jelesarov et al. (1998) and Thoreson and Stella (2000). Perutz et al. (1994) showed that Cl^- exerts an allosteric-like effect on hemoglobin oxygen affinity that does not depend on binding, but rather neutralization of electrostatic repulsion of positive charges in the hemoglobin-binding cavity. Jelesarov et al. (1998) showed that salts, anions in particular, affect hydrophobic interactions in peptides that can alter 3-dimensional conformation. Thoreson and Stella (2000) demonstrated in vertebrate photoreceptors a Cl^- specific regulation of Ca^{2+} channel open probability that was attributed to anion interactions at the membrane/protein surface (Thoreson and Stella, 2000). All three studies are consistent with the lyotropic or Hofmeister anion series, where charge density determines ion mobility at water-solute interfaces (Collins and Washabaugh 1985; Collins 2004).

6.2.2 Alterations in N-terminal T1 domain conformation can affect voltage-gating kinetics

As all the Kv channel family members are made up of four subunits (six transmembrane domains) with highly conserved membrane spanning and tetramerization domains (Kreusch et al. 1998; Coetzee et al. 1999), differences in channel gating kinetics must be due to small changes in protein sequence or interactions with additional proteins that alter channel conformation in such a way as to affect field potentials across the 'S4' voltage sensor. Scanning mutagenesis studies have shown that polar amino acids in the tetramerization (T1) domain of *Shaker* Kv1 channels can have a large impact on channel gating kinetics (Cushman et al. 2000; Minor et al. 2000). It is highly unusual for the T1 domain (protein-protein interaction site) to contain so many buried polar residues. In fact, most protein interaction complexes are composed of nonpolar, closely-packed residues (Jones and Thornton 1997). "The polar nature of the residues in the T1 interface is strongly conserved (Kreusch et al. 1998), suggesting that the stability penalties incurred by these types of interactions are balanced against a strong functional requirement" (Minor et al. 2000). Indeed, replacement of the T1 domain with a four stranded coiled-coil resulted in dramatically altered gating kinetics of the channel, suggesting the T1 structure functions in channel gating (Minor et al. 2000). Minor et al. (2000) proposed that a conformational change in the T1 domain is coupled to voltage sensing through alterations in local field potentials (see Fig. 6.3A for illustration). Mutational analysis of several polar residues on the outside of the C-terminal end of the T1 domain (T50, F77, D79, Q93, V102, D107 and E111; Fig. 6.3B), which are accessible for interaction with other parts of the channel including the voltage sensor, affect gating kinetics and thereby couple the T1 structure to channel gating. Sequence alignments of T1 domains from several Kv channel subunits demonstrate consistent polar residue positioning among the different subunits used in the present studies. The most pertinent point with regards to experiments presented in this thesis is that Minor et al. (2000) also showed that small changes in conformation, produced by a mutation of the buried polar residue T46 (Fig. 6.3B open box) that

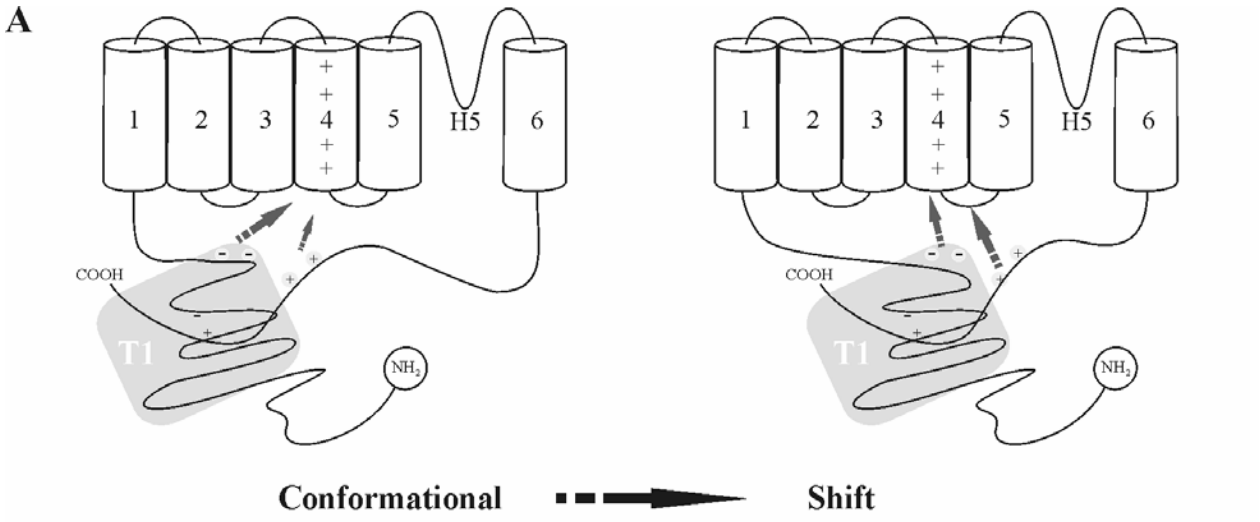

Figure 6.3. Simplified schematic demonstrating how conformation of the T1/C-terminal complex can impact the field potential across the S4 voltage-sensor. A) Charges in the C-terminal interact and modulate T1 conformation and charges in both the T1and C-terminal can influence voltage-gating kinetics. Screening of charges with ions or binding of accessory proteins/cytoskeleton all impact conformation of cytoplasmic structure of Kv channels, possibly modulating gating kinetics. B) Sequence alignments of ~75 residues of the T1 domains of different Kv channels illustrating the residues (grey boxes) on the outermost face of the T1 domain capable of affecting surface field potentials across the channel. Alanine replacement of these polar residues resulted in alterations of channel gating kinetics (Minor et al. 2000). The open box represents a buried polar residue that when mutated results in a small change in T1 conformation resulting in a shift of gating kinetics mediated through charges on the surface (grey boxes).

does not interact with the voltage sensor directly, can change the energetic coupling of the outside polar residues (mentioned above) with the voltage gate, altering half-activation kinetics. Therefore, binding of any protein to the T1 domain that alters its conformation may have an impact on channel gating kinetics.

6.2.3 Cytoskeletal interaction and anion concentration may impact T1 domain conformation and indirectly affect voltage-gating kinetics

The seeming importance of even minute changes in N-terminal conformation (T1 in particular) on channel gating provides enormous opportunity for modulation of channel behavior. Binding of accessory cytoplasmic or membrane proteins, interaction with cytoskeletal elements as well as simple phosphorylation may all serve to alter N-terminal T1 domain conformation. The effects of chloride on steady-state activation and/or inactivation kinetics in both astrocytes and HEK cells presented in this thesis may be accounted for by small conformational changes in

the Kv channel N-terminal T1 domain such as those demonstrated by Cushman et al. (2000) and Minor et al. (2000) in response to anion-mediated charge screening (Curtis et al. 1998; Jelesarov et al. 1998). Anion-mediated charge screening was shown to affect 3-dimensional folding of a negatively charged peptide into a coiled-coil (leucine zipper; Jelesarov et al. 1998) that was consistent with the lyotropic or Hofmeister series, which predicts that SO_4^{2-} and F^- are equally less effective at approaching protein-water interfaces than $Cl^- < NO_3^- < Br^- < I^- < SCN^-$ (Collins and Washabaugh 1985; Washabaugh and Collins 1986; Jelesarov et al. 1998; Collins 2004). In other words, the effect has to do with relative mobilities of anions in solution (waters of hydration). Consequently, these results demonstrate that anion concentrations play a significant role in conformational stability of charged protein structures; such as the Kv channel T1 domain. A recent study by Hatano et al. (2004) provides strong evidence that the N-terminal side of the C-terminal also plays a large role in voltage gating kinetics in the Kv4 subfamily, possibly through electrostatic interaction with the T1 domain. This may mean that both the C-terminal and T1 domain form a quaternary complex that together controls the electrostatic field potential across the voltage sensor (Fig. 6.3A). Together, this means that with small (perhaps even large) changes in Cl^- concentration in the vicinity of the membrane in response to $GABA_A$ receptor opening, changes in T1/C-terminal conformation, and the resulting changes in field potentials across the channel voltage sensor, could explain rapid changes in gating kinetics seen in astrocytes in the present studies. Support for this hypothesis can be found in anion replacement experiments where iodide demonstrated an increased sensitivity for modulation of Kv currents, as effects were seen at lower concentrations (Fig. 5.2A). This increased sensitivity to iodide followed the lyotropic or Hofmeister anion series in which ions to the right of Cl^- have a weaker charge density and therefore have weaker interactions with water and as a result are able to approach proteins for screening charges with greater ease.

Additional support for an anion effect on gating kinetics in astrocytes is demonstrated in isolated Kv channel expression studies in HEK cells. However, a Cl^- effect was only revealed after cytoskeletal interactions with the Kv channels were interrupted (Fig. 5.6). Also worthy of noting in HEK cells is that, in contrast to the depolarizing shift in astrocytic activation kinetics (Fig 5.4), Kv channels showed a hyperpolarizing shift under low Cl^- conditions (Fig. 5.6). This may be related to charges in the C-terminal, as Hatano et al. (2004) demonstrated a hyperpolarizing shift in mutational studies of two positively charged arginines in the C-terminal of Kv4.2/4.3. However, anion screening of these two charges cannot account for what is observed in HEK cells because, if it were the case, the adjustment to lower Cl^- conditions should result in a corresponding depolarizing shift. Further studies are needed in order to understand this disparity, but it may be possible that accessory proteins, differing cytoskeletal interactions or the heterogeneous Kv channel population are responsible in astrocytes.

The presence of a Cl^- concentration-dependent effect on Kv channels expressed in HEK293 cells only after cytoskeletal disruption (Fig. 5.6) suggests that cytoskeletal elements may bind and stabilize the T1/N-terminal conformation in this cell preparation. Consistent with this, Cukovic et al. (2001) demonstrated that both Kv1.4 and Kv1.5 bind to the cytoskeleton through α-actinin-2 mediated interactions with the initial segment of the T1 domain. However, in contrast to the low Cl^- experimental conditions in this thesis, they demonstrated that disruption of this cytoskeletal interaction with use of the antibiotic cytochalasin D had no impact on gating kinetics of Kv1.5 (Maruoka et al. 2000) or Kv4.2 (Wang et al. 2004). The most probable reason for this is that high Cl^- concentrations were used in their whole-cell pipette solutions. In the present study, no effect on gating kinetics under high Cl^- conditions were seen either (Fig. 5.6 inset), suggesting that the high, non-physiological Cl^- concentrations commonly used in whole-cell

patch-clamp studies screen the charges most sensitive under lower physiological Cl^- conditions. Additional support for a conformational change in T1 with protein binding is the notable hyperpolarizing shift in activation kinetics of Kv1.5 with binding of Kvβ1.3 (Uebele et al. 1998; Kwak et al. 1999a, b), Kvβ1.2 (Accili et al. 1997) or Kvβ2.1 (Uebele et al. 1996) to the T1 domain. As noted earlier the Kvβ1.2/3 subunits contain an N-terminal inactivation 'ball and chain', whereas the Kvβ2.1 does not. This may mean that binding of Kvβ1.3 or Kvβ2.1 to the T1 domain alters its conformation resulting in a change of the electrostatic field potential across the voltage sensor via the polar residues on the outside face of the T1 three-dimensional structure as described by Minor et al. (2000). Furthermore, rapid N-terminal inactivation is not required for an effect on gating as when the inactivation ball domain is removed from Kvβ1.2 or Kvβ1.3, with loss of fast inactivation, there is no impact on the hyperpolarizing shift in activation kinetics (Accili et al. 1997 and Uebele et al. 1998, respectively). Of course, a role of C-terminal polar residues must not be ruled out as it has been shown to interact with the N-terminal T1 domain as well (Hatano et al. 2004; Fig. 6.3A).

6.2.4 Modulation of cytoskeletal-Kv channel interaction in astrocytes does not account for anion-mediated effects

Although cytoskeletal disruption in astrocytes does not remove the effect of chloride on Kv channel gating, it significantly reduces sensitivity and removes the selectivity for inactivating A-type currents. These effects most likely have nothing to do with chloride-mediated modulation of gating kinetics, but rather remove co-localization of inactivating Kv subunits with $GABA_A$ receptor channels. This can be seen in the much more dramatic decrease in amplitude of the normalized block of A-type currents (Fig. 5.7B). Under cytoskeletal disruptive conditions, changes in intracellular Cl^- concentration in response to $GABA_A$ channel opening must travel a similar distance to that of delayed Kv channels in order to exert an effect on channel gating kinetics and thereby amplitude of block (Fig. 5.7). In support of this mislocalization hypothesis, it is worth noting that the $GABA_A$ current density increased after cytoskeleton disruption (data not shown). This may be consistent with cytoskeletal disruption preventing localization of receptor channels to astrocytic cell processes where current clamp is limited (Fraser et al. demonstrated localization of the $GABA_A$ receptor to cell soma and distant cell processes; 1995).

6.2.5 Anion (salt) concentrations appear to play a fundamental role in protein function and should therefore be more commonly considered when designing and interpreting experiments

It has been well established that both ion selective filtration and voltage "sensing" are susceptible to surface electrostatic changes or electrolyte screening (MacKinnon et al. 1989; Green and Andersen 1991). Furthermore, as discussed earlier (section 6.2), chloride has also been shown to affect function of other cellular proteins as well as conformational changes in 3-dimensional protein structures (Jelesarov et al. 1998). Anion impact on protein conformation seems to have almost unlimited potential for modulation of many cellular enzymes and structures. Therefore, it is becoming increasingly more difficult to ignore the impact anions have in cellular function and especially in experimental solutions. The cytoskeletal impact on gating kinetics under low chloride conditions of Kv channels in HEK cells shown in this study, compared to finding no cytoskeletal effect on kinetics under high chloride conditions in the study by Wang et al. (2004), is a prime example of how anion concentrations can impact findings and interpretations.

7.0 - CONCLUSIONS

Based on studies of cultured hippocampal astrocytes herein, the following conclusions can be made:

- Electrophysiological recordings from astrocytes demonstrate that inactivating potassium currents are comprised of Kv4 (~70%), Kv3 (~10%) and Kv1 (<5%) α-subunits with additional KChIP (possibly Ca^{2+}-sensitive) modulation.
- Astrocytes target A-type subfamily members to different subcellular locations, possibly for functional purposes similar to targeting of Kv channels seen in neurons. Future studies are required to address this function in more detail; perhaps using imaging with voltage-sensitive dyes to better visualize what is happening in glial processes.
- Inactivating A-type currents in astrocytes may enable large membrane oscillations at high frequency, possibly to allow synchronized responses to high frequency synaptic events.

Expression of multiple voltage gated channel currents in the so-called 'non-excitable' astrocyte may seem paradoxical at first, but might provide astrocytes with the ability to establish rapid membrane oscillations in response to high K^+ and neurotransmitter release from rapid firing neurons. During extracellular K^+ accumulation astrocytes would take up KCl (thereby increasing internal Cl^-) that may serve to increase A-type channel activity (higher $[Cl^-]_i$, larger A-current amplitude in astrocytes in these studies) allowing improved and more rapid control of astrocytic membrane repolarization. The ability to mirror neuronal activity may allow astrocytes to maintain membrane depolarization gradients across the glial syncytium for K^+ buffering and siphoning capability. In addition to the rapid membrane voltage oscillations, under high frequency firing conditions or ligand mediated effects on Kv channels, summation of oscillations may lead to sustained membrane depolarizations resulting in increased intracellular Ca^{2+} signaling. This signaling may lead to feedback signaling to neurons for potentiation or depression of synaptic events or for regulation of blood flow. Further investigations into the role of specific glial ion currents in cellular processes such as long-term potentiation and depression, regulation of blood flow, migration, changes in cell morphology, and reactive gliosis are necessary to elucidate potential roles for voltage-gated channels in cell signaling processes.

Based on studies of anion-mediated effects on Kv channels both in astrocytes and in isolation in HEK293 cells, the following conclusions can be made:

- $GABA_A$-mediated effects on Kv currents in astrocytes are dependent on intracellular anion concentration and are consistent with the lyotropic or Hofmeister series relating charge density to waters of hydration and ease of approach to water-solute interfaces.
- As alterations in N-terminal T1 domain conformation can affect voltage-gating kinetics and anions are able to screen polar residues in proteins that modulate conformation, it is proposed that anion concentration changes lead to changes in Kv channel voltage-gating kinetics.

- Similarly, as cytoskeletal interactions with the T1 domain affect voltage-gating kinetics in HEK cells in the present studies, it is proposed that cytoskeletal binding alters the conformation of the T1/C-terminal quaternary protein complex.
- The selective $GABA_A$-mediated block of inactivating Kv currents in astrocytes is related to cytoskeletal colocalization, but not anion-mediated alterations of the cytoskeletal interaction with inactivating Kv channels specifically.

Taken together, the present studies demonstrate voltage-gated K^+ channel activity to be highly electrostatic in nature and validate the possibility that anions alter or screen electrostatic charges on or near the voltage "sensor", thereby affecting channel kinetics. Thoreson and Stella (2000) found an almost identical scenario in their retinal preparation with anion effects on voltage-gated Ca^{2+} channels suggesting anion concentrations are not merely passive charge neutralizers.

In summary, these results indicate that hippocampal astrocytes *in vitro* express multiple A-type Kv channel α-subunits with accessory, possibly Ca^{2+}-sensitive, cytoplasmic subunits that appear to be specifically localized to subcellular compartments. Furthermore, it is hypothesized that these channels, possibly in concert with glial voltage-gated Na^+ channels, enable astrocytes to respond rapidly with membrane voltage oscillations to high frequency signals, perhaps synchronizing glial functions with neuronal activity. Results also indicate that anion concentrations are important to proper function and modulation of Kv channel gating kinetics.

8.0 - REFERENCES

Abbott GW, Goldstein SA, Sesti F (2001) Do all voltage-gated potassium channels use MiRPs? Circ Res 88:981.

Abbott NJ (2002) Astrocyte-endothelial interactions and blood-brain barrier permeability. J Anat 200:629.

Accili EA, Kiehn J, Yang Q, Wang Z, Brown AM, Wible BA (1997) Separable Kvbeta subunit domains alter expression and gating of potassium channels. J Biol Chem 272:25824.

Adams DJ, Oxford GS (1983) Interaction of internal anions with potassium channels of the squid giant axon. J Gen Physiol 82:429.

Aiyar J, Nguyen AN, Chandy KG, Grissmer S (1994) The P-region and S6 of Kv3.1 contribute to the formation of the ion conduction pathway. Biophys J 67:2261.

Alkayed NJ, Birks EK, Hudetz AG, Roman RJ, Henderson L, Harder DR (1996) Inhibition of brain P-450 arachidonic acid epoxygenase decreases baseline cerebral blood flow. Am J Physiol 271:H1541.

An WF, Bowlby MR, Betty M, Cao J, Ling HP, Mendoza G, Hinson JW, Mattsson KI, Strassle BW, Trimmer JS, Rhodes KJ (2000) Modulation of A-type potassium channels by a family of calcium sensors. Nature 403:553.

Anderson CM, Swanson RA (2000) Astrocyte glutamate transport: review of properties, regulation, and physiological functions. Glia 32:1.

Araque A, Carmignoto G, Haydon PG (2001) Dynamic signaling between astrocytes and neurons. Annu Rev Physiol 63:795.

Araque A, Parpura V, Sanzgiri RP, Haydon PG (1998a) Glutamate-dependent astrocyte modulation of synaptic transmission between cultured hippocampal neurons. Eur J Neurosci 10:2129.

Araque A, Sanzgiri RP, Parpura V, Haydon PG (1998b) Calcium elevation in astrocytes causes an NMDA receptor-dependent increase in the frequency of miniature synaptic currents in cultured hippocampal neurons. J Neurosci 18:6822.

Araque A, Parpura V, Sanzgiri RP, Haydon PG (1999) Tripartite synapses: glia, the unacknowledged partner. Trends Neurosci 22:208.

Aronica E, Troost D, Rozemuller AJ, Yankaya B, Jansen GH, Isom LL, Gorter JA (2003) Expression and regulation of voltage-gated sodium channel beta1 subunit protein in human gliosis-associated pathologies. Acta Neuropathol (Berl) 105:515.

Ashcroft FM (2000) Voltage-gated K+ Channels. In: Ion channels and Disease: Channelopathies (Ashcroft FM, ed), pp 97-123. New York: Academic Press.

Attali B, Wang N, Kolot A, Sobko A, Cherepanov V, Soliven B (1997) Characterization of delayed rectifier Kv channels in oligodendrocytes and progenitor cells. J Neurosci 17:8234.

Bahring R, Boland LM, Varghese A, Gebauer M, Pongs O (2001) Kinetic analysis of open- and closed-state inactivation transitions in human Kv4.2 A-type potassium channels. J Physiol 535:65.

Ballanyi K, Grafe P, ten Bruggencate G (1987) Ion activities and potassium uptake mechanisms of glial cells in guinea-pig olfactory cortex slices. J Physiol 382:159.

Barres BA, Chun LL, Corey DP (1990) Ion channels in vertebrate glia. Annu Rev Neurosci 13:441-74.:441.

Bauer HC, Bauer H (2000) Neural induction of the blood-brain barrier: still an enigma. Cell Mol Neurobiol 20:13.

Beck EJ, Bowlby M, An WF, Rhodes KJ, Covarrubias M (2002) Remodelling inactivation gating of Kv4 channels by KChIP1, a small-molecular-weight calcium-binding protein. J Physiol 538:691.

Bekar LK, Walz W (1999) Evidence for chloride ions as intracellular messenger substances in astrocytes. J Neurophysiol 82:248.

Bekar LK, Jabs R, Walz W (1999) GABAA receptor agonists modulate K+ currents in adult hippocampal glial cells in situ. Glia 26:129.

Bekar LK, Walz W (2002) Intracellular chloride modulates A-type potassium currents in astrocytes. Glia. 39:207.

Bevensee MO, Apkon M, Boron WF (1997) Intracellular pH regulation in cultured astrocytes from rat hippocampus. II. Electrogenic Na/HCO3 cotransport. J Gen Physiol 110:467.

Bixby KA, Nanao MH, Shen NV, Kreusch A, Bellamy H, Pfaffinger PJ, Choe S (1999) Zn2+-binding and molecular determinants of tetramerization in voltage-gated K+ channels. Nat Struct Biol 6:38.

Black JA, Westenbroek R, Ransom BR, Catterall WA, Waxman SG (1994) Type II sodium channels in spinal cord astrocytes in situ: immunocytochemical observations. Glia 12:219.

Black JA, Westenbroek R, Minturn JE, Ransom BR, Catterall WA, Waxman SG (1995) Isoform-specific expression of sodium channels in astrocytes in vitro: immunocytochemical observations. Glia 14:133.

Boland LM, Jiang M, Lee SY, Fahrenkrug SC, Harnett MT, O'Grady SM (2003) Functional properties of a brain-specific NH2-terminally spliced modulator of Kv4 channels. Am J Physiol Cell Physiol 285:C161.
Bordey A, Sontheimer H (1997) Postnatal development of ionic currents in rat hippocampal astrocytes in situ. J Neurophysiol 78:461.
Bordey A, Sontheimer H (1998a) Properties of human glial cells associated with epileptic seizure foci. Epilepsy Res 32:286.
Bordey A, Sontheimer H (1998b) Electrophysiological properties of human astrocytic tumor cells In situ: enigma of spiking glial cells. J Neurophysiol 79:2782.
Bordey A, Sontheimer H (1999) Differential inhibition of glial K(+) currents by 4-AP. JNeurophysiol 82:3476.
Bordey A, Sontheimer H (2000) Ion channel expression by astrocytes in situ: comparison of different CNS regions. Glia 30:27.
Borges K, Kettenmann H (1995) Blockade of K+ channels induced by AMPA/kainate receptor activation in mouse oligodendrocyte precursor cells is mediated by Na+ entry. J Neurosci Res 42:579.
Brown AM, Baltan Tekkok S, Ransom BR (2004) Energy transfer from astrocytes to axons: the role of CNS glycogen. Neurochem Int 45:529.
Brown AM, Sickmann HM, Fosgerau K, Lund TM, Schousboe A, Waagepetersen HS, Ransom BR (2005) Astrocyte glycogen metabolism is required for neural activity during aglycemia or intense stimulation in mouse white matter. J Neurosci Res 79:74.
Burke NA, Takimoto K, Li D, Han W, Watkins SC, Levitan ES (1999) Distinct structural requirements for clustering and immobilization of K+ channels by PSD-95. J Gen Physiol 113:71.
Buzsaki G, Haas HL, Anderson EG (1987) Long-term potentiation induced by physiologically relevant stimulus patterns. Brain Res 435:331.
Caballero R, Gomez R, Moreno I, Nunez L, Gonzalez T, Arias C, Guizy M, Valenzuela C, Tamargo J, Delpon E (2004) Interaction of angiotensin II with the angiotensin type 2 receptor inhibits the cardiac transient outward potassium current. Cardiovasc Res 62:86.
Cantiello HF, Stow JL, Prat AG, Ausiello DA (1991) Actin filaments regulate epithelial Na+ channel activity. Am J Physiol 261:C882.
Chen C, Magee JC, Bazan NG (2002) Cyclooxygenase-2 regulates prostaglandin E2 signaling in hippocampal long-term synaptic plasticity. J Neurophysiol 87:2851.
Chen KC, Nicholson C (2000) Spatial buffering of potassium ions in brain extracellular space. Biophys J 78:2776.
Cherubini E, Gaiarsa JL, Ben Ari Y (1991) GABA: an excitatory transmitter in early postnatal life. Trends Neurosci 14:515.
Chesler M (1990) The regulation and modulation of pH in the nervous system. Prog Neurobiol 34:401.
Chipperfield AR, Harper AA (2000) Chloride in smooth muscle. Prog Biophys Mol Biol 74:175.
Christie JM, Westbrook GL (2003) Regulation of backpropagating action potentials in mitral cell lateral dendrites by A-type potassium currents. J Neurophysiol 89:2466.
Ciorba MA, Heinemann SH, Weissbach H, Brot N, Hoshi T (1999) Regulation of voltage-dependent K+ channels by methionine oxidation: effect of nitric oxide and vitamin C. FEBS Lett 442:48.
Coetzee WA, Amarillo Y, Chiu J, Chow A, Lau D, McCormack T, Moreno H, Nadal MS, Ozaita A, Pountney D, Saganich M, Vega-Saenz de Miera E, Rudy B (1999) Molecular diversity of K+ channels. Ann N Y Acad Sci 868:233.
Collins KD (2004) Ions from the Hofmeister series and osmolytes: effects on proteins in solution and in the crystallization process. Methods 34:300.
Collins KD, Washabaugh MW (1985) The Hofmeister effect and the behaviour of water at interfaces. Q Rev Biophys 18:323.
Cornell-Bell AH, Finkbeiner SM, Cooper MS, Smith SJ (1990) Glutamate induces calcium waves in cultured astrocytes: long-range glial signaling. Science 247:470.
Cotrina ML, Nedergaard M (2005) Intracellular calcium control mechanisms in glia. In: Neuroglia, 2nd Edition (Kettenmann H, Ransom B, eds), pp 229-239. New York: Oxford University Press.
Cukovic D, Lu GW, Wible B, Steele DF, Fedida D (2001) A discrete amino terminal domain of Kv1.5 and Kv1.4 potassium channels interacts with the spectrin repeats of alpha-actinin-2. FEBS Lett 498:87.
Curtis RA, Prausnitz JM, Blanch HW (1998) Protein-protein and protein-salt interactions in aqueous protein solutions containing concentrated electrolytes. Biotechnol Bioeng 57:11.
Cushman SJ, Nanao MH, Jahng AW, DeRubeis D, Choe S, Pfaffinger PJ (2000) Voltage dependent activation of potassium channels is coupled to T1 domain structure. Nat Struct Biol 7:403.

D'Ambrosio R, Gordon DS, Winn HR (2002) Differential role of KIR channel and Na(+)/K(+)-pump in the regulation of extracellular K(+) in rat hippocampus. J Neurophysiol 87:87.
D'Ambrosio R, Maris DO, Grady MS, Winn HR, Janigro D (1999) Impaired K(+) homeostasis and altered electrophysiological properties of post-traumatic hippocampal glia. J Neurosci 19:8152.
Dani JA, Sanchez JA, Hille B (1983) Lyotropic anions. Na channel gating and Ca electrode response. J Gen Physiol 81:255.
Dani JW, Chernjavsky A, Smith SJ (1992) Neuronal activity triggers calcium waves in hippocampal astrocyte networks. Neuron 8:429.
Deitmer JW (1996) pH regulation. In: Neuroglia (Kettenmann H, Ransom B, eds), pp 230-245. New York: Raven.
Deitmer JW, Rose CR (1996) pH regulation and proton signalling by glial cells. Prog Neurobiol 48:73.
Dinudom A, Young JA, Cook DI (1993) Na+ and Cl- conductances are controlled by cytosolic Cl- concentration in the intralobular duct cells of mouse mandibular glands. J Membr Biol 135:289.
Duprat F, Guillemare E, Romey G, Fink M, Lesage F, Lazdunski M, Honore E (1995) Susceptibility of cloned K+ channels to reactive oxygen species. Proc Natl Acad Sci U S A 92:11796.
Edwards L, Nashmi R, Jones O, Backx P, Ackerley C, Becker L, Fehlings MG (2002) Upregulation of Kv 1.4 protein and gene expression after chronic spinal cord injury. J Comp Neurol 443:154.
Eldstrom J, Doerksen KW, Steele DF, Fedida D (2002) N-terminal PDZ-binding domain in Kv1 potassium channels. FEBS Lett 531:529.
Elinder F, Arhem P (1998) The functional surface charge density of a fast K channel in the myelinated axon of Xenopus laevis. J Membr Biol 165:175.
Elinder F, Arhem P (1999) Role of individual surface charges of voltage-gated K channels. Biophys J 77:1358.
England SK, Uebele VN, Kodali J, Bennett PB, Tamkun MM (1995) A novel K+ channel beta-subunit (hKv beta 1.3) is produced via alternative mRNA splicing. J Biol Chem 270:28531.
Enkvist MO, McCarthy KD (1994) Astroglial gap junction communication is increased by treatment with either glutamate or high K+ concentration. J Neurochem 62:489.
Evanko DS, Zhang Q, Zorec R, Haydon PG (2004) Defining pathways of loss and secretion of chemical messengers from astrocytes. Glia 47:233.
Fedoroff S, Hall C (1979) Effect of horse serum on neural cell differentiation in tissue culture. In Vitro 15:641.
Fellin T, Carmignoto G (2004) Neurone-to-astrocyte signalling in the brain represents a distinct multifunctional unit. J Physiol 559:3.
Fernandez FR, Morales E, Rashid AJ, Dunn RJ, Turner RW (2003) Inactivation of Kv3.3 potassium channels in heterologous expression systems. J Biol Chem 278:40890.
Ferroni S, Valente P, Caprini M, Nobile M, Schubert P, Rapisarda C (2003) Arachidonic acid activates an open rectifier potassium channel in cultured rat cortical astrocytes. J Neurosci Res 72:363.
Fili O, Michaelevski I, Bledi Y, Chikvashvili D, Singer-Lahat D, Boshwitz H, Linial M, Lotan I (2001) Direct interaction of a brain voltage-gated K+ channel with syntaxin 1A: functional impact on channel gating. J Neurosci 21:1964.
Filosa JA, Bonev AD, Nelson MT (2004) Calcium dynamics in cortical astrocytes and arterioles during neurovascular coupling. Circ Res 95:e73.
Fraser DD, Duffy S, Angelides KJ, Perez-Velazquez JL, Kettenmann H, MacVicar BA (1995) GABAA/benzodiazepine receptors in acutely isolated hippocampal astrocytes. J Neurosci 15:2720.
Gallo V, Zhou JM, McBain CJ, Wright P, Knutson PL, Armstrong RC (1996) Oligodendrocyte progenitor cell proliferation and lineage progression are regulated by glutamate receptor-mediated K^+ channel block. J Neurosci 16:2659.
Gautron S, Gruszczynski C, Koulakoff A, Poiraud E, Lopez S, Cambier H, Dos Santos G, Berwald-Netter Y (2001) Genetic and epigenetic control of the Na-G ion channel expression in glia. Glia 33:230.
Gebauer M, Isbrandt D, Sauter K, Callsen B, Nolting A, Pongs O, Bahring R (2004) N-type inactivation features of Kv4.2 channel gating. Biophys J 86:210.
Gebremedhin D, Yamaura K, Zhang C, Bylund J, Koehler RC, Harder DR (2003) Metabotropic glutamate receptor activation enhances the activities of two types of Ca2+-activated k+ channels in rat hippocampal astrocytes. J Neurosci 23:1678.
Geiger JR, Jonas P (2000) Dynamic control of presynaptic Ca(2+) inflow by fast-inactivating K(+) channels in hippocampal mossy fiber boutons. Neuron 28:927.
Ghiani CA, Yuan X, Eisen AM, Knutson PL, DePinho RA, McBain CJ, Gallo V (1999) Voltage-activated K^+ channels and membrane depolarization regulate accumulation of the cyclin-dependent kinase inhibitors p27(Kip1) and p21(CIP1) in glial progenitor cells. J Neurosci 19:5380.

Gnatenco C, Han J, Snyder AK, Kim D (2002) Functional expression of TREK-2 K+ channel in cultured rat brain astrocytes. Brain Res 931:56.
Green WN, Andersen OS (1991) Surface charges and ion channel function. Annu Rev Physiol 53:341.
Grichtchenko, II, Chesler M (1994) Depolarization-induced alkalinization of astrocytes in gliotic hippocampal slices. Neuroscience 62:1071.
Grosche J, Matyash V, Moller T, Verkhratsky A, Reichenbach A, Kettenmann H (1999) Microdomains for neuron-glia interaction: parallel fiber signaling to Bergmann glial cells. Nat Neurosci 2:139.
Gulbis JM, Zhou M, Mann S, MacKinnon R (2000) Structure of the cytoplasmic beta subunit-T1 assembly of voltage- dependent K+ channels. Science 289:123.
Harbury PB, Zhang T, Kim PS, Alber T (1993) A switch between two-, three-, and four-stranded coiled coils in GCN4 leucine zipper mutants. Science 262:1401.
Harder DR, Alkayed NJ, Lange AR, Gebremedhin D, Roman RJ (1998) Functional hyperemia in the brain: hypothesis for astrocyte-derived vasodilator metabolites. Stroke 29:229.
Hatano N, Ohya S, Muraki K, Clark RB, Giles WR, Imaizumi Y (2004) Two arginines in the cytoplasmic C-terminal domain are essential for voltage-dependent regulation of A-type K+ current in the Kv4 channel subfamily. J Biol Chem 279:5450.
Heinemann SH, Rettig J, Graack HR, Pongs O (1996) Functional characterization of Kv channel beta-subunits from rat brain. J Physiol. 493:625.
Higashijima T, Ferguson KM, Sternweis PC (1987) Regulation of hormone-sensitive GTP-dependent regulatory proteins by chloride. J Biol Chem 262:3597.
Hirase H, Qian L, Bartho P, Buzsaki G (2004) Calcium dynamics of cortical astrocytic networks in vivo. PLoS Biol 2:E96.
Hoffman DA, Johnston D (1998) Downregulation of transient K+ channels in dendrites of hippocampal CA1 pyramidal neurons by activation of PKA and PKC. J Neurosci 18:3521.
Hoffman DA, Magee JC, Colbert CM, Johnston D (1997) K+ channel regulation of signal propagation in dendrites of hippocampal pyramidal neurons. Nature 387:869.
Hofmeister F (1888) Naunyn-Schmiedebergs. Arch Exp Pathol Pharmakol 24:247.
Holmqvist MH, Cao J, Knoppers MH, Jurman ME, Distefano PS, Rhodes KJ, Xie Y, An WF (2001) Kinetic modulation of Kv4-mediated A-current by arachidonic acid is dependent on potassium channel interacting proteins. J Neurosci 21:4154.
Holmqvist MH, Cao J, Hernandez-Pineda R, Jacobson MD, Carroll KI, Sung MA, Betty M, Ge P, Gilbride KJ, Brown ME, Jurman ME, Lawson D, Silos-Santiago I, Xie Y, Covarrubias M, Rhodes KJ, Distefano PS, An WF (2002) Elimination of fast inactivation in Kv4 A-type potassium channels by an auxiliary subunit domain. Proc Natl Acad Sci U S A 99:1035.
Hoppe D, Kettenmann H (1989) Carrier-mediated Cl- transport in cultured mouse oligodendrocytes. J Neurosci Res 23:467.
Ikura M (1996) Calcium binding and conformational response in EF-hand proteins. Trends Biochem Sci 21:14.
Irwin A, Walz W (1999) Spreading depression waves as mediators of secondary injury and of protective mechanisms. In: Cerebral ischemia: molecular and cellular pathophysiology (Walz W, ed), pp 35-44. Totowa: Human Press.
Islas LD, Sigworth FJ (2001) Electrostatics and the gating pore of Shaker potassium channels. J Gen Physiol 117:69.
Jabs R, Kirchhoff F, Kettenmann H, Steinhauser C (1994) Kainate activates Ca(2+)-permeable glutamate receptors and blocks voltage-gated K+ currents in glial cells of mouse hippocampal slices. Pflugers Arch 426:310.
Jan LY, Jan YN (1992) Structural elements involved in specific K+ channel functions. Annu Rev Physiol 54:537.
Jan LY, Jan YN (1997) Cloned potassium channels from eukaryotes and prokaryotes. Annu Rev Neurosci 20:91.
Jelesarov I, Durr E, Thomas RM, Bosshard HR (1998) Salt effects on hydrophobic interaction and charge screening in the folding of a negatively charged peptide to a coiled coil (leucine zipper). Biochemistry 37:7539.
Jerng HH, Covarrubias M (1997) K+ channel inactivation mediated by the concerted action of the cytoplasmic N- and C-terminal domains. Biophys J 72:163.
Jerng HH, Shahidullah M, Covarrubias M (1999) Inactivation gating of Kv4 potassium channels: molecular interactions involving the inner vestibule of the pore. J Gen Physiol 113:641.
Jing J, Peretz T, Singer-Lahat D, Chikvashvili D, Thornhill WB, Lotan I (1997) Inactivation of a voltage-dependent K+ channel by beta subunit. Modulation by a phosphorylation-dependent interaction between the distal C terminus of alpha subunit and cytoskeleton. J Biol Chem 272:14021.

Jing J, Chikvashvili D, Singer-Lahat D, Thornhill WB, Reuveny E, Lotan I (1999) Fast inactivation of a brain K+ channel composed of Kv1.1 and Kvbeta1.1 subunits modulated by G protein beta gamma subunits. EMBO J 18:1245.

Jones S, Thornton JM (1997) Prediction of protein-protein interaction sites using patch analysis. J Mol Biol 272:133.

Jugloff DG, Khanna R, Schlichter LC, Jones OT (2000) Internalization of the Kv1.4 potassium channel is suppressed by clustering interactions with PSD-95. J Biol Chem 275:1357.

Kang J, Jiang L, Goldman SA, Nedergaard M (1998) Astrocyte-mediated potentiation of inhibitory synaptic transmission. Nat Neurosci 1:683.

Kasischke KA, Vishwasrao HD, Fisher PJ, Zipfel WR, Webb WW (2004) Neural activity triggers neuronal oxidative metabolism followed by astrocytic glycolysis. Science 305:99.

Kettenmann H, Steinhauser C (2005) Receptors for neurotransmitters and hormones. In: Neuroglia, 2nd Edition (Kettenmann H, Ransom B, eds), pp 131-145. New York: Oxford University Press.

Kettenmann H, Backus KH, Schachner M (1987) gamma-Aminobutyric acid opens Cl-channels in cultured astrocytes. Brain Res 404:1.

Kim E, Niethammer M, Rothschild A, Jan YN, Sheng M (1995) Clustering of Shaker-type K+ channels by interaction with a family of membrane-associated guanylate kinases. Nature 378:85.

Kimelberg HK (1981) Active accumulation and exchange transport of chloride in astroglial cells in culture. Biochim Biophys Acta 646:179.

Kimelberg HK, Biddlecome S, Bourke RS (1979) SITS-inhibitable Cl- transport and Na+-dependent H+ production in primary astroglial cultures. Brain Res 173:111.

Klausberger T, Marton LF, Baude A, Roberts JD, Magill PJ, Somogyi P (2004) Spike timing of dendrite-targeting bistratified cells during hippocampal network oscillations in vivo. Nat Neurosci 7:41.

Klausberger T, Magill PJ, Marton LF, Roberts JD, Cobden PM, Buzsaki G, Somogyi P (2003) Brain-state- and cell-type-specific firing of hippocampal interneurons in vivo. Nature %20;421:844.

Knutson P, Ghiani CA, Zhou JM, Gallo V, McBain CJ (1997) K^+ channel expression and cell proliferation are regulated by intracellular sodium and membrane depolarization in oligodendrocyte progenitor cells. J Neurosci 17:2669.

Kondo T, Katafuchi T, Hori T (2002) Stem cell factor modulates paired-pulse facilitation and long-term potentiation in the hippocampal mossy fiber-CA3 pathway in mice. Brain Res 946:179.

Konietzko U, Muller CM (1994) Astrocytic dye coupling in rat hippocampus: topography, developmental onset, and modulation by protein kinase C. Hippocampus 4:297.

Kreft M, Stenovec M, Rupnik M, Grilc S, Krzan M, Potokar M, Pangrsic T, Haydon PG, Zorec R (2004) Properties of Ca(2+)-dependent exocytosis in cultured astrocytes. Glia 46:437.

Kreisman NR, Smith ML (1993) Potassium-induced changes in excitability in the hippocampal CA1 region of immature and adult rats. Brain Res Dev Brain Res 76:67.

Kreusch A, Pfaffinger PJ, Stevens CF, Choe S (1998) Crystal structure of the tetramerization domain of the Shaker potassium channel. Nature 392:945.

Kunec S, Bose A (2003) High-frequency, depressing inhibition facilitates synchronization in globally inhibitory networks. Network 14:647.

Kuryshev YA, Gudz TI, Brown AM, Wible BA (2000) KChAP as a chaperone for specific K(+) channels. Am J Physiol Cell Physiol 278:C931.

Kuryshev YA, Wible BA, Gudz TI, Ramirez AN, Brown AM (2001) KChAP/Kvbeta1.2 interactions and their effects on cardiac Kv channel expression. Am J Physiol Cell Physiol 281:C290.

Kwak YG, Navarro-Polanco RA, Grobaski T, Gallagher DJ, Tamkun MM (1999a) Phosphorylation is required for alteration of kv1.5 K(+) channel function by the Kvbeta1.3 subunit. J Biol Chem 274:25355.

Kwak YG, Hu N, Wei J, George AL, Jr., Grobaski TD, Tamkun MM, Murray KT (1999b) Protein kinase A phosphorylation alters Kvbeta1.3 subunit-mediated inactivation of the Kv1.5 potassium channel. J Biol Chem 274:13928.

Labrakakis C, Patt S, Weydt P, Cervos-Navarro J, Meyer R, Kettenmann H (1997) Action potential-generating cells in human glioblastomas. J Neuropathol Exp Neurol. 56:243.

Labrakakis C, Patt S, Hartmann J, Kettenmann H (1998) Glutamate receptor activation can trigger electrical activity in human glioma cells. Eur J Neurosci. 10:2153.

Lascola CD, Nelson DJ, Kraig RP (1998) Cytoskeletal actin gates a Cl- channel in neocortical astrocytes. J Neurosci 18:1679.

Latour I, Gee CE, Robitaille R, Lacaille JC (2001) Differential mechanisms of Ca2+ responses in glial cells evoked by exogenous and endogenous glutamate in rat hippocampus. Hippocampus 11:132.

Latour I, Hamid J, Beedle AM, Zamponi GW, MacVicar BA (2003) Expression of voltage-gated Ca2+ channel subtypes in cultured astrocytes. Glia 41:347.
Laube G, Roper J, Pitt JC, Sewing S, Kistner U, Garner CC, Pongs O, Veh RW (1996) Ultrastructural localization of Shaker-related potassium channel subunits and synapse-associated protein 90 to septate-like junctions in rat cerebellar Pinceaux. Brain Res Mol Brain Res 42:51.
Lenz RA, Pitler TA, Alger BE (1997) High intracellular Cl- concentrations depress G-protein-modulated ionic conductances. J Neurosci 17:6133.
Levin G, Chikvashvili D, Singer-Lahat D, Peretz T, Thornhill WB, Lotan I (1996) Phosphorylation of a K+ channel alpha subunit modulates the inactivation conferred by a beta subunit. Involvement of cytoskeleton. J Biol Chem 271:29321.
Lew TS, Chang CS, Fang KP, Chen CY, Chen CH, Lin SC (2004) The involvement of Kv3.4 voltage-gated potassium channel in the growth of an oral squamous cell carcinoma cell line. J Oral Pathol Med 33:543.
Lewit-Bentley A, Rety S (2000) EF-hand calcium-binding proteins. Curr Opin Struct Biol 10:637.
Li D, Takimoto K, Levitan ES (2000) Surface expression of Kv1 channels is governed by a C-terminal motif. J Biol Chem 275:11597.
Li M, Unwin N, Stauffer KA, Jan YN, Jan LY (1994) Images of purified Shaker potassium channels. Curr Biol 4:110.
Lien CC, Jonas P (2003) Kv3 potassium conductance is necessary and kinetically optimized for high-frequency action potential generation in hippocampal interneurons. J Neurosci 23:2058.
Liu QS, Xu Q, Arcuino G, Kang J, Nedergaard M (2004) Astrocyte-mediated activation of neuronal kainate receptors. Proc Natl Acad Sci USA 101:3172.
Longuemare MC, Rose CR, Farrell K, Ransom BR, Waxman SG, Swanson RA (1999) K(+)-induced reversal of astrocyte glutamate uptake is limited by compensatory changes in intracellular Na+. Neuroscience 93:285.
Lou HC, Edvinsson L, MacKenzie ET (1987) The concept of coupling blood flow to brain function: revision required? Ann Neurol 22:289.
Lytle C, Forbush B, 3rd (1996) Regulatory phosphorylation of the secretory Na-K-Cl cotransporter: modulation by cytoplasmic Cl. Am J Physiol 270:C437.
MacFarlane SN, Sontheimer H (1997) Electrophysiological changes that accompany reactive gliosis in vitro. J Neurosci. 17:7316.
MacFarlane SN, Sontheimer H (2000) Changes in ion channel expression accompany cell cycle progression of spinal cord astrocytes. Glia 30:39.
MacKinnon R, Latorre R, Miller C (1989) Role of surface electrostatics in the operation of a high-conductance Ca2+-activated K+ channel. Biochemistry 28:8092.
Magistretti PJ, Pellerin L, Rothman DL, Shulman RG (1999) Energy on demand. Science 283:496.
Maguire G, Connaughton V, Prat AG, Jackson GR, Jr., Cantiello HF (1998) Actin cytoskeleton regulates ion channel activity in retinal neurons. Neuroreport 9:665.
Manganas LN, Trimmer JS (2000) Subunit composition determines Kv1 potassium channel surface expression. J Biol Chem 275:29685.
Martin DL (1996) The role of glia in the inactivation of neurotransmitters. In: Neuroglia (Kettenmann H, Ransom B, eds), pp 732-745. New York: Raven.
Maruoka ND, Steele DF, Au BP, Dan P, Zhang X, Moore ED, Fedida D (2000) alpha-actinin-2 couples to cardiac Kv1.5 channels, regulating current density and channel localization in HEK cells. FEBS Lett 473:188.
Matsutani S, Yamamoto N (1997) Neuronal regulation of astrocyte morphology in vitro is mediated by GABAergic signaling. Glia 20:1.
Matthias K, Kirchhoff F, Seifert G, Huttmann K, Matyash M, Kettenmann H, Steinhauser C (2003) Segregated expression of AMPA-type glutamate receptors and glutamate transporters defines distinct astrocyte populations in the mouse hippocampus. J Neurosci 23:1750.
McCormack K, McCormack T, Tanouye M, Rudy B, Stuhmer W (1995) Alternative splicing of the human Shaker K+ channel beta 1 gene and functional expression of the beta 2 gene product. FEBS Lett 370:32.
McKhann GM, 2nd, D'Ambrosio R, Janigro D (1997) Heterogeneity of astrocyte resting membrane potentials and intercellular coupling revealed by whole-cell and gramicidin-perforated patch recordings from cultured neocortical and hippocampal slice astrocytes. J Neurosci 17:6850.
Minor DL, Lin YF, Mobley BC, Avelar A, Jan YN, Jan LY, Berger JM (2000) The polar T1 interface is linked to conformational changes that open the voltage-gated potassium channel. Cell 102:657.
Monaghan MM, Trimmer JS, Rhodes KJ (2001) Experimental localization of Kv1 family voltage-gated K+ channel alpha and beta subunits in rat hippocampal formation. J Neurosci 21:5973.

Moody W, Jr. (1984) Effects of intracellular H+ on the electrical properties of excitable cells. Annu Rev Neurosci 7:257.
Morohashi Y, Hatano N, Ohya S, Takikawa R, Watabiki T, Takasugi N, Imaizumi Y, Tomita T, Iwatsubo T (2002) Molecular cloning and characterization of CALP/KChIP4, a novel EF-hand protein interacting with presenilin 2 and voltage-gated potassium channel subunit Kv4. J Biol Chem 277:14965.
Mulligan SJ, MacVicar BA (2004) Calcium transients in astrocyte endfeet cause cerebrovascular constrictions. Nature 431:195.
Nadal MS, Amarillo Y, Vega-Saenz de Miera E, Rudy B (2001) Evidence for the presence of a novel Kv4-mediated A-type K(+) channel-modifying factor. J Physiol 537:801.
Nadal MS, Ozaita A, Amarillo Y, Vega-Saenz de Miera E, Ma Y, Mo W, Goldberg EM, Misumi Y, Ikehara Y, Neubert TA, Rudy B (2003) The CD26-related dipeptidyl aminopeptidase-like protein DPPX is a critical component of neuronal A-type K+ channels. Neuron 37:449.
Nagai Y, Tsugane M, Oka J, Kimura H (2004) Hydrogen sulfide induces calcium waves in astrocytes. FASEB J 18:557.
Nakahira K, Shi G, Rhodes KJ, Trimmer JS (1996) Selective interaction of voltage-gated K+ channel beta-subunits with alpha-subunits. J Biol Chem 271:7084.
Nakamura TY, Pountney DJ, Ozaita A, Nandi S, Ueda S, Rudy B, Coetzee WA (2001) A role for frequenin, a Ca2+-binding protein, as a regulator of Kv4 K+-currents. Proc Natl Acad Sci USA 98:12808.
Nedergaard M, Ransom B, Goldman SA (2003) New roles for astrocytes: redefining the functional architecture of the brain. Trends Neurosci 26:523.
Nerbonne JM (2000) Molecular basis of functional voltage-gated K+ channel diversity in the mammalian myocardium. J Physiol 525 Pt 2:285.
Newman EA (1993) Inward-rectifying potassium channels in retinal glial (Muller) cells. J Neurosci 13:3333.
Newman EA (1996) Acid efflux from retinal glial cells generated by sodium bicarbonate cotransport. J Neurosci 16:159.
Newman EA (2003) New roles for astrocytes: regulation of synaptic transmission. Trends Neurosci 26:536.
Oh Y, Waxman SG (1994) The beta 1 subunit mRNA of the rat brain Na+ channel is expressed in glial cells. Proc Natl Acad Sci U S A 91:9985.
Oh Y, Waxman SG (1995) Differential Na+ channel beta 1 subunit mRNA expression in stellate and flat astrocytes cultured from rat cortex and cerebellum: a combined in situ hybridization and immunocytochemistry study. Glia 13:166.
Oh Y, Black JA, Waxman SG (1994) The expression of rat brain voltage-sensitive Na+ channel mRNAs in astrocytes. Brain Res Mol Brain Res 23:57.
Oh Y, Lee YJ, Waxman SG (1997) Regulation of Na+ channel beta 1 and beta 2 subunit mRNA levels in cultured rat astrocytes. Neurosci Lett 234:107.
Oudit GY, Kassiri Z, Sah R, Ramirez RJ, Zobel C, Backx PH (2001) The molecular physiology of the cardiac transient outward potassium current (I(to)) in normal and diseased myocardium. J Mol Cell Cardiol 33:851.
Patt S, Labrakakis C, Bernstein M, Weydt P, Cervos-Navarro J, Nisch G, Kettenmann H (1996) Neuron-like physiological properties of cells from human oligodendroglial tumors. Neuroscience. 71:601.
Park JB, Kim HJ, Ryu PD, Moczydlowski E (2003) Effect of phosphatidylserine on unitary conductance and Ba2+ block of the BK Ca2+-activated K+ channel: re-examination of the surface charge hypothesis. J Gen Physiol 121:375.
Parpura V, Haydon PG (2000) Physiological astrocytic calcium levels stimulate glutamate release to modulate adjacent neurons. Proc Natl Acad Sci U S A 97:8629.
Pasti L, Volterra A, Pozzan T, Carmignoto G (1997) Intracellular calcium oscillations in astrocytes: a highly plastic, bidirectional form of communication between neurons and astrocytes in situ. J Neurosci 17:7817.
Pasti L, Zonta M, Pozzan T, Vicini S, Carmignoto G (2001) Cytosolic calcium oscillations in astrocytes may regulate exocytotic release of glutamate. J Neurosci 21:477.
Patel SP, Campbell DL, Strauss HC (2002) Elucidating KChIP effects on Kv4.3 inactivation and recovery kinetics with a minimal KChIP2 isoform. J Physiol 545:5.
Patel SP, Parai R, Parai R, Campbell DL (2004) Regulation of Kv4.3 voltage-dependent gating kinetics by KChIP2 isoforms. J Physiol 557:19.
Pellerin L, Magistretti PJ (2004a) Neuroscience. Let there be (NADH) light. Science 305:50.
Pellerin L, Magistretti PJ (2004b) Neuroenergetics: calling upon astrocytes to satisfy hungry neurons. Neuroscientist 10:53.

Perez-Garcia MT, Lopez-Lopez JR, Gonzalez C (1999) Kvbeta1.2 subunit coexpression in HEK293 cells confers O2 sensitivity to kv4.2 but not to Shaker channels. J Gen Physiol 113:897.
Peri R, Wible BA, Brown AM (2001) Mutations in the Kv beta 2 binding site for NADPH and their effects on Kv1.4. J Biol Chem 276:738.
Perutz MF, Shih DT, Williamson D (1994) The chloride effect in human haemoglobin. A new kind of allosteric mechanism. J Mol Biol 239:555.
Petersen KR, Nerbonne JM (1999) Expression environment determines K+ current properties: Kv1 and Kv4 alpha-subunit-induced K+ currents in mammalian cell lines and cardiac myocytes. Pflugers Arch 437:381.
Petrecca K, Miller DM, Shrier A (2000) Localization and enhanced current density of the Kv4.2 potassium channel by interaction with the actin-binding protein filamin. J Neurosci 20:8736.
Pongs O (1999) Voltage-gated potassium channels: from hyperexcitability to excitement. FEBS Lett 452:31.
Pongs O, Leicher T, Berger M, Roeper J, Bahring R, Wray D, Giese KP, Silva AJ, Storm JF (1999) Functional and molecular aspects of voltage-gated K+ channel beta subunits. Ann NY Acad Sci 868:344-55.:344.
Ponomarenko AA, Knoche A, Korotkova TM, Haas HL (2003) Aminergic control of high-frequency (approximately 200 Hz) network oscillations in the hippocampus of the behaving rat. Neurosci Lett 348:101.
Porter JT, McCarthy KD (1996) Hippocampal astrocytes in situ respond to glutamate released from synaptic terminals. J Neurosci 16:5073.
Porter JT, McCarthy KD (1997) Astrocytic neurotransmitter receptors in situ and in vivo. Prog Neurobiol 51:439.
Ramakers GM, Storm JF (2002) A postsynaptic transient K(+) current modulated by arachidonic acid regulates synaptic integration and threshold for LTP induction in hippocampal pyramidal cells. Proc Natl Acad Sci USA 99:10144.
Ransom B, Behar T, Nedergaard M (2003) New roles for astrocytes (stars at last). Trends Neurosci 26:520.
Ransom BR (1992) Glial modulation of neural excitability mediated by extracellular pH: a hypothesis. Prog Brain Res 94:37.
Ransom CB, Sontheimer H (1995) Biophysical and pharmacological characterization of inwardly rectifying K+ currents in rat spinal cord astrocytes. J Neurophysiol 73:333.
Reese KA, Caldwell JH (1999) Immunocytochemical localization of NaCh6 in cultured spinal cord astrocytes. Glia 26:92.
Reichenbach A (1991) Glial K+ permeability and CNS K+ clearance by diffusion and spatial buffering. Ann N Y Acad Sci 633:272.
Rettig J, Heinemann SH, Wunder F, Lorra C, Parcej DN, Dolly JO, Pongs O (1994) Inactivation properties of voltage-gated K+ channels altered by presence of beta-subunit. Nature 369:289.
Rhodes KJ, Carroll KI, Sung MA, Doliveira LC, Monaghan MM, Burke SL, Strassle BW, Buchwalder L, Menegola M, Cao J, An WF, Trimmer JS (2004) KChIPs and Kv4 alpha subunits as integral components of A-type potassium channels in mammalian brain. J Neurosci 24:7903.
Riazanski V, Becker A, Chen J, Sochivko D, Lie A, Wiestler OD, Elger CE, Beck H (2001) Functional and molecular analysis of transient voltage-dependent K+ currents in rat hippocampal granule cells. J Physiol 537:391.
Rivera JF, Ahmad S, Quick MW, Liman ER, Arnold DB (2003) An evolutionarily conserved dileucine motif in Shal K+ channels mediates dendritic targeting. Nat Neurosci 6:243.
Robert A, Magistretti PJ (1997) AMPA/kainate receptor activation blocks K+ currents via internal Na+ increase in mouse cultured stellate astrocytes. Glia 20:38.
Roy ML, Saal D, Perney T, Sontheimer H, Waxman SG, Kaczmarek LK (1996) Manipulation of the delayed rectifier Kv1.5 potassium channel in glial cells by antisense oligodeoxynucleotides. Glia 18:177.
Rubin LL, Staddon JM (1999) The cell biology of the blood-brain barrier. Annu Rev Neurosci 22:11.
Rubin LL, Hall DE, Porter S, Barbu K, Cannon C, Horner HC, Janatpour M, Liaw CW, Manning K, Morales J, et al. (1991) A cell culture model of the blood-brain barrier. J Cell Biol 115:1725.
Ruppersberg JP, Stocker M, Pongs O, Heinemann SH, Frank R, Koenen M (1991) Regulation of fast inactivation of cloned mammalian IK(A) channels by cysteine oxidation. Nature 352:711.
Schlief T, Schonherr R, Heinemann SH (1996) Modification of C-type inactivating Shaker potassium channels by chloramine-T. Pflugers Arch 431:483.
Schools GP, Zhou M, Kimelberg HK (2003) Electrophysiologically "complex" glial cells freshly isolated from the hippocampus are immunopositive for the chondroitin sulfate proteoglycan NG2. J Neurosci Res 73:765.
Schroder W, Seifert G, Huttmann K, Hinterkeuser S, Steinhauser C (2002) AMPA receptor-mediated modulation of inward rectifier K+ channels in astrocytes of mouse hippocampus. Mol Cell Neurosci 19:447.

Schulteis CT, Nagaya N, Papazian DM (1996) Intersubunit interaction between amino- and carboxyl-terminal cysteine residues in tetrameric shaker K+ channels. Biochemistry 35:12133.
Seifert G, Steinhauser C (1995) Glial cells in the mouse hippocampus express AMPA receptors with an intermediate Ca2+ permeability. Eur J Neurosci 7:1872.
Sheng M, Tsaur ML, Jan YN, Jan LY (1992) Subcellular segregation of two A-type K+ channel proteins in rat central neurons. Neuron 9:271.
Sheng M, Liao YJ, Jan YN, Jan LY (1993) Presynaptic A-current based on heteromultimeric K+ channels detected in vivo. Nature 365:72.
Shevchenko T, Teruyama R, Armstrong WE (2004) High-threshold, Kv3-like potassium currents in magnocellular neurosecretory neurons and their role in spike repolarization. J Neurophysiol 92:3043.
Shi G, Nakahira K, Hammond S, Rhodes KJ, Schechter LE, Trimmer JS (1996) Beta subunits promote K+ channel surface expression through effects early in biosynthesis. Neuron 16:843.
Shibasaki K, Nakahira K, Trimmer JS, Shibata R, Akita M, Watanabe S, Ikenaka K (2004) Mossy fibre contact triggers the targeting of Kv4.2 potassium channels to dendrites and synapses in developing cerebellar granule neurons. J Neurochem 89:897.
Shibata R, Misonou H, Campomanes CR, Anderson AE, Schrader LA, Doliveira LC, Carroll KI, Sweatt JD, Rhodes KJ, Trimmer JS (2003) A fundamental role for KChIPs in determining the molecular properties and trafficking of Kv4.2 potassium channels. J Biol Chem 278:36445.
Shimizu Y, Kubo T, Furukawa Y (2002) Cumulative inactivation and the pore domain in the Kv1 channels. Pflugers Arch 443:720.
Simard M, Nedergaard M (2004) The neurobiology of glia in the context of water and ion homeostasis. Neuroscience 129:877.
Simard M, Arcuino G, Takano T, Liu QS, Nedergaard M (2003) Signaling at the gliovascular interface. J Neurosci 23:9254.
Singer-Lahat D, Dascal N, Lotan I (1999) Modal behavior of the Kv1.1 channel conferred by the Kvbeta1.1 subunit and its regulation by dephosphorylation of Kv1.1. Pflugers Arch 439:18.
Slesinger PA, Jan YN, Jan LY (1993) The S4-S5 loop contributes to the ion-selective pore of potassium channels. Neuron 11:739.
Smart SL, Bosma MM, Tempel BL (1997) Identification of the delayed rectifier potassium channel, Kv1.6, in cultured astrocytes. Glia 20:127.
Sobko A, Peretz A, Shirihai O, Etkin S, Cherepanova V, Dagan D, Attali B (1998) Heteromultimeric delayed-rectifier K+ channels in schwann cells: developmental expression and role in cell proliferation. J Neurosci 18:10398.
Song WJ, Tkatch T, Baranauskas G, Ichinohe N, Kitai ST, Surmeier DJ (1998) Somatodendritic depolarization-activated potassium currents in rat neostriatal cholinergic interneurons are predominantly of the A type and attributable to coexpression of Kv4.2 and Kv4.1 subunits. J Neurosci 18:3124.
Sontheimer H (1994) Voltage-dependent ion channels in glial cells. Glia 11:156.
Sontheimer H, Waxman SG (1993) Expression of voltage-activated ion channels by astrocytes and oligodendrocytes in the hippocampal slice. J Neurophysiol 70:1863.
Sontheimer H, Black JA, Ransom BR, Waxman SG (1992) Ion channels in spinal cord astrocytes in vitro. I. Transient expression of high levels of Na+ and K+ channels. J Neurophysiol 68:985.
Sontheimer H, Minturn JE, Black JA, Ransom BR, Waxman SG (1991) Two types of Na(+)-currents in cultured rat optic nerve astrocytes: changes with time in culture and with age of culture derivation. J Neurosci Res 30:275.
Sontheimer H, Fernandez-Marques E, Ullrich N, Pappas CA, Waxman SG (1994) Astrocyte Na+ channels are required for maintenance of Na+/K(+)-ATPase activity. J Neurosci 14:2464.
Spray DC, Bennett MV (1985) Physiology and pharmacology of gap junctions. Annu Rev Physiol 47:281.
Staba RJ, Wilson CL, Fried I, Engel J, Jr. (2002) Single neuron burst firing in the human hippocampus during sleep. Hippocampus 12:724.
Stephens GJ, Owen DG, Robertson B (1996) Cysteine-modifying reagents alter the gating of the rat cloned potassium channel Kv1.4. Pflugers Arch 431:435.
Strang C, Cushman SJ, DeRubeis D, Peterson D, Pfaffinger PJ (2001) A central role for the T1 domain in voltage-gated potassium channel formation and function. J Biol Chem 276:28493.
Strop P, Bankovich AJ, Hansen KC, Garcia KC, Brunger AT (2004) Structure of a human A-type potassium channel interacting protein DPPX, a member of the dipeptidyl aminopeptidase family. J Mol Biol 343:1055.
Takimoto K, Yang EK, Conforti L (2002) Palmitoylation of KChIP splicing variants is required for efficient cell surface expression of Kv4.3 channels. J Biol Chem 277:26904.

Tamargo J, Caballero R, Gomez R, Valenzuela C, Delpon E (2004) Pharmacology of cardiac potassium channels. Cardiovasc Res 62:9.
Tanaka H, Habuchi Y, Nishio M, Suto F, Yoshimura M (1998) Modulation by chloramine-T of 4-aminopyridine-sensitive transient outward current in rabbit atrial cells. Eur J Pharmacol 358:85.
Thoreson WB, Stella SL (2000) Anion modulation of calcium current voltage dependence and amplitude in salamander rods. Biochim Biophys Acta 1464:142.
Thoreson WB, Nitzan R, Miller RF (1997) Reducing extracellular Cl- suppresses dihydropyridine-sensitive Ca2+ currents and synaptic transmission in amphibian photoreceptors. J Neurophysiol 77:2175.
Tipparaju SM, Saxena N, Liu SQ, Kumar R, Bhatnagar A (2005) Differential regulation of voltage-gated K+ channels by oxidized and reduced pyridine nucleotide coenzymes. Am J Physiol Cell Physiol 288:C366.
Tohda H, Foskett JK, O'Brodovich H, Marunaka Y (1994) Cl- regulation of a Ca(2+)-activated nonselective cation channel in beta-agonist-treated fetal distal lung epithelium. Am J Physiol 266:C104.
Tombaugh GC, Sapolsky RM (1990) Mild acidosis protects hippocampal neurons from injury induced by oxygen and glucose deprivation. Brain Res 506:343.
Tontsch U, Bauer HC (1991) Glial cells and neurons induce blood-brain barrier related enzymes in cultured cerebral endothelial cells. Brain Res 539:247.
Trimmer JS, Rhodes KJ (2004) Localization of voltage-gated ion channels in mammalian brain. Annu Rev Physiol 66:477.
Tseng GN (1999) Different state dependencies of 4-aminopyridine binding to rKv1.4 and rKv4.2: role of the cytoplasmic halves of the fifth and sixth transmembrane segments. J Pharmacol Exp Ther 290:569.
Uebele VN, England SK, Chaudhary A, Tamkun MM, Snyders DJ (1996) Functional differences in Kv1.5 currents expressed in mammalian cell lines are due to the presence of endogenous Kv beta 2.1 subunits. J Biol Chem 271:2406.
Uebele VN, England SK, Gallagher DJ, Snyders DJ, Bennett PB, Tamkun MM (1998) Distinct domains of the voltage-gated K+ channel Kv beta 1.3 beta- subunit affect voltage-dependent gating. Am J Physiol 274:C1485.
Ullrich N, Bordey A, Gillespie GY, Sontheimer H (1998) Expression of voltage-activated chloride currents in acute slices of human gliomas. Neuroscience 83:1161.
Van Hoorick D, Raes A, Keysers W, Mayeur E, Snyders DJ (2003) Differential modulation of Kv4 kinetics by KCHIP1 splice variants. Mol Cell Neurosci 24:357.
Vautier F, Belachew S, Chittajallu R, Gallo V (2004) *Shaker*-type potassium channel subunits differentially control oligodendrocyte progenitor proliferation. Glia 48:337.
Vega-Saenz de Miera E, Rudy B (1992) Modulation of K+ channels by hydrogen peroxide. Biochem Biophys Res Commun 186:1681.
Veh RW, Lichtinghagen R, Sewing S, Wunder F, Grumbach IM, Pongs O (1995) Immunohistochemical localization of five members of the Kv1 channel subunits: contrasting subcellular locations and neuron-specific co-localizations in rat brain. Eur J Neurosci 7:2189.
Verkhratsky A, Kettenmann H (1996) Calcium signalling in glial cells. Trends Neurosci 19:346.
Verkhratsky A, Orkand RK, Kettenmann H (1998) Glial calcium: homeostasis and signaling function. Physiol Rev 78:99.
Villarroel A, Schwarz TL (1996) Inhibition of the Kv4 (Shal) family of transient K+ currents by arachidonic acid. J Neurosci 16:2522.
Walz W (1987) Swelling and potassium uptake in cultured astrocytes. Can J Physiol Pharmacol 65:1051.
Walz W (1996) Distribution and transport of chloride and bicarbonate ions across membranes. In: Neuroglia (Kettenmann H, Ransom B, eds), pp 221-229. New York: Raven.
Walz W (2000) Role of astrocytes in the clearance of excess extracellular potassium. Neurochem Int. 36:291.
Walz W (2004) Potassium homeostasis in the brain at the organ and cell level. In: Molecular and cell biology (Hertz L, ed), pp 569-609. San Diego: Elsevier.
Walz W, Hertz L (1983) Comparison between fluxes of potassium and of chloride in astrocytes in primary cultures. Brain Res 277:321.
Walz W, Hinks EC (1986) A transmembrane sodium cycle in astrocytes. Brain Res 368:226.
Walz W, Hinks EC (1987) Extracellular hydrogen ions influence channel-mediated and carrier-mediated K+ fluxes in cultured mouse astrocytes. Neuroscience 20:341.
Walz W, Mukerji S (1988) KCl movements during potassium-induced cytotoxic swelling of cultured astrocytes. Exp Neurol 99:17.

Wang S, Patel SP, Qu Y, Hua P, Strauss HC, Morales MJ (2002) Kinetic properties of Kv4.3 and their modulation by KChIP2b. Biochem Biophys Res Commun 295:223.
Wang X, Marunaka Y, Fedorko L, Dho S, Foskett JK, O'Brodovich H (1993) Activation of Cl- currents by intracellular chloride in fibroblasts stably expressing the human cystic fibrosis transmembrane conductance regulator. Can J Physiol Pharmacol 71:645.
Wang Z, Kiehn J, Yang Q, Brown AM, Wible BA (1996) Comparison of binding and block produced by alternatively spliced Kvbeta1 subunits. J Biol Chem 271:28311.
Wang Z, Eldstrom JR, Jantzi J, Moore ED, Fedida D (2004) Increased focal Kv4.2 channel expression at the plasma membrane is the result of actin depolymerization. Am J Physiol Heart Circ Physiol 286:H749.
Washabaugh MW, Collins KD (1986) The systematic characterization by aqueous column chromatography of solutes which affect protein stability. J Biol Chem 261:12477.
Watanabe S, Hoffman DA, Migliore M, Johnston D (2002) Dendritic K+ channels contribute to spike-timing dependent long-term potentiation in hippocampal pyramidal neurons. Proc Natl Acad Sci U S A 99:8366.
Wesemann DR, Benveniste EN (2005) cytokine and chemokine receptors and signaling. In: Neuroglia, 2nd Edition (Kettenmann H, Ransom B, eds), pp 146-162. New York: Oxford University Press.
Whitaker-Azmitia PM, Clarke C, Azmitia EC (1993) Localization of 5-HT1A receptors to astroglial cells in adult rats: implications for neuronal-glial interactions and psychoactive drug mechanism of action. Synapse 14:201.
Wong W, Newell EW, Jugloff DG, Jones OT, Schlichter LC (2002) Cell surface targeting and clustering interactions between heterologously expressed PSD-95 and the Shal voltage-gated potassium channel, Kv4.2. J Biol Chem 277:20423.
Xu J, Yu W, Jan YN, Jan LY, Li M (1995) Assembly of voltage-gated potassium channels. Conserved hydrophilic motifs determine subfamily-specific interactions between the alpha-subunits. J Biol Chem 270:24761.
Yang EK, Alvira MR, Levitan ES, Takimoto K (2001) Kvbeta subunits increase expression of Kv4.3 channels by interacting with their C termini. J Biol Chem 276:4839.
Ye ZC, Wyeth MS, Baltan-Tekkok S, Ransom BR (2003) Functional hemichannels in astrocytes: a novel mechanism of glutamate release. J Neurosci 23:3588.
Yellen G (2002) The voltage-gated potassium channels and their relatives. Nature 419:35.
Yi BA, Minor DL, Jr., Lin YF, Jan YN, Jan LY (2001) Controlling potassium channel activities: Interplay between the membrane and intracellular factors. Proc Natl Acad Sci U S A 98:11016.
Zhang M, Jiang M, Tseng GN (2001) minK-related peptide 1 associates with Kv4.2 and modulates its gating function: potential role as beta subunit of cardiac transient outward channel? Circ Res 88:1012.
Zhang Q, Fukuda M, Van Bockstaele E, Pascual O, Haydon PG (2004a) Synaptotagmin IV regulates glial glutamate release. Proc Natl Acad Sci U S A 101:9441.
Zhang Q, Pangrsic T, Kreft M, Krzan M, Li N, Sul JY, Halassa M, Van Bockstaele E, Zorec R, Haydon PG (2004b) Fusion-related release of glutamate from astrocytes. J Biol Chem 279:12724.
Zhou M, Kimelberg HK (2000) Freshly isolated astrocytes from rat hippocampus show two distinct current patterns and different [K(+)](o) uptake capabilities. J Neurophysiol 84:2746.
Zonta M, Carmignoto G (2002) Calcium oscillations encoding neuron-to-astrocyte communication. J Physiol Paris 96:193.
Zonta M, Sebelin A, Gobbo S, Fellin T, Pozzan T, Carmignoto G (2003a) Glutamate-mediated cytosolic calcium oscillations regulate a pulsatile prostaglandin release from cultured rat astrocytes. J Physiol 553:407.
Zonta M, Angulo MC, Gobbo S, Rosengarten B, Hossmann KA, Pozzan T, Carmignoto G (2003b) Neuron-to-astrocyte signaling is central to the dynamic control of brain microcirculation. Nat Neurosci 6:43.